NASA Contractor Report 189552

Measurement of Mechanical and Thermophysical Properties of Dimensionally Stable Materials for Space Applications

S. P. Rawal
M. S. Misra

Martin Marietta Astronautics Group
Denver, Colorado

Contract NAS1-18230 - Task 12
February 1992

National Aeronautics and
Space Administration

Langley Research Center
Hampton, Virginia 23665-5225

FOREWORD

Work reported in this final report was conducted under NASA Contract NAS1-18230, Task 12 during the period from 12 November 1990 through 22 August 1991. The work was funded by Strategic Defense Initiative Office (SDIO) work package directive PMA 1504, Advanced Materials for Space Structures. Technical effort was directed to generate a viable database of advanced composites and to determine the effect of thermal cycling on material properties. The technical monitor for the program was Mr. Louis A. Teichman of National Aeronautics and Space Administration (NASA), Langley Research Center, Materials Division. Mr. Allan W. Gunderson was the Wright Research and Development Center, Materials Laboratory advisor to the program.

Martin Marietta Astronautics Group was the prime contractor for this program. Major subcontractors included: (1) Thermophysical Properties Research Laboratory (TPRL), Purdue University, West Lafayette, IN, for thermal-physical property tests; and (2) Harrop Industries, Columbus, OH, for thermal expansion tests.

Team members, their tasks, and organization are listed below:

Name	Task	Organization
Dr. Suraj P. Rawal	Program Manager/Principal Investigator	Martin Marietta
Dr. Mohan S. Misra	Technical Advisor	Martin Marietta
Mr. Walt Thiemet	Specimen Preparation	Martin Marietta
Mr. Ron Vasquez	Material Property Tests	Martin Marietta

Subcontractors

Name	Task	Organization
Dr. Raymond E. Taylor	Task Leader	TPRL, IN
Mr. Edward Whalen	Task Leader	Harrop Industries, OH

TABLE OF CONTENTS

Page

Page

LIST OF FIGURES *

* Figures Related to Material Properties Test Data from Chapter 2 is Presented in Matrix Form.

LIST OF FIGURES - MATRIX: IM7/PEEK

TEST DATA	IM7/PEEK					
	$[0]_8$ PANEL		$[0, \pm 45, 90]_s$ PANEL		$[\pm 30, 0_4]_s$ PANEL	
	Figure #	Page #	Figure #	Page #	Figure #	Page #
• **As Fabricated**						
• Ultrasonic C-Scan	2.1-1	2-4	2.2-1,2	2-22	------	------
Microstructure	2.1-2	2-5	2.2-2	2-23	2.2-3	2-24
Thermal Expansion	2.1-3,4	2-14,15	2.2-4,5	2-40,41	2.2-6,7	2-42,43
Specific Heat	2.2-8	2-49	2.2-8	2-49	2.2-8	2-49
Thermal Conductivity (x)	2.2-9	2-49	2.2-9	2-49	2.2-9	2-49
Thermal Conductivity (y, z)	2.2-10,11	2-50	2.2-10,11	2-50	2.2-10,11	2-50
Electrical Resistivity	------	------	------	------	------	------
Hemispherical Emissivity	------	------	------	------	------	------
Reflectance vs. Wavelength	2.1-5	2-19	2.2-12	2-51	2.2-13	2-51
Fabrication Process	------	------	------	------	------	------
Dimensions	------	------	------	------	------	------

LIST OF TABLES *

* Tables of Material Properties Test Data from Chapter 2 & 3 are Presented in Matrix Form.

LIST OF TABLES-MATRIX: IM7/PEEK TEST DATA

TEST DATA	IM7/PEEK					
	$[0]_8$ PANEL		$[0, \pm 45, 90]_s$ PANEL		$[\pm 30, 0_4]_s$ PANEL	
	Table #	Page #	Table #	Page #	Table #	Page #
• **As Fabricated** Dimensions	------	------	------	------	------	------
Fiber Volume	------	------	------	------	------	------
Tension	2.1-1,2	2-7,8	2.2-1,2	2-26,27	2.2-3,4	2-28,29
Compression	2.1-3,4	2-9,10	2.2-5,6	2-30,31	2.2-7,8	2-32,33
Inplane Shear	2.1-6	2-12	2.2-10	2-36	2.2-11	2-37
Flexure	2.1-5	2-11	2.2-9	2-35	2.2-9	2-35
Interlaminar Shear	2.1-7	2-13	2.2-12	2-38	2.2-12	2-38
Coefficient of Thermal Exp.	------	------	2.2-13	2-44	2.2-13	2-44
Thermophysical	2.1-8,9,10	2-17,18	2.2-14,15,16	2-45,46,47	2.2-14,15,16	2-45,46,47
Torsion	------	------	------	------	------	------
Test Data Summary	2.3-1	2-54	2..3-2	2-55	2.3-3	2-56

LIST OF TABLES-MATRIX: 25 V/O DISCONTINUOUS SiC/2124-T6 TEST DATA

TEST DATA	25 v/o Discontinuous SiC/2124-T6			
	SiC_p/Al PANEL		SiC_w/Al PANEL	
	Table #	Page #	Table #	Page #
• **As Fabricated** Dimensions	------	------	------	------
Fiber Volume	------	------	------	------
Tension	3.1-1,2	3-5,6	3.1-3,4	3-8,9
Compression	3.1-5,6	3-11,12	3.1-7,8	3-13,14
Inplane Shear	3.1-11,12,13	3-18,19,20	3.1-11,12,13	3-18,19,20
Flexure	3.1-9	3-16	3.1-10	3-17
Interlaminar Shear	------	------	------	------
Coefficient of Thermal Exp.	------	------	------	------
Thermophysical	------	------	------	------
Torsion	------	------	------	------
Test Data Summary	3.2-1	3-22	3.2-2	3-23

SPECIMEN INDEXING CODES

Each test specimen of different composite materials was given a Martin Marietta I.D. # using an alpha-numeric code outline below:

- 10 Digit Code --- (12)(34)(56)-789-10

(reinforcement, matrix)(vendor, layup)(condition,form)-test,orientation-test#

Reinforcement Codes:

P-Silicon Carbide Particulate

G-Graphite fibers

C-Carbon (AS4)

W-Silicon Carbide Whisker

Matrix Codes:

A-Aluminum

C-Carbon

E-Epoxy

K-PEEK

M-Magnesium

P-PPS

S-Glass

Z-PES

Form Codes:

P-Panel

T-Tube

Test Codes:

TN-Tension

CM Compression

TO-Torsion

IL-Interlaminar Shear

FX-Flexure

TE-Thermal Expansion

NE-Normal Emissivity

IP-Inplane Shear

TK-Thermal Conductivity

VO-Fiber Volume Analysis

CP-Specific Heat

TD-Thermal Diffusivity

HE-Hemispherical Emissivity

AB-Absorptance

Vendor Codes:

A-Amercom

B-Specmat

C-ACMC

D-DWA

H-Hitco

M-MCI

P-ACPI

S-Martin Marietta

Layup Codes:

Q-Quasi-isotropic

Z-Zero CTE

U-Unidirectional

B-Bidirectional

Q-Particulate

Q-Whisker

Condition Codes:

A-As Fabricated

T-Thermally Cycled

Orientation Codes:

L-Longitudinal (x)

T-Transverse (y)

O-(Out-of-Plane) (z)

Example: (GA)(DU)(AP)-TNL-1 is the Graphite-Aluminum: DWA's Unidirectional As Fabricated Plate: a Tension Longitudinal Specimen #1.

(GK)(PQ)(TP)-FXT-5 is the fifth transverse flexure specimen of thermal cycled quasi-isotropic graphite reinforced PEEK from ACPI.

ACRONYMS

AF	As Fabricated
aF	Acceleration Factor
Al	Aluminum
ATCC	Accelerated Thermal Cycling Chamber
ACMC	Advanced Composite Material Corp., SC
ACPI	Advanced Composite Producted Inc., CT
ASTM	American Society for Testing and Materials
BP-DWA	British Petroleum - Dolowy Webb Associates, CA
C	Carbon
CTE	Coefficient of Thermal Expansion
CV	Coefficient of Variation
D	Thermal Diffusivity
DoD	Department of Defense
E	Epoxy
GEO	Geosynchronous Earth Orbit
Gl	Glass
GN_2	Gas Nitrogen
Gr	Graphite
LEO	Low Earth Orbit
LN_2	Liquid Nitrogen
MCI	Material Concepts Inc., Columbus, OH
Mg	Magnesium
MMC	Metal Matrix Composites
MMES	Martin Marietta Energy systems, Oakridge, TN
MTBF	Mean Time Between Failures

NDE	Non-Destructive Evaluation
OMC	Organic Matrix Composites
P	Particulate
p (subscript)	Pitch
QI	Quasi-isotropic
ROM	Rule of Mixture
RT	Room Temperature
SDS	Strategic Defense System
SiC	Silicon Carbide
SOA	State-of-the-Art
Std. Dev.	Standard Deviation
TP	Thermoplastic
UTRC	United Technology Research Center, CT
w (subscript)	Whisker

SYMBOLS

v/o	Percentage Fiber Volume
V_f	Fiber Volume Fraction
V_v	Void Volume
t	Specimen Thickness
θ	Ply Orientation
ρ	Density
E_x^T	Longitudinal Tensile Modulus
E_x^C	Longitudinal Compressive Modulus
E_y^T	Transverse Tensile Modulus
E_y^C	Transverse Compressive Modulus
σ_x^{TU}	Longitudinal Ultimate Tensile Strength
σ_x^{CU}	Longitudinal Ultimate Compressive Strength
σ_y^{TU}	Transverse Ultimate Tensile Strength
σ_y^{CU}	Transverse Ultimate Compressive Strength
ν_{xy}	Longitudinal Tensile Poisson Ratio
ν_{yx}	Transverse Tensile Poisson Ratio
G_{xy}	Inplane Shear Modulus
IPSS	Inplane Shear Strength
ILSS	Interlaminar Shear Strength
$\alpha_x = CTE_x$	Longitudinal Coefficient of Thermal Expansion
$\alpha_y = CTE_y$	Transverse Coefficient of Thermal Expansion
$\alpha_z = CTE_z$	Through Thickness Coefficient of Thermal Expansion
C_p	Specific Heat
D	Thermal Diffusivity
K_x	Longitudinal Thermal Conductivity

K_y	Transverse Thermal Conductivity
K_z	Through Thickness Thermal Conductivity
ε_H	Total Hemispherical Emissivity
ε_N	Total Normal Emittance
α_s	Solar Absorptance
CV	Coefficient of Variation
μm	Mirocrometer = Micron

CONVERSION FACTORS

1-in. = 2.54 cm

1-lb.= 0.454 kgm

1-lb/in^3 = 27.68 gm/cm^3 = 27.68 x 10^3 kg/m^3

1 ksi = 6.895 Mega Pascals (MPa)

1 Msi = 6.895 Giga Pascals (GPa)

°F = 1.8°C + 32

1 ppm/°F = 1.8 ppm/°C

1 watt-sec (W.s) = 1 Joule

Btu/(lb·°F) = 4184 W.s/(Kg.K) = 4.184 W.s/(gm.K)

1 Btu//(hr·ft·°F) = 12 Btu-in//(hr·ft^2·°F)

Btu/(hr·ft·°F) = 0.0833 Btu//(hr·in·°F)

1 Btu//(hr·ft·°F) = 1.73 W/(m.K) = 0.0173 W/(cm.K)

1 Btu-in/hr·ft^2·°F) = 0.144 W/m.K)

Microhm.cm = 10^{-8} ohm.m

1.0 INTRODUCTION AND SUMMARY

Future NASA and DoD spacecraft missions offer demanding challenges for advanced materials to satisfy mission performance and reliability requirements. For example, the beam expander metering structure for the Space Based Laser (SBL) spacecraft, and parabolic panels for Large Deployable Reflector Telescope will be required to maintain ultra-precision alignment and dimensional stability in the presence of dynamic and thermal disturbances. Conventional materials do not provide adequate specific stiffness and thermal response to maintain this level of precision. However, composite materials provide the necessary characteristics to produce light-weight and dimensionally stable structures because of their unique combination of high specific stiffness and low coefficient of thermal expansion (Ref 1-10).

Composites include both continuous and discontinuous reinforced organic matrix, metal matrix, ceramic matrix, and carbon/carbon (C/C) composite materials. Of the organic matrix composites, graphite/epoxy (Gr/E) has been used for various structural applications such as antenna support structures, waveguides, multi-horn feed support towers, and parabolic reflectors. Although, Gr/E composites have proven adequate in antenna applications to date, they are prone to microcracking during exposure to thermal cycling and radiation conditions encountered in the space environment (Ref 11-18). As a result of microdamage, the long term dimensional stability of the composites may be significantly reduced. For long-life space missions (10-20 years) and large high frequency antennas, the durability of these materials in the hostile space environment has been identified as a key material technology need. Therefore, damage resistant organic matrix composites and other composite materials are being developed for structures requiring long term dimensional stability.

Composite material development is an ongoing process. In some space applications such as precision pointing and optical bench structures, composites will provide an enabling technology

only to satisfy system performance requirements, while in others (e.g., Brilliant Pebbles, Submillimeter Explorer, Large Multiple Aperture Telescope, and Space Surveillance and Tracking System), they will provide cost savings and weight reduction. However, for composites to be utilized in the design of Strategic Defense system (SDS) spacecraft or other near term structural applications, data must be available to aid designers in performing preliminary design trade studies and assist in material selection efforts. In several Department of Defense (DoD) sponsored programs, mechanical and/or thermophysical property data of various composite systems (Ref 19-47) have been obtained at different stages of the material development. As the fabrication technology is nearing maturity, reliable and reproducible test data for State-of-the-Art (SOA) composites need to be generated using standardized or recommended test procedures (Ref 48-64). This data will facilitate the verification of analytical models that are used to predict properties. The accuracy of property prediction shall enable the assessment of performance of these materials during their operational life. In addition, there is a critical need to assess the reproducibility and reliability of materials using SOA non-destructive evaluation (NDE) techniques. After verifying the material property data and establishing the reliability of the components, the designers will be able to integrate composites into structural applications. The major thrust of this program was to generate a viable database of advanced composite material properties by utilizing a single contractor and implementing the same test methods and environments for composites considered under this program.

In the overall program, extensive mechanical and thermophysical property tests of various SOA composites have been conducted, and a reliable database has been constructed for spacecraft material selection. The composites included Gr/E, graphite/thermoplastic (Gr/TP), carbon/thermoplastics (C/TP), discontinuous silicon carbide/aluminum (SiC/Al), graphite/aluminum (Gr/Al), graphite/magnesium (Gr/Mg), carbon/glass (C/Gl), and C/C materials. Of the test methods, American Society for Testing and Materials (ASTM) standards were used whenever they were applicable. In the absence of an ASTM

Standard, DoD/NASA, Thermophysical Property Research Laboratory (TPRL), Society of Advanced Composite Materials Association (SACMA) or Martin Marietta Astronautics Group recommended test methods were used.

During 1987 -1990, in this program, material property tests of different composites were conducted at room temperature (RT). These results were documented in the NASA contractor report 187472 (August 1990) entitled "Composites Materials for Space Applications"(65). A copy of the summary of the test data is included in the Appendix A.

This report documents the results of mechanical and thermophysical property tests (in the present 1991 follow-on effort), of IM7/PEEK and discontinuous SiC/Al (both particulate (p) and whisker (w) reinforced) composites which were tested at three different temperatures: -150°, RT and 250° F to determine the effect of temperature on material properties. The specific material systems tested were as follows:

- IM7/PEEK $[0]_8$;
- IM7/PEEK $[0, \pm 45, 90]_s$;
- IM7/PEEK $[\pm 30, 0_4]_s$;
- 25 volume percent (v/o) SiC_p/Al; and;
- 25 v/o SiC_w/Al.

Room temperature material property results of IM7/PEEK were in excellent agreement with the predicted values, providing a measure of consolidation integrity attained during fabrication. Results of mechanical property tests indicated that modulus values at each test temperature were identical, whereas the strength (e.g. tensile, compressive, flexural and shear) values were the same at -150°F and RT, and gradually decreased as the test temperature was increased to 250° F. Similar trend in the strength values was also observed in discontinuous SiC/Al composites. Based on these results, the effect of temperature was more pronounced on the strength values as compared to the modulus values as compared

to the modulus values.

For the as-fabricated IM7/PEEK and discontinuous SiC/Al , the test results are discussed in detail in the chapters 2 and 3 respectively.

1.1 OBJECTIVE

The objective of the program was to:

- Generate mechanical, thermal, and physical property test data for as-fabricated advanced composite materials at RT, -150° and 250° F.

1.2 PROGRAM PLAN

Figure 1-1 shows a systematic test plan that was used to accomplish the program objectives. The plan included composite material acquisition, product evaluation, specimen preparation, material property tests, and data analysis. Of these tests, all physical and mechanical property measurements were conducted at Martin Marietta Astronautics Group, Denver, CO, thermal expansion measurements at Harrop Industries, Columbus, OH, and remaining thermal and electrical property tests were conducted at TPRL, IN. This report includes the test results of only as-fabricated composites. Later, several specimens will be thermal cycled between -150° and 150°F and the results of subsequent material property tests will be documented in a separate report.

1.3 TEST MATERIALS

Table 1-1 lists the advanced composite materials that were obtained in the flat panel form from the major composite manufacturers and tested to obtain mechanical and thermophysical property data.

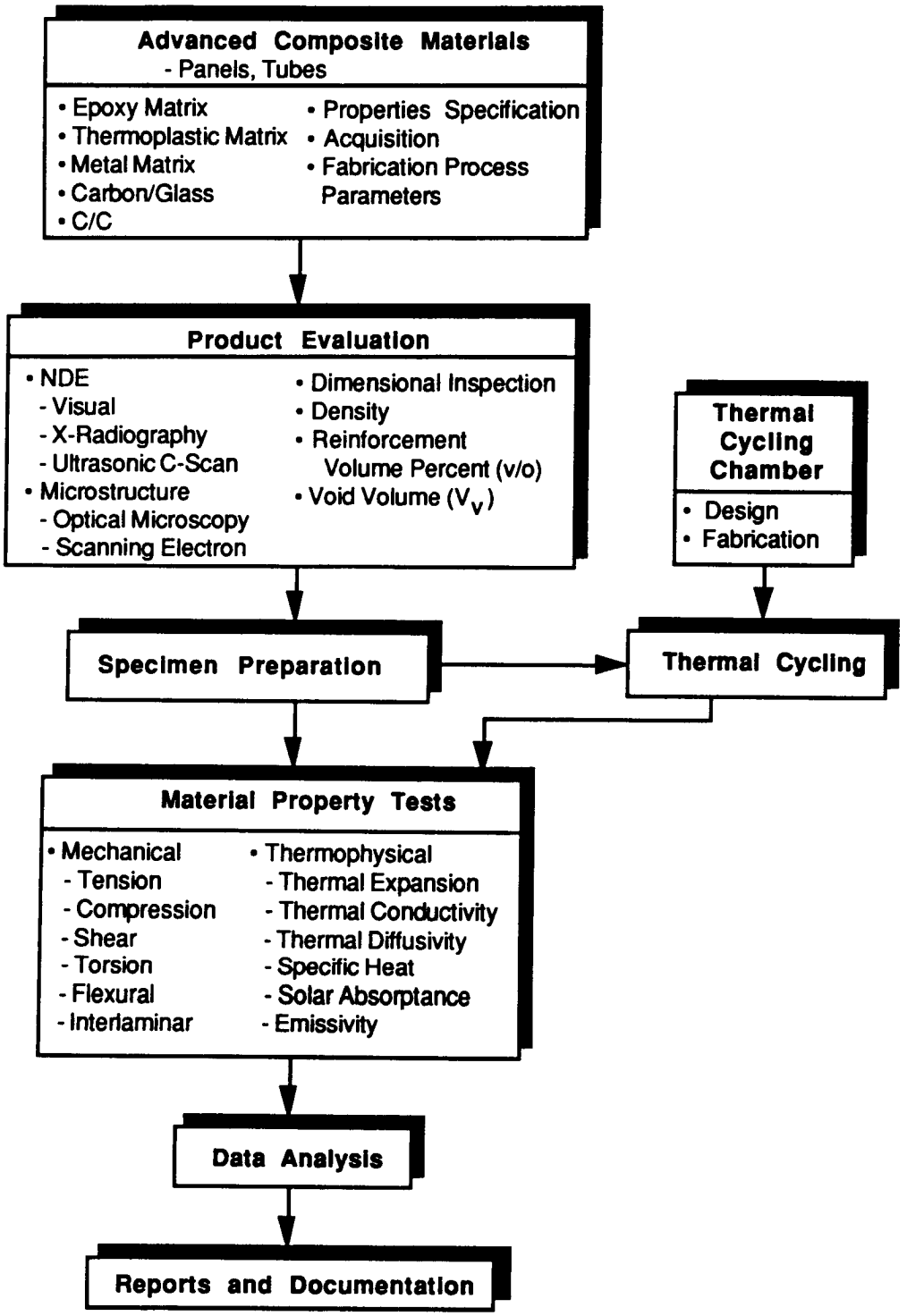

Figure 1-1 Program Test Plan Flowchart

Table 1-1 List of Composite Materials Tested in This Program

Advanced Composites	Test Material • Ply Orietnation	Form	Manufacturer
Continuously Reinforced Graphite/ Thermoplastic	IM7/PEEK • $[0]_8$ • $[0, \pm 45, 90]_s$ • $[\pm 30, 0_4]_s$	 Flat Panel Flat Panel Flat Panel	ICI/Fiberite,AZ
Discontinuously Reinforced Metal Matrix Composites	25 SiC_p /2124 Al–T6 25 SiC_w /2124 Al–T6	Flat Panel Flat Panel	ACMC, SC ACMC, SC

In the case of IM7/PEEK flat lamina (unidirectional) panels were included to obtain the input material properties required for analytical modeling to predict laminate response. Also, the laminates were obtained with two types of ply orientation: quasi-isotropic $[0, \pm 45, 90]_s$, and $[\pm 30, 0_4]_s$. Both the silicon carbide particulate and whisker reinforced 2124-T6 aluminum (SiC_p/2124-T6 and SiC_w/2124-T6) flat panels were obtained from Advanced Composite Materials Corporation, SC (ACMC).

Typical composite panels were 12-in. x 12-in. from which about 50 specimens were carefully cut for microstructural evaluation, reinforcement volume analysis, mechanical and thermophysical property tests.

1.4 EXPERIMENTAL PROCEDURES

Each composite material was extensively characterized by NDE techniques to evaluate the product quality, dimensionally inspected to determine flatness/bow and wall thickness variation, and tested to determine mechanical and thermophysical properties. The test matrix for as-fabricated composites is listed in Table 1-2. A minimum of 5 specimens were used for each

mechanical property test. While the details of product evaluation and property tests for each composite are discussed in subsequent chapters, the experimental procedures and results are summarized below.

Table 1-2 Test Matrix for Composite Materials

Material Property Tests	IM7/PEEK $[0]_8,[0,\pm45,90]_s,[\pm30,0_4]_s$			Dis. SiC/Al 25 v/o SiC_p/Al 25 v/o SiC_w/Al		
	-150°F	RT	250°F	-150°F	RT	250°F
Mechanical Properties						
• Tension (x, y)	10*	10	10	10		10
• Compression (x, y)	10	10	10	10		10
• Inplane Shear (x, y)	10	10	10	10		10
• Flexure (x, y)	10	10	10	10		10
• Interlaminar Shear (x, y)	10	10	10	10		10
Thermophysical Properties						
• CTE (x, y)		5				
• Specific Heat (Cp)		5				
• Thermal Conductivity, K(x&y)		5				
• Thermal Diffusivity (D)		1				
• Electrical Resistivity (ρ_e)		(5)				
• Emissivity (ε_H)		3				
• Solar Absorptance (α_s)		3				
Miscellaneous						
• Density		5				
• Fiber Volume & Porosity		5				
• Microstructure		3				
* (5 (x), 5 (y) specimens)						

1.4.1 Product Evaluation

Comprehensive evaluation of each flat panel included:

- Fabrication data;
- Non-Destructive Evaluation;

- Dimensional Inspection;
- Microstructural Evaluation;
- Specific Gravity and Density; and
- Reinforcement Content.

Fabrication data was supplied by the manufacturer. The NDE techniques included visual examination to observe surface imperfections; X-radiography to assess fiber collimation, fiber breakage, voids or other defects; ultrasonic C-scanning to find delaminations and voids, and thermography to find delamination or voids. Microstructural evaluation using optical and scanning electron microscopy was used to reveal the consolidation quality, ply orientation, voids, microcracks and fiber-matrix distribution.

While NDE results and microstructures provided an adequate means to detect internal defects, the specific gravity, reinforcement volume percentage (v/o), and void volume (Vv) measurements also provided an assessment of the material or processing quality. The specific gravity and density of each composite was determined by the displacement method described in ASTM-D792. To determine the v/o, ASTM-D3171 test method was used for IM7/PEEK composites, and ASTM-D3553 method was used for metal matrix composites. The Vv in the IM7/PEEK was determined by the procedures described in ASTM-D2734.

The measured values of density, v/o, Vv, and ply thickness for each composite are listed in Table 1-3. These results of low void volume ($\leq$0.8%) and uniform ply thickness indicated that the consolidation quality of the laminates was satisfactory.

1.4.2 Test Methods

After completing the product evaluation of each panel, the specimens were prepared for

Table 1-3 Measured Density and Reinforcement Volume of Composite Materials

Material	Density (lb/in^3)			Reinforcement Volume (v/o)		Void Volume* V_v	Ply Thickness (-in)
	Matrix	Reinforcement	Composite				
IM7/PEEK							
• $[0]_8$	0.046	0.0643	0.0571	62.5	(1.0)*	≤0.5	0.005
• $[0,\pm45,90]_s$	0.046	0.0643	0.0571	62.0	(0.9)	≤0.5	0.005
• $[\pm30,0_4]_s$	0.046	0.0643	0.0571	62.0	(0.9)	≤0.5	0.005
SiC_p/Al							
• 25 v/o							
SiC_w/Al							
• 25 v/o	0.098	0.134	0.104	25	(1.1)	≤0.1	N/A
	0.098	0.134	0.104	25	(1.1)	≤0.1	N/A

* Standard Deviation

mechanical and thermophysical property tests. From each panel the test specimens were cut with the 2-in. dia. diamond-coated band saw. Subsequently, edges of each specimens were polished to the final dimensions using 320 grit abrasive paper. On flat specimens for tension and compression tests , the fiber glass end tabs providing 15° taper near the gage length, were bonded using FM-300-2 adhesive which offered good bond strength at RT and ± 250°F. For each test either an ASTM standard or SACMA recommended method was used as listed in Table 1-4. The details of test method including specimen dimension, specimen configuration, and fixture designs are described in Appendix B.

1.5 MATERIAL PROPERTY TEST DATA SUMMARY

Figure 1-2 shows the composite axes used in the presentation of test data. For example, in a composite laminate with $[0, \pm45, 90]_s$ layup, the elastic modulus in the longitudinal (i.e., along 0° ply) direction is abbreviated as E_x (equivalently E_1) and longitudinal tensile poisson ratios as ν_{xy}.

Table 1-4 Test Methods for Composite Materials

Material Property Tests	Test Methods †
Mechanical	
• Tension (x, y)	ASTM D-3552 (MMC, CMC, C-C) † ASTM D-3039 (OMC)
• Hoop	NOL Ring Test
• Compression (x,y)	ASTM D-3410 (Celanese Fixture) †
• Inplane Shear	Iosipescu Test
• Interlaminar Shear (Short Beam - 4 point bend)	ASTM-D-2344
• Flexure Test	ASTM D-790M-84
• Torsion	Designed Fixture
Thermophysical Properties	
• Thermal Expansion (x,y)	ASTM E-80/ASTM E-228 (Push Rod Dilatometer)
• Thermal Conductivity* (x,y)	Kohlrausch Method
• Electrical Resistivity* (x,y)	Kohlrausch Method
• Specific Heat*	ASTM E1269
• Solar Absorptance	ASTM E-903
• Hemispherical Emissivity*	ASTM C-835
• Total Normal Emissivity	ASTM E-408B
• Thermal Diffusivity*	Laser Flash
• Density	ASTM D-792
• Fiber Volume	ASTM D-3171 (OMC), D2734 ASTM D-3553 (MMC)

* Tests were conducted at Thermophysical Properties Research Lab, Purdue Univ., West Lafayette, IN.

† Tension and compression tests of the tube specimens were performed by using a fixture and test method recommended for ASTM standards

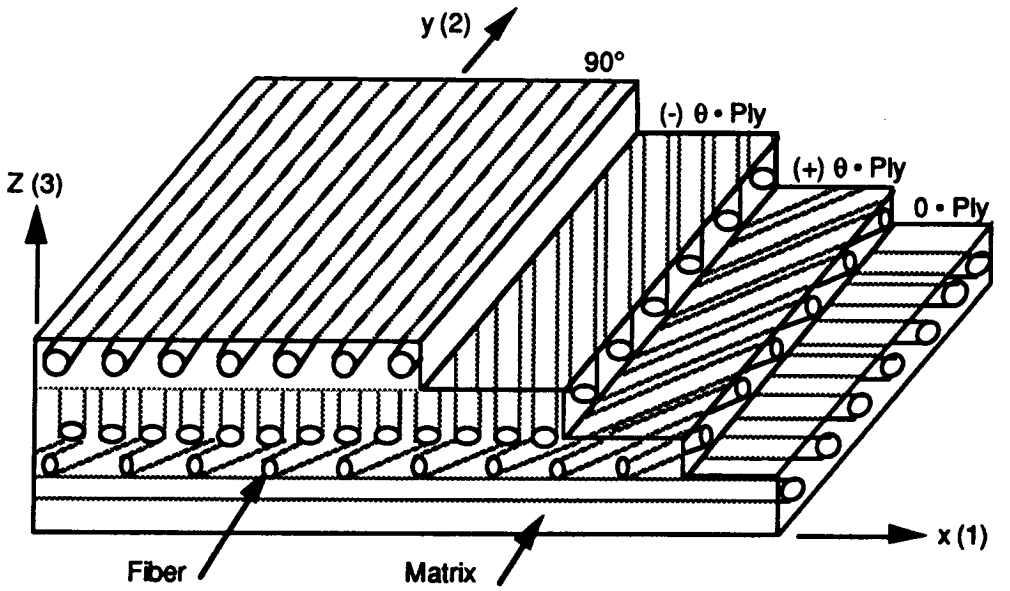

Figure 1-2 Composite Axes Used to Describe the Fiber Architecture and Test Direction

The average mechanical and thermophysical properties of as-fabricated IM7/PEEK and 25 v/o SiC/2124 Al composites obtained from tests at -150°F, RT, and 250°F are summarized in Table 1-5 and details of these results are discussed in Chapters 2 and 3. Measured properties of the composites are in agreement with the values predicted from the simple rule of mixture (ROM) equations (Appendix C) and the laminate properties estimated by the computer analysis. Quantitative comparison for each composite system are presented in respective chapters. In the modulus and strength measurements, the coefficient of variation (CV) is less than 6%, whereas in Poisson ratio measurements the CV is about 12%. This level of scatter is reasonable to expect in SOA composites. Of the various tests, in general compressive property measurements indicated more scatter in the data than other mechanical and thermophysical property tests. The extent of scatter in compressive properties can be attributed both to the test method (Celanese compression - using 0.5 in. gauge length) and to inherent material response.

Overall, the reasonable agreement between the measured and predicted properties (e.g., E_x^T, σ_x^T, CTE_x)(Table 1-6) and low CV indicated that SOA composites have adequate consolidation quality. The predicted values were obtained by using the general dominate (GENLAM) analysis code. Table 1-6 shows that the measured longitudinal CTE values are in nearly perfect agreement with the predicted CTE values. Of the measured modulus values, the tensile modulus for IM7/PEEK $[0]_8$ and $[\pm 30, 0_4]_S$ is about 90% of the predicted values, and 80% of the predicted value for $[0, \pm 45, 90]_S$ layup. In each case the measured tensile strength values are in complete agreement with the expected strength values.

The effect of temperature on tensile modulus and strength for IM7/PEEK composites is shown in Figures 1-3 and 1-4 respectively. At -150°F, RT, and 250°F the measured modulus values are nearly the same, indicating that fiber dominated property such as modulus are not affected by temperature over this range. Whereas, Figure 1-3 shows that matrix dominated property such as strength gradually decreases as the temperature increases to 250°F (Glass Transition temperature for PEEK: Tg = 290°F). In the case of discontinuous SiC/Al (Table 1-7) measured modulus

Table 1-5 As-Fabricated IM7/PEEK Tested at -150°F, RT and 250°F

Material Property			Gr/TP: IM7/PEEK $[0]_8$			Gr/TP: IM7/PEEK $[0, \pm45, 90]_s$			Gr/TP: IM7/PEEK $[\pm30, 0_4]_s$		
Density	ρ	lb/in^3		0.057			0.057			0.057	
Fiber Volume Fraction	V_f			0.62			0.62			0.62	
Nominal Ply Thickness	t	in.		0.005			0.005			0.005	
Max. Continuous Use Temp.	T	°F		250			250			250	
Test Temperature		°F	-150	RT	250	-150	RT	250	-150	RT	250
Longitudinal Tensile Strength	σ_x^{TU}	ksi	389.0	391.27	318.1	130.97	130.3	114.5	304.4	297.4	238.7
Transverse Tensile Strength	σ_y^{TU}	ksi	11.08	10.5	9.03	145.4	134.8	116.4	15.57	14.72	12.6
Longitudinal Comp. Strength	σ_x^{CU}	ksi	163.6	146.8	105.2	96.85	67.7	55.06	154.2	127.6	106.38
Transverse Comp. Strength	σ_y^{CU}	ksi	25.86	17.8	12.3	61.25	49.0	39.0	38.13	23.0	18.9
In-Plane Shear Strength	IPSS	ksi	23.85	19.18	9.0	44.72	45.2	33.1	34.6	36.3	25.7
Interlaminar Shear Strength	ILSS	ksi		15.39		9.48	11.45	7.95	17.68	16.5	10.51
Longitudinal Tensile Strain **	ε_x^T	%									
Transverse Tensile Strain **	ε_y^T	%									
Longitudinal Comp. Strain **	ε_x^C	%									
Transverse Comp. Strain **	ε_y^C	%									
Longitudinal Tensile Modulus	E_x	Msi	21.9	23.87	24.3	7.17	7.3	7.26	17.32	18.1	18.81
Transverse Tensile Modulus	E_y	Msi	1.46	1.4	1.18	7.57	7.71	7.3	1.69	1.62	1.15
Longitudinal Comp Modulus	E_x	Msi	22.53	22.8	21.72	9.13	7.1	7.7	16.39	17.2	15.94
Transverse Comp Modulus	E_y	Msi	1.41	1.4	1.22	8.98	9.36	8.71	2.0	1.9	1.41
In-Plane Shear Modulus	G	Msi	1.08	1.12	0.80	2.91	2.70	2.46	2.04	1.93	1.81
Longitudinal Flexural Modulus	F_x	Msi		23.13			13.5			11.21	
Transverse Flexural Modulus	F_y	Msi		1.32			3.2			2.0	
Long. Tensile Poisson's Ratio	ν_{xy}	---	0.295	0.289	0.276	0.291	0.291	0.33	1.09	1.02	
Trans. Tensile Poisson's Ratio	ν_{yx}	---	0.018	0.02	0.016	0.31	0.334	0.31	0.080	0.084	0.093
Long. Thermal Conductivity	K_x	(1)	0.21	0.253	0.30	0.13	0.158	0.18	0.194	0.24	0.27
Trans. Thermal Conductivity	K_y	(1)	0.026	0.031	0.041	0.109	1.151	0.155	0.047	0.055	0.058
Thru Thickness thermal Cond.	K_z	(1)	0.026	0.033	0.04	0.022	0.033	0.041	0.028	0.034	0.041
Specific Heat	Cp	(2)	0.10	0.20	0.26	0.10	0.20	0.26	0.10	0.20	0.26
Longitudinal CTE	α_x	(3)		-0.07			1.37			-0.62	
Transverse CTE	α_y	(3)		17.42			1.16			12.56	
Through Thickness CTE	α_z	(3)									

** Strain to failure (1) Btu/(hr•in•°F) (2) Btu/lb•°F) (3) µin/in/°F

Table 1-5 As-fabricated 25 v/o SiC_p/2124 Al Tested at -150°F, RT and 250°F

Material Property			MMC: SiC_p/2124 Al			MMC: SiC_w/2124 Al		
Density	ρ	lb/in^3		0.104			0.104	
Fiber Volume Fraction	V_f			0.25			0.25	
Max. Continuous Use Temp.	T	°F		550			550	
Test Temperature		°F	-150°F	RT*	250°F	-150°F	RT*	250°F
Longitudinal Tensile Strength	σ_x^{TU}	ksi	92.66	84.5	79.89	108.8	102.0	93.02
Transverse Tensile Strength	σ_y^{TU}	ksi	91.42	77.5	73.97	94.16	97.4	76.0
Longitudinal Comp. Strength	σ_x^{CU}	ksi	109.7	80.8	73.16	106.56	102.5	81.28
Transverse Comp. Strength	σ_y^{CU}	ksi	109.4	75.8	72.44	102.18	91.0	67.11
In-Plane Shear Strength	IPSS	ksi	34.31	39.54	47.91	48.2	44.0	46.3
Interlaminar Shear Strength	ILSS	ksi	NA	NA	NA	NA	NA	NA
Longitudinal Tensile Strain **	ε_x^T	%		1.258			1.62	
Transverse Tensile Strain **	ε_y^T	%		1.18			1.83	
Longitudinal Comp. Strain **	ε_x^C	%		0.618			1.11	
Transverse Comp. Strain **	ε_y^C	%		0.620			1.26	
Longitudinal Tensile Modulus	E_x	Msi	16.75	16.64	15.58	17.21	17.6	17.67
Transverse Tensile Modulus	E_y	Msi	16.12	17.0	15.65	17.03	16.42	15.31
Longitudinal Comp Modulus	E_x	Msi	17.42	18.5	16.16	17.57	18.15	17.33
Transverse Comp Modulus	E_y	Msi	16.28	17.9	15.78	17.44	16.5	14.61
In-Plane Shear Modulus	G	Msi	6.0	5.94	5.03	6.19	5.40	5.23
Longitudinal Flexural Modulus	F_x	Msi	16.76	13.51	16.45	17.59	13.1	17.2
Transverse Flexural Modulus	F_y	Msi	16.44	13.02	16.82	17.0	11.8	16.75
Long. Tensile Poisson's Ratio	ν_{xy}	---	0.297	0.267	0.269	0.298	0.2934	0.295
Trans. Tensile Poisson's Ratio	ν_{yx}	---	0.289	0.279	0.261	0.297	0.2717	0.256
Long. Thermal Conductivity	K_x	(1)	3.373	5.740	6.486		4.87	
Trans. Thermal Conductivity	K_y	(1)	3.3026	5.6116	6.111		4.71	
Thru Thickness Thermal Cond.	K_z	(1)					4.57	
Specific Heat	Cp	(2)	0.123	0.1984	0.243		0.199	
Longitudinal CTE	α_x	(3)		8.16			8.03	
Transverse CTE	α_y	(3)		7.86			7.77	
Through Thickness CTE	α_z	(3)						

* RT test panesl (0.040-in. thick) were from a different batch than the -150°F and 250°F test panels (0.06-in. thick)

** Strain to failure

(1) Btu/(hr•in•°F)

(2) Btu/lb•°F)

(3) µin/in/°F

Table 1-6 Comparison of Measured and Predicted Properties of Selected Composite Materials at RT

COMPOSITE	E_X^T (Msi)		CTE_L (ppm/°F)		σ_X^T (ksi)	
	MEASURED	PREDICTED	MEASURED	PREDICTED	MEASURED	PREDICTED
IM7/PEEK						
$[0]_8$	23.87	25.8	-0.07	-0.1	391.3	392
$0, \pm 45, 90_s$	7.3	9.4	1.27	1.27	134.8	139
$[\pm 30, 0_4]_s$	18.1	19.8	-0.62	-0.63	297.4	303
25 v/o SiC/Al	16.64	16.8	8.16	8.56	–	–

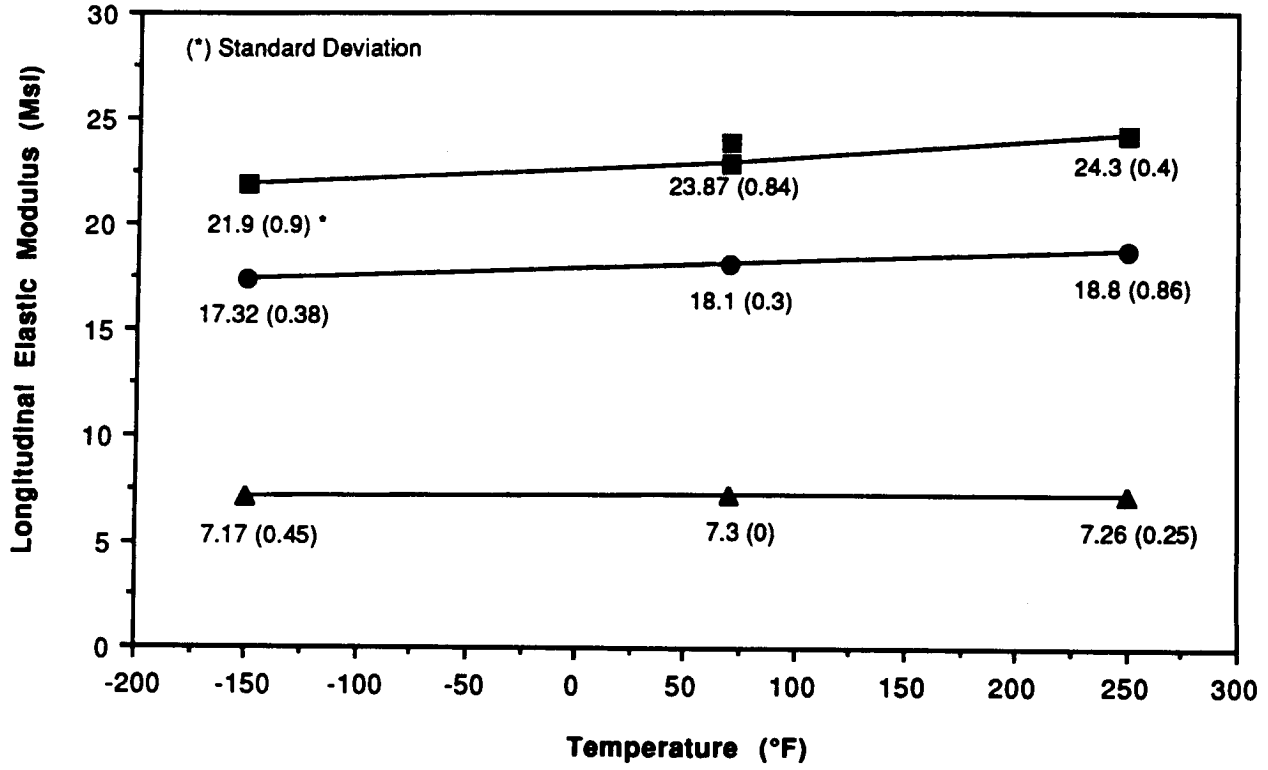

Figure 1-3 Effect of Temperature on the Longitudinal Elastic Modulus of IM7/PEEK

values were also nearly the same at each test temperature (i.e., -150°, RT, and 250°F) but the ultimate strength slightly decreased with increasing temperature (e.g., for 25 v/o SiC_p/Al, UTS = 92.66 ksi @ -150°F, and UTS = 73.89 ksi @ 250°F in manner similar to the 2124 Al matrix.

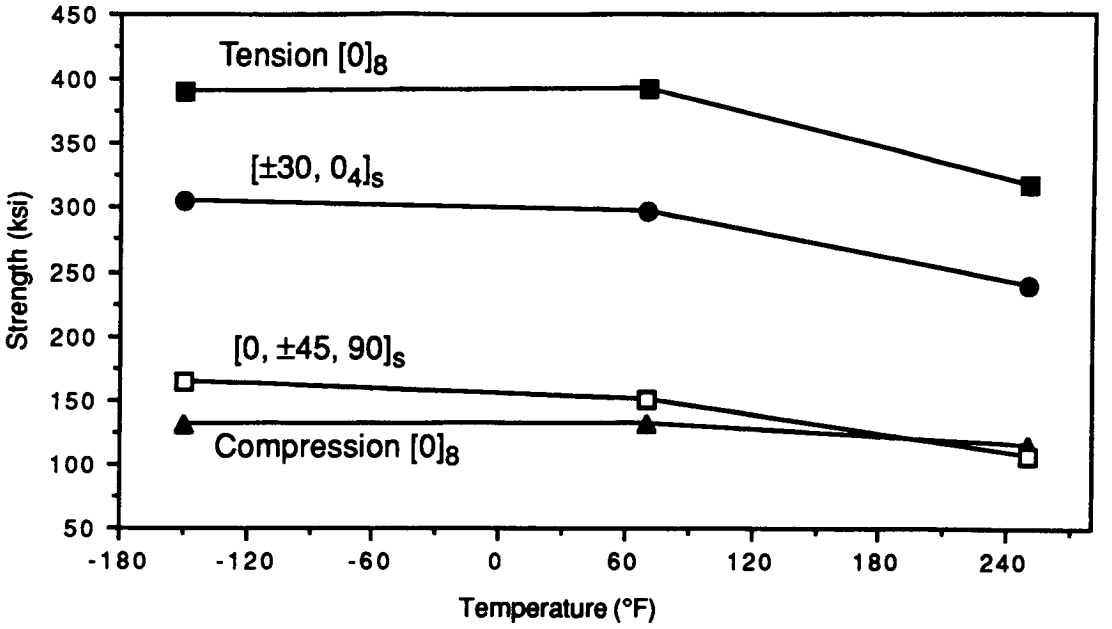

Figure 1-4 Effect of Temperature on the Ultimate Strength of IM7/PEEK

Table 1-7 Effect of Temperature on Tensile Modulus and Strength of Discontinuous SiC/Al

Properties	25 v/o SiCp/Al at			25 v/o SiCw/Al at		
	-150°F	RT*	250°F	-150°F	RT*	250°F
E (Msi)	16.75	16.64	15.58	17.21	17.6	17.67
UTS (ksi)	92.66	84.5	73.89	108.8	102.0	93.02
0.2% Ys (ksi)	73.67	70.44	63.65	78.61	76.2	72.59

* RT values from a different batch of composite material (65)

1.6 CONCLUDING REMARKS

Although extensive material property data of several composites exist, use of this data in structural design efforts is severely limited due to lack of standardized test methods and procedures, and the large number of organizations reporting only limited data. In response to these needs, the current program was designed to generate a viable database of advanced composite material properties by utilizing a single contractor and implementing the same test methods and environments for the composites considered. This database, although limited, should prove extremely valuable to spacecraft designers for preliminary material trade-off studies. The test data generated in this program (listed in Appendix A, and chapters 2 and 3) provides the typical material properties of SOA composites. The results of the as-fabricated (and also thermal cycled composites) have been included in the "Strategic Defense System (SDS) Spacecraft Structural Composite Materials Selection Guide" prepared by Ketema, Inc., Composite Materials Division, CA (Ref 21). While extensive data has been generated in this technical effort, a large number of specimens from different production batches should be tested before and after thermal cycling to build confidence in the reproducibility and reliability of composite material properties.

2.0 GRAPHITE/THERMOPLASTIC: IM7/PEEK

A high performance graphite/thermoplastic composite, IM7/PEEK, is being developed for spacecraft structural applications. Therefore, flat panels with the following fiber layups:

(1) $[0]_8$: Unidirectional;

(2) $[0, \pm 45, 90]_S$: Quasi-isotropic (QI); and

(3) $[\pm 30, 0_4]_S$: Laminate

were procured for material property characterization. The $[\pm 30, 0_4]_S$ layup was selected to obtain near zero CTE in the laminate, therefore it has also been referred to as zero CTE laminate in the report (65). The fabrication data, and the results of product evaluation, mechanical, and thermophysical property tests of these materials are discussed in this chapter.

2.1 IM7/PEEK $[0]_8$ FLAT PANELS

2.1.1 Fabrication Data:

Material System:	IM7/PEEK
Fiber Layup:	$[0]_8$
Manufacturer:	Fiberite/ICI, AZ
Prepreg Source:	Fiberite/ICI, AZ
Martin Marietta ID#:	(CK)(SU)(AP)
Fiberite Code No.:	12736 P1-P5
Fabrication Process:	ICI-Fiberite autoclave cycle C-29 All panels were consolidated in a platen press at 735°F under an applied pressure of 100 psi for 20 min. The panels were cooled down at ≥ 13°F/minute while the 100 psi pressure was maintained until below 200°F. Full vacuum was maintained throughout consolidation cycle.

Condition:	as-fabricated
Dimensions:	12-in. x 12-in. x 0.040-in.
Ply Thickness:	0.005-in.
Nominal Fiber weight/area per ply:	145 gm/m^2
Nominal Resin Content/ply:	32 weight%
Roll Numbers:	31

2.1.2 Product Evaluation

(a) Density:

IM7 Fiber:	0.0643 lb/in^3 (1.78 gm/cm^3)
PEEK :	0.046 lb/in^3 (1.28 gm/cm^3)
IM7/PEEK:	0.0571 lb/in^3 (1.58 gm/cm^3)

(b) Fiber Volume:

Fiber Volume (v/o):	62.0%
Std. Dev:	0.6%
Void Volume (%Vv):	≤0.4%

(c) Non-Destructive Evaluation

Visual, X-radiographic and ultrasonic techniques were used to inspect all IM7/PEEK $[0]_8$ flat panels. Each panel appeared to be of good quality without any surface imperfections. X-

radiographic inspection examination revealed that fiber collimation was excellent. Typical ultrasonic C-scans of a $[0]_8$ panels are shown in Figure 2.1-1. Ultrasonic C-scan showed no major defect such as cracks or delaminations except one or two air-bubble sites on the entire panel.

(d) Microstructure

Longitudinal and transverse microstructures of IM7/PEEK $[0]_8$ lamina are shown in Figure 2.1-2(a) and (b). Each photomicrograph shows that the overall fiber matrix distribution is uniform and fibers are aligned along the longitudinal direction.

2.1.3 Mechanical Properties

(a) Tension

Prior to testing the longitudinal specimens, computer analysis was performed to determine the predicted mechanical properties. Based on this analysis:

$E_L = 25.8$ Msi

Ultimate Tensile Strength = 392 ksi

From the$[0]_8$ plates, tensile test specimens (10-in. long x 0.5-in.wide x 0.040-in. thick) were prepared in accordance with ASTM D-3039. Preliminary tests of this high strength composite indicated the critical need for obtaining adequate adhesive bond strength by selecting optimum surface preparation techniques, bonded area and adhesives. The end tabs were bonded using the FM-300-2 adhesive (bond line thickness 0.005-in.) because it offered good bond strength at RT, and ±250°F. In these preliminary tests, IM7/PEEK $[0]_8$ specimens exhibited elastic modulus values between 23.5 and 25.5 Msi, and strength values between 300 and 392 ksi. But a few of

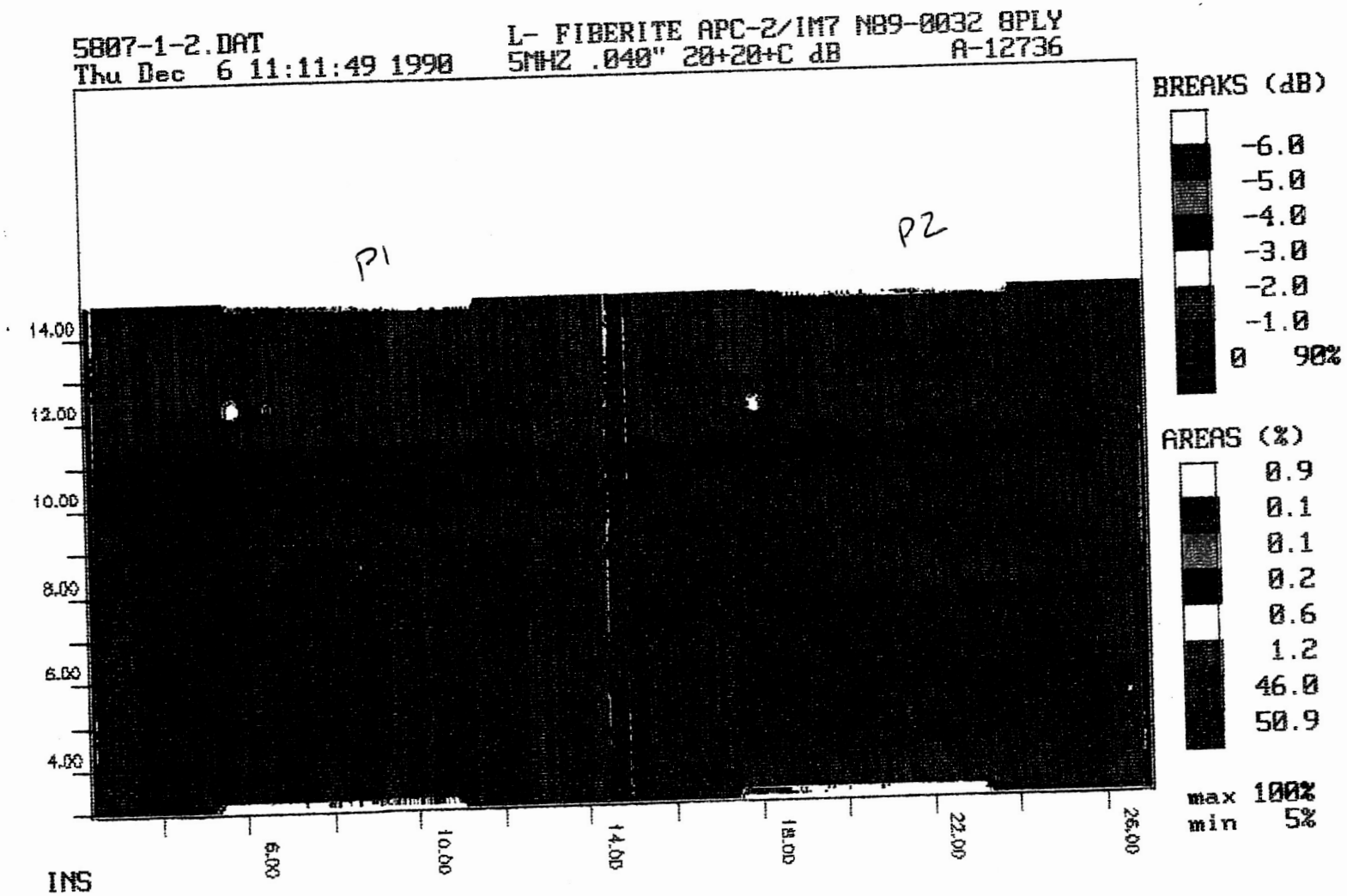

Figure 2.1-1 Ultrasonic C-Scans of IM7/PEEK $[0]_8$ Panels Showing No Defects

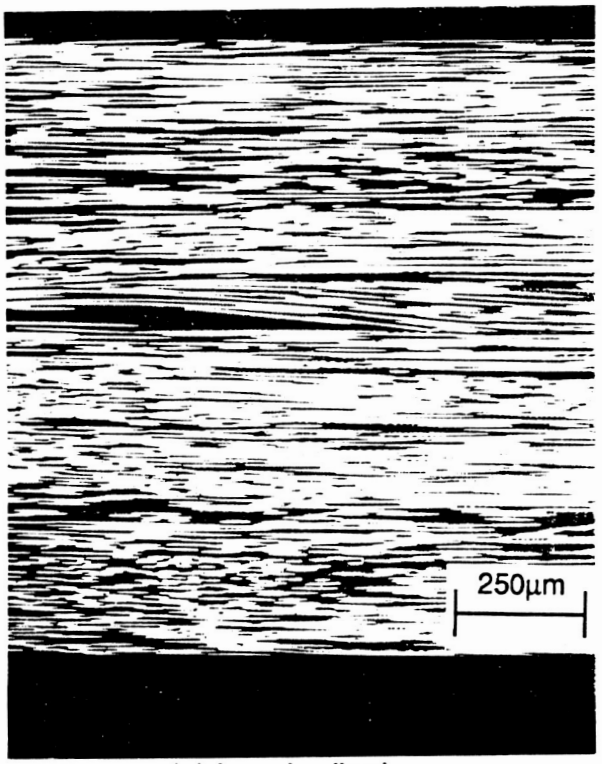

(a) Longitudinal

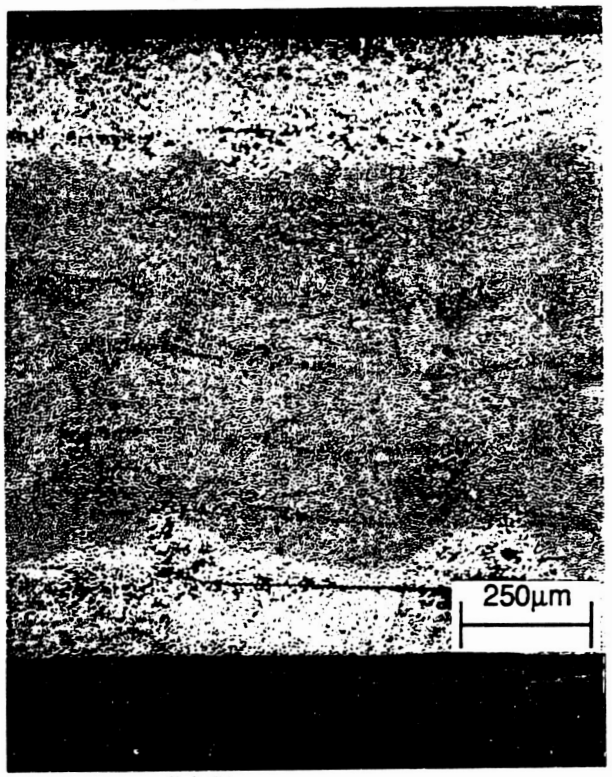

(b) Transverse

Figure 2.1-2 Photomicrographs of IM7/PEEK $[0]_8$ Showing Uniform Fiber/Matrix Distribution

these specimens exhibited adhesive failure at the end tab/specimen interface at the test load levels (≈ 380 ksi), thus making it difficult to determine the ultimate tensile strength. To minimize this adhesive failure, test specimens were prepared from a thinner (0.025-in.) $[0]_s$ panel with the uniform bond line thickness of 0.005-in.

Each specimen exhibited tensile failure within the gage length region and reproducible data was obtained at different test temperatures: -150°F, RT, and 250°F . Typical stress-strain response of each specimen exhibited linear elastic behavior until failure. Results of these longitudinal tensile tests are listed in Table 2.1-1. At RT, the measured elastic modulus of 23.87 Msi and ultimate strength of 391.27 ksi were in excellent agreement with the predicted modulus value of 25.8 Msi and strength value of 392 ksi. Also, these results indicate that the average elastic modulus value at each test temperature was 23.35 Msi (Std. Dev. 1.27) with a 5.4% coefficient of variation. Measured ultimate strength values at -150°F and RT were 391 and 389 ksi respectively, however at 250°F strength decreased to about 318 ksi. Measured strain to failure at RT was 1.6% and Poisson ratio was 0.26 - 0.33. Results of transverse tensile properties are listed in Table 2.1-2, indicating an average modulus of 1.4 Msi and 10.5 ksi strength.

(b) Compression

Longitudinal and transverse compressive properties of unidirectional IM7/PEEK are listed in Table 2.1-3 and 2.1-4 respectively. At room temperature, the average longitudinal modulus value was about 9% lower than the tensile modulus, and the ultimate compressive strength was nearly 40% of the tensile strength. The compressive stress-strain curves showed non-linear response beyond 0.3 - 0.4% strain level, with a typical strain to failure value of 1.35%. At 250°F measured compressive strength was 105 ksi compared to 146.8 ksi at RT and 163 ksi at -150°F.

Table 2.1-1 Longitudinal Tensile Properties of IM7/PEEK $[0]_8$ at Different Test Temperatures

(a) at -150°F

Specimen # (CK) (SU) (AP)	Elastic Modulus E_x^T (Msi)	Ultimate Tensile Strength (ksi)	Poisson Ratio ν_{xy}
TNL-1a	22.36	398.90	0.27
TNL-2a	22.73	394.30	0.30
TNL-3a	20.37	381.00	0.29
TNL-4	22.48	390.00	0.32
TNL-5	21.56	381.00	—
Mean Value	21.90	389.04	0.295
Std. Dev.	0.90	7.98	0.02
CV (%)	4.10	2.05	6.78

(b) at RT

Specimen # (CK) (SU) (AP)	Elastic Modulus E_x^T (Msi)	Ultimate Tensile Strength (ksi)	Poisson Ratio ν_{xy}
TNL-11	23.61	392.84	0.26
TNL-12	26.97	394.87	----
TNL-13	22.52	382.54	0.28
TNL-14	22.42	398.35	----
TNL-15	23.83	387.76	0.33
Mean Value	23.87	391.27	0.289
Std. Dev.	1.84	6.20	0.035
CV (%)	7.70	1.60	12.20

(c) at +250°F

Specimen # (CK) (SU) (AP)	Elastic Modulus E_x^T (Msi)	Ultimate Tensile Strength (ksi)	Poisson Ratio ν_{xy}
TNL-6	—	308.00	—
TNL-7	24.4	336.00	0.250
TNL-8	24.5	307.00	0.250
TNL-9	23.7	336.00	0.320
TNL-10	24.6	303.60	0.290
Mean Value	24.3	318.10	0.276
Std. Dev.	0.4	16.41	0.035
CV (%)	1.7	5.17	12.500

Table 2.1-2 Transverse Tensile Properties of IM7/PEEK $[0]_8$ at Different Test Temperatures

(a) at -150°F

Specimen # (CK) (SU) (AP)	Elastic Modulus E_y^T (Msi)	Ultimate Tensile Strength (ksi)	Poisson Ratio ν_{yx}
TNL-1	1.400	11.50	0.019
TNL-2	1.500	10.60	0.020
TNL-3	1.480	11.14	0.015
TNL-4	—	—	—
TNL-5	—	—	—
Mean Value	1.46	11.08	0.018
Std. Dev.	0.0530	0.45	0.003
CV (%)	3.600	4.06	14.400

(b) at RT

Specimen # (CK) (SU) (AP)	Elastic Modulus E_y^T (Msi)	Ultimate Tensile Strength (ksi)	Poisson Ratio ν_{yx}
TNL-11	—	—	—
TNL-12	—	—	—
TNL-13	1.3	10.9	0.020
TNL-14	1.5	11.1	0.020
TNL-15	1.3	11.1	0.020
Mean Value	1.4	10.5	0.020
Std. Dev.	0.1	1.20	0.000
CV (%)	8.5	11.30	0.000

(c) at +250°F

Specimen # (CK) (SU) (AP)	Elastic Modulus E_y^T (Msi)	Ultimate Tensile Strength (ksi)	Poisson Ratio ν_{yx}
TNL-6	1.10	8.90	0.020
TNL-7	1.20	8.91	0.016
TNL-8	—	—	—
TNL-9	1.20	9.20	0.012
TNL-10	1.20	9.10	0.016
Mean Value	1.18	9.03	0.016
Std. Dev.	0.05	0.147	0.003
CV (%)	4.24	1.63	18.700

Table 2.1-3 Longitudinal Compressive Properties of IM7/PEEK $[0]_8$

(a) at -150°F

Specimen # (CK) (SU) (AP)	Elastic Modulus E_x^C (Msi)	Ultimate Compressive Strength (ksi)	Poisson Ratio ν_{xy}
CML-1	23.25	163.8	0.420
CML-2	23.91	183.3	0.390
CML-3	20.19	161.1	0.350
CML-4	23.40	171.1	0.460
CML-5	21.89	138.4	0.390
Mean Value	22.53	163.6	0.402
Std. Dev.	1.50	16.5	0.041
CV (%)	6.70	10.1	10.200

(b) at RT

Specimen # (CK) (SU) (AP)	Elastic Modulus E_x^C (Msi)	Ultimate Compressive Strength (ksi)	Poisson Ratio ν_{xy}
CML-11	21.9	149.3	0.330
CML-12	22.9	140.6	0.340
CML-13	23.5	142.0	0.280
CML-14	22.7	152.6	0.330
CML-15	23.0	149.8	0.300
Mean Value	22.8	146.8	0.320
Std. Dev.	0.6	5.	0.030
CV (%)	2.5	3.60	8.300

(c) at +250°F

Specimen # (CK) (SU) (AP)	Elastic Modulus E_x^C (Msi)	Ultimate Compressive Strength (ksi)	Poisson Ratio ν_{xy}
CML-6	20.11	119.6	0.350
CML-7	24.50	123.6	0.320
CML-8	18.58	90.1	0.340
CML-9	19.68	107.6	0.330
CML-10	25.79	85.1	0.380
Mean Value	21.72	105.2	0.340
Std. Dev.	3.21	17.2	0.020
CV (%)	14.80	16.4	6.800

Table 2.1-4 Transverse Compressive Properties of IM7/PEEK $[0]_8$

(a) at -150°F

Specimen # (CK) (SU) (AP)	Elastic Modulus E_y^C (Msi)	Ultimate Compressive Strength (ksi)	Poisson Ratio ν_{yx}
CMT-1	1.62	25.44	0.008
CMT-2	1.60	29.93	0.010
CMT-3	1.30	23.05	0.009
CMT-4	1.14	24.48	0.010
CMT-5	1.41	26.38	0.007
Mean Value	1.41	25.86	0.009
Std. Dev.	0.20	2.59	0.001
CV (%)	14.10	10.00	14.400

(b) at RT

Specimen # (CK) (SU) (AP)	Elastic Modulus E_y^C (Msi)	Ultimate Compressive Strength (ksi)	Poisson Ratio ν_{yx}
CMT-11	—	—	—
CMT-12	1.2	14.4	0.007
CMT-13	1`.4	17.9	0.005
CMT-14	1.6	19.8	—
CMT-15	1.3	19.3	0.008
Mean Value	1.4	17.8	0.007
Std. Dev.	0.2	2.4	0.001
CV (%)	12.3	13.6	19.100

(c) at +250°F

Specimen # (CK) (SU) (AP)	Elastic Modulus E_y^C (Msi)	Ultimate Compressive Strength (ksi)	Poisson Ratio ν_{yx}
CMT-6	—	14.2	—
CMT-7	1.140	11.6	0.010
CMT-8	1.100	11.5	0.010
CMT-9	1.310	12.5	0.010
CMT-10	1.350	12.0	0.010
Mean Value	1.220	12.3	0.010
Std. Dev.	0.012	1.1	0.00
CV (%)	9.800	8.8	0.000

(c) Flexure

Longitudinal and transverse flexural modulus and strength values of unidirectional IM7/PEEK determined by 4-point bend tests are listed in Table 2.1-5. As expected, these results showed that the longitudinal flexural modulus (23.13 Msi) and strength (286.63 ksi) were significantly higher than the transverse flexural modulus (1.32 Msi) and strength (19.86 ksi) values.

Table 2.1-5 Four Point Bend Flexure Test Results of IM7/PEEK $[0]_8$ at RT

	Longitudinal Flexural			Transverse Flexural	
Specimen # (CK)(SU)(AP)	Modulus (Msi)	Strength (ksi)	Specimen # (CK)(SU)(AP)	Modulus (Msi)	Strength (ksi)
FXL-1	23.11	279.50	FXT-1	1.35	21.10
FXL-2	21.77	257.90	FXT-2	1.32	19.10
FXL-3	21.99	260.20	FXT-3	1.31	19.50
FXL-4	24.45	331.90	FXT-4	1.35	19.10
FXL-5	24.36	303.60	FXT-5	1.27	20.50
Mean	23.13	286.63	Mean	1.32	19.86
Std. Dev.	1.26	31.25	Std. Dev.	0.03	0.89
CV (%)	5.50	10.90	CV (%)	2.50	4.50

(d) Inplane Shear

Longitudinal and transverse shear modulus and strength values obtained by losipescu shear test method are listed in Table 2.1-6. These results indicate an average longitudinal shear modulus of 1.12, 1.08 and 0.80 Msi at RT, -150°F, and 250°F respectively. Based on these measurements, shear strength gradually decreased with increasing temperatures: 23.85 ksi at -150°F, 19.18 ksi at RT and 9.00 ksi at 250°F.

Table 2.1-6 Inplane Shear Properties of IM7/PEEK $[0]_8$

(a) at -150°F

Specimen # (CK)(SU)(AP)	Longitudinal Shear Modulus (Msi)	Longitudinal Shear Strength (ksi)	Specimen # (CK)(SU)(AP)	Transverse Shear Modulus (Msi)	Transverse Shear Strength (ksi)
IPL-1	1.08	24.02	IPT-1	0.73	17.46
IPL-2	1.34	25.00	IPT-2	0.88	17.50
IPL-3	0.95	23.38	IPT-3	0.78	16.17
IPL-4	0.93	23.02	IPT-4	0.74	14.86
IPL-5	—	—	IPT-5	—	—
Mean	1.08	23.85	Mean	0.78	16.49
Std. Dev.	0.19	0.87	Std. Dev.	0.068	1.25
CV (%)	17.60	3.60	CV (%)	8.70	7.58

(b) at RT

Specimen # (CK)(SU)(AP)	Longitudinal Shear Modulus (Msi)	Longitudinal Shear Strength (ksi)	Specimen # (CK)(SU)(AP)	Transverse Shear Modulus (Msi)	Transverse Shear Strength (ksi)
IPL-11	1.06	—	IPT-11	0.650	11.5
IPL-12	1.16	19.70	IPT-12	0.690	12.3
IPL-13	1.14	18.20	IPT-13	0.696	11.4
IPL-14	1.06	18.60	IPT-14	0.655	11.2
IPL-15	1.16	20.20	IPT-15	0.646	12.1
Mean	1.12	19.18	Mean	0.666	11.7
Std. Dev.	0.05	0.93	Std. Dev.	0.022	0.7
CV (%)	4.48	4.80	CV (%)	3 .300	5.6

(c) at 250°F

Specimen # (CK)(SU)(AP)	Longitudinal Shear Modulus (Msi)	Longitudinal Shear Strength (ksi)	Specimen # (CK)(SU)(AP)	Transverse Shear Modulus (Msi)	Transverse Shear Strength (ksi)
IPL-6	0.840	7.88	IPT-6	0.50	7.58
IPL-7	0.800	9.19	IPT-7	0.60	7.85
IPL-8	0.830	9.27	IPT-8	0.52	8.31
IPL-9	0.810	9.23	IPT-9	0.46	8.09
IPL-10	0.740	9.42	IPT-10	0.49	7.85
Mean	0.800	9.00	Mean	0.51	7.94
Std. Dev.	0.042	0.63	Std. Dev.	0.04	0.27
CV (%)	5.230	7.0	CV (%)	8.80	3.49

(e) Interlaminar Shear Strength

The apparent interlaminar shear strength values of unidirectional IM7/PEEK specimens determined by short beam shear (three point bend) tests are listed in Table 2.1-7. Optical microscopic examination of the 0.5-in. specimens indicated that failure was primarily interlaminar shear.

Table 2.1-7 Interlaminar Shear Strength of IM7/PEEK at RT

IM7/PEEK: Unidirectional $[0]_8$	
Specimen # (CK)(SU)(AP)	ILSS (ksi) Longitudinal)
IL-1	15.46
IL-2	15.26
IL-3	15.88
IL-4	15.19
IL-5	15.14
Mean	15.39
Std. Dev.	0.30
CV (%)	1.95

2.1.4 Thermophysical Properties

(a) Coefficient of Thermal Expansion

Thermal expansion response of IM7 $[0]_8$ specimens was determined by push-rod-dilatometer (PRD) method (Appendix B) in a heat-cool-heat cycle between -150° and 150°F. The thermal strain sensitivity of PRD method is about 10 ppm. For the first cycle, typical thermal expansion behavior of longitudinal and transverse specimens is shown in Figures 2.1-3 and 2.1-4 respectively. From this first cycle response, the average CTE was obtained as the slope of the

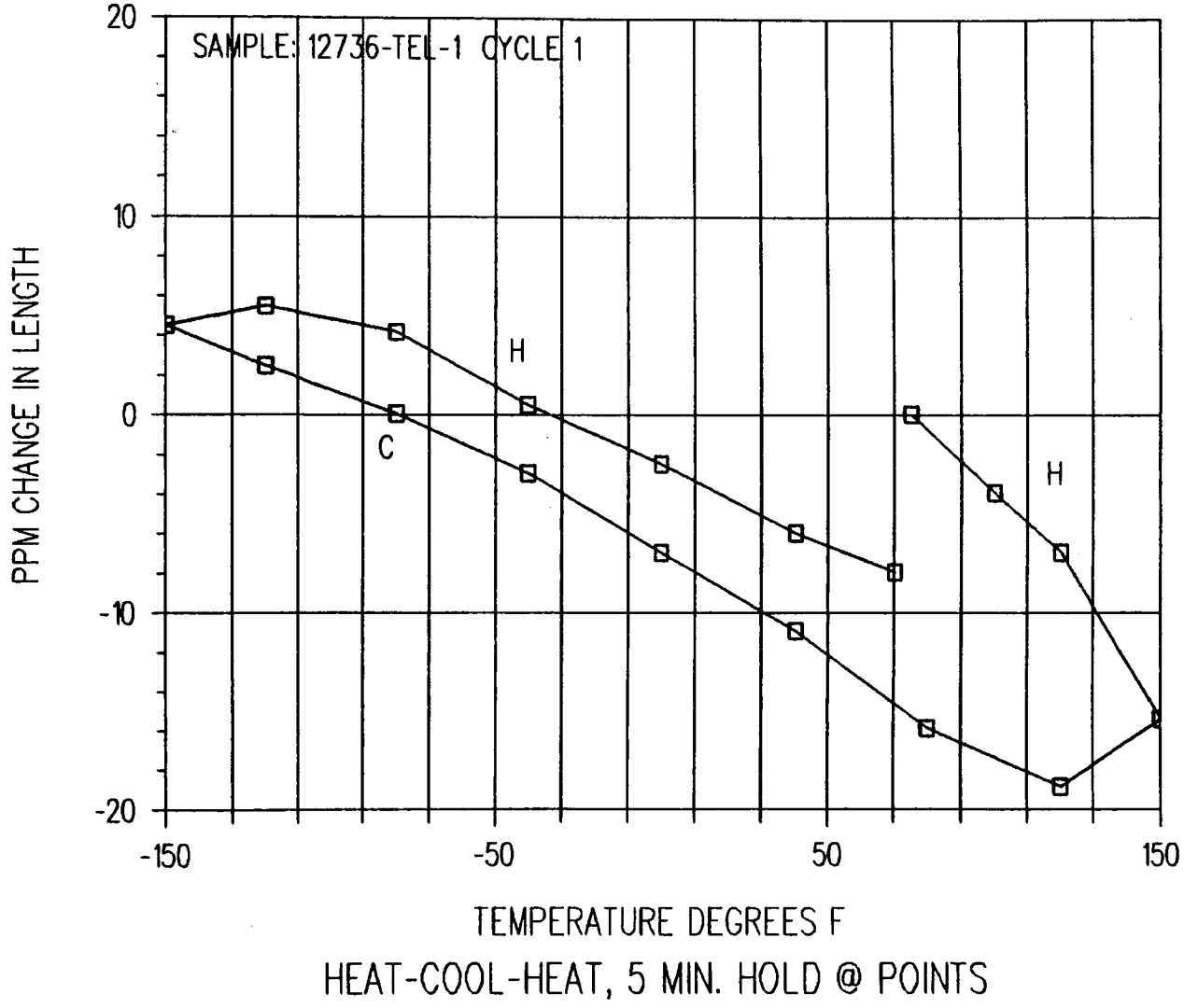

Figure 2.1-3 Longitudinal Thermal Expansion Response of IM7/PEEK $[0]_8$, v/o = 62.0%, Obtained With a Push Rod Diatometer

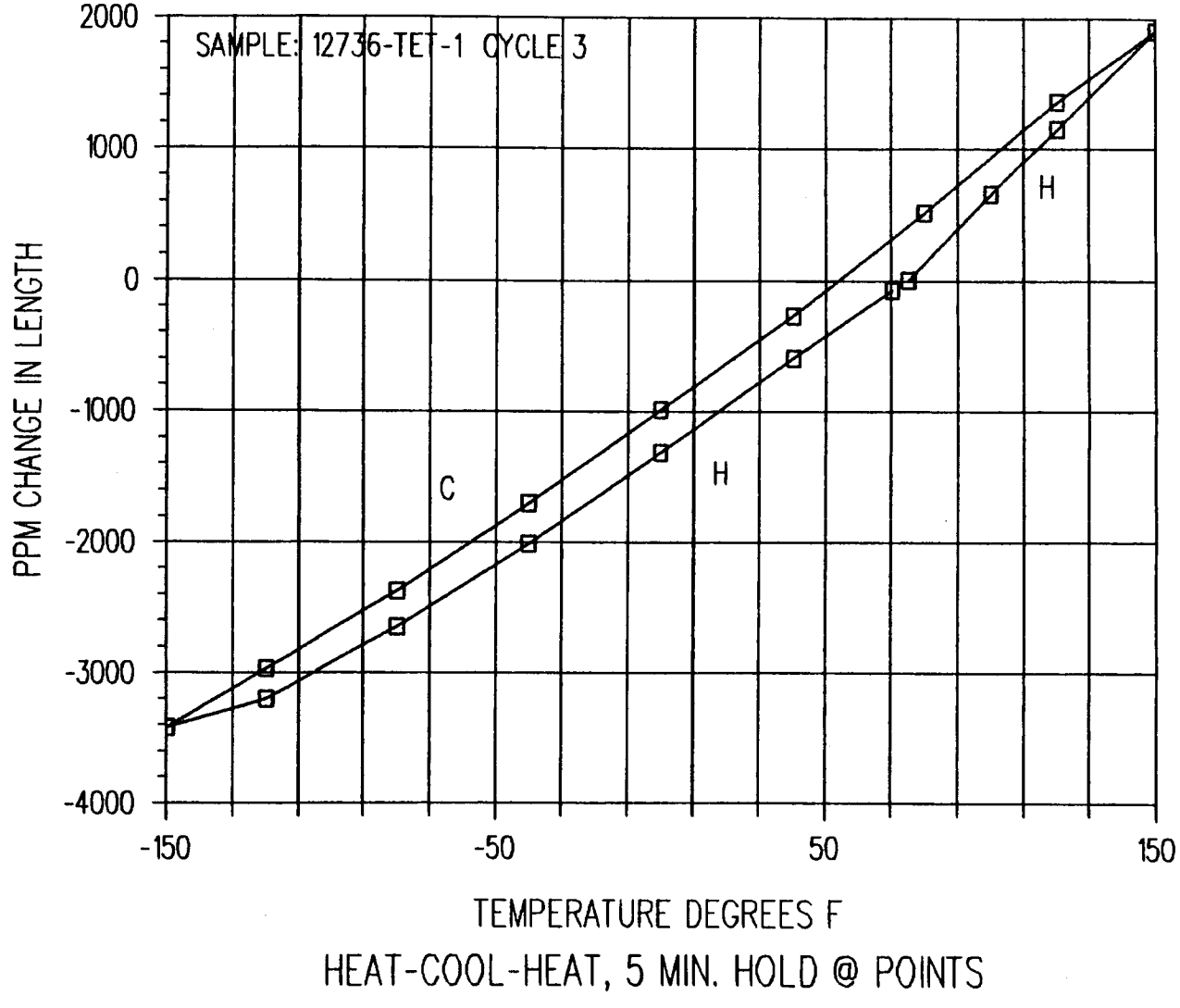

Figure 2.1-3 Transverse Thermal Expansion Response of IM7/PEEK $[0]_8$, v/o = 62.5%, Obtained With a Push Rod Diatometer

line connecting the strain values at temperature extremes (±150°F). The average longitudinal CTE value of -0.07 ppm/°F is in good agreement with the predicted value of -0.1 ppm/°F and measured transverse CTE value of 17.42 ppm/°F is in good agreement with the predicted value of 16.6 ppm°F. These CTE results are summarized below.

	Longitudinal $[0]_8$	Transverse $[0]_8$
CTE (ppm/°F)	-0.07	17.42
RT Hysteresis (ppm)	-15.92	613
Residual Strain (ppm)	-7.96	-255.78

(b) Specific Heat, Thermal Diffusivity and Thermal Conductivity

The thermophysical property test results of IM7/PEEK specimens for $[0]_8$ are listed in Table 2.1-8 (Longitudinal), Table 2.1-9 (Transverse) and Table 2.1-10 (through-the-thickness) respectively. The specific heat (Cp) values at different temperatures are as follows:

		Cp ($Ws\ gm^{-1}\ K^{-1}$)
IM7/PEEK $[0]_8$:	at RT	0.8230
	at -150°F	0.43
	at 250°F	1.1

For thermal conductivity tests, our experience has shown that Kohlrausch technique cannot be used for organic matrix composites because of the high electrical resistivity of constituent fiber and matrix. Therefore, diffusivity (D) and bulk density (ρ) measurements were made to calculate thermal conductivity (K) using the following relationship:

$$K = -D \cdot Cp \cdot \rho,$$

Test specimens were prepared for transverse, longitudinal, and through-the-thickness diffusivity measurements. The measured bulk density values (Table 2.1-8) obtained by weighing the

Table 2.1-8 Results of IM7/PEEK Thermophysical Property Test (Longitudinal)

Material	Temp. (C)	Density (gm/cm^{-3})	Specific Heat ($W\,s\,mg^{-1}K^{-1}$)	Diffusivity (cm^2sec^{-1})	Conduct-ivity ($W\,cm^{-1}K^{-1}$)	Conduct-ivity (BTU Units *)	Temp (F)
IM7/PEEK							
$[0]_8$	-150.0	1.549	0.2210	0.06620	0.02266	15.71	-238.0
$[0]_8$	-100.0	1.549	0.4300	0.05480	0.03650	25.31	-148.0
$[0]_8$	-50.0	1.549	0.6010	0.04720	0.04394	30.47	-58.0
$[0]_8$	0.0	1.549	0.7600	0.04230	0.04980	34.53	32.0
$[0]_8$	23.0	1.549	0.8230	0.04130	0.05265	36.50	73.4
$[0]_8$	75.0	1.549	0.9850	0.03950	0.06027	41.79	167.0
$[0]_8$	150.0	1.549	1.2390	0.03720	0.07139	49.50	302.0
$[0]_8$	225.0	1.549	1.4790	0.03550	0.08133	56.39	437.0
$[0]_8$	300.0	1.549	1.6570	0.03420	0.08778	60.86	572.0
$[0]_8$	350.0	1.549	1.8600**	0.03400	0.09796	67.92	662.0

Table 2.1-9 Results of IM7/PEEK Thermophysical Property Test (Transverse)

Material	Temp. (C)	Density (gm/cm^{-3})	Specific Heat ($W\,s\,mg^{-1}K^{-1}$)	Diffusivity (cm^2sec^{-1})	Conduct-ivity ($W\,cm^{-1}K^{-1}$)	Conduct-ivity (BTU Units *)	Temp (F)
IM7/PEEK							
$[0]_8$	-150.0	1.536	0.2210	0.00781	0.00265	1.84	-238.0
$[0]_8$	-100.0	1.536	0.4300	0.00672	0.00444	3.08	-148.0
$[0]_8$	-50.0	1.536	0.6010	0.00606	0.00559	3.88	-58.0
$[0]_8$	0.0	1.536	0.7600	0.00552	0.00644	4.47	32.0
$[0]_8$	23.0	1.536	0.8230	0.00525	0.00664	4.60	73.4
$[0]_8$	75.0	1.536	0.9850	0.00471	0.00713	4.94	167.0
$[0]_8$	150.0	1.536	1.2390	0.00437	0.00832	5.77	302.0
$[0]_8$	225.0	1.536	1.4790	0.00394	0.00895	6.21	437.0
$[0]_8$	300.0	1.536	1.6570	0.00365	0.00929	6.44	572.0
$[0]_8$	350.0	1.536	1.8600	0.00361	0.01031	7.15	662.0

Table 2.1-10 Results of IM7/PEEK Thermophysical Property Test (Through-the-Thickness)

Material	Temp. (C)	Density (gm/cm^{-3})	Specific Heat ($W\,s\,mg^{-1}K^{-1}$)	Diffusivity (cm^2sec^{-1})	Conduct-ivity ($W\,cm^{-1}K^{-1}$)	Conduct-ivity (BTU Units *)	Temp (F)
IM7/PEEK							
$[0]_8$	-150.0	1.579	0.2210	0.00802	0.00280	1.94	-238.0
$[0]_8$	-100.0	1.579	0.4300	0.00680	0.00462	3.20	-148.0
$[0]_8$	-50.0	1.579	0.6010	0.00584	0.00554	3.84	-58.0
$[0]_8$	0.0	1.579	0.7600	0.00558	0.00670	4.64	32.0
$[0]_8$	23.0	1.579	0.8230	0.00532	0.00691	4.79	73.4
$[0]_8$	75.0	1.579	0.9850	0.00497	0.00773	5.36	167.0
$[0]_8$	150.0	1.579	1.2390	0.00447	0.00875	6.06	302.0
$[0]_8$	225.0	1.579	1.4790	0.00396	0.00925	6.41	437.0
$[0]_8$	300.0	1.579	1.6570	0.00356	0.00931	6.46	572.0
$[0]_8$	350.0	1.579	1.8600 **	0.00340	0.00999	6.92	662.0

specimens of known geometry are about two percent lower than the values obtained by ASTM D-792, based on Archimedes principle.

Measured thermal conductivity values as listed in Tables 2.1-8 to 2.1-10 show an increase in conductivity with the increasing temperature for IM7/PEEK. Also, the longitudinal thermal conductivity value of 0.0526 W/cm-K (at RT) is significantly lower than the 0.91 W/cm-K value for unidirectional P75/1962 Epoxy composite because P75 fiber has significantly higher thermal conductivity compared to IM7 fiber. The thermal conductivity values at different temperatures are as follows:

	K_L	K_T	K_Z
IM7/PEEK $[0]_8$		(W/cm-K)	(W/cm-K)
At RT	0.0526	0.0066	0.0069
-150°F	0.0365	0.0044	0.0046
250°F	0.0655	0.0077	0.0082

(c) Optical Properties

Solar Absorptance:	0.91
I.R. Emittance:	0.77

Reflectance vs. wavelength plot - for the as-consolidated $[0]_8$ plate surface the percent reflectance spectra from 2.0 - 14.0 microns is shown in Figure 2.1-5. For example, at 10.6 μm the reflectance value of 0.23 (23%) suggested the emittance value of 0.77; consistent with the normal emittance value obtained from Gier-Dunkel model DE-100.

Figure 2.1-5 FTIR Reflectance Spectra of $[0]_8$ IM7/PEEK

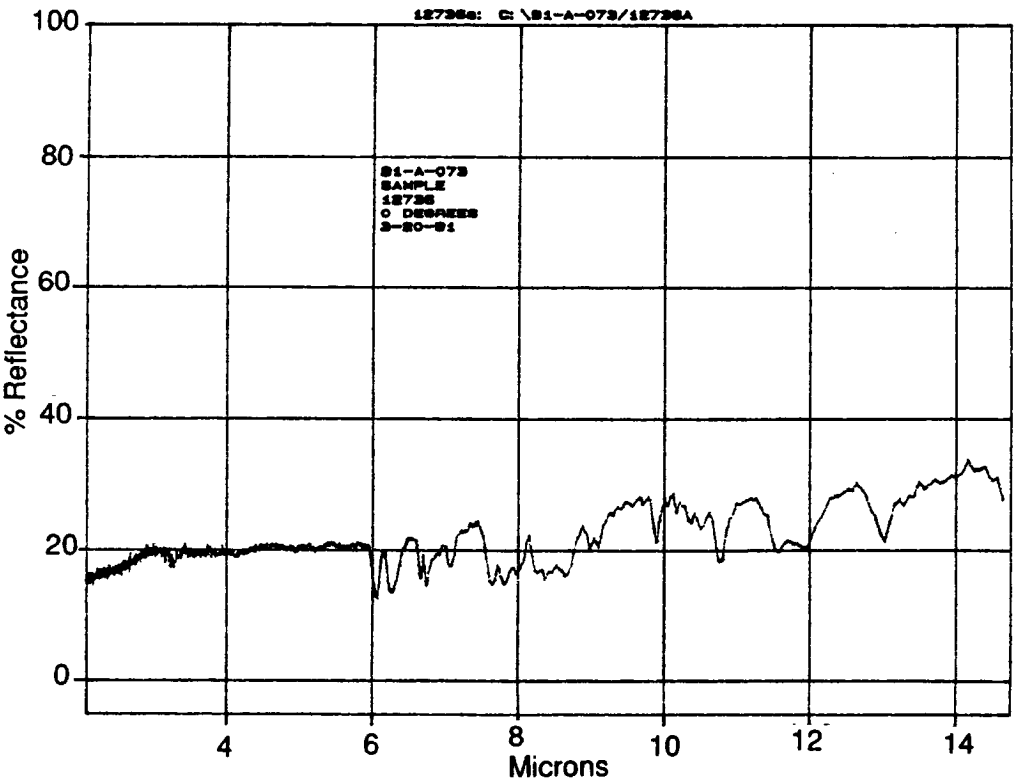

2.2 IM7/PEEK $[0, \pm 45,90]_S$ AND $[\pm 30, 0_4]_S$ FLAT PANELS

2.2.1 Fabrication Data

Material system:	IM7/PEEK(IM7/APC2)	IM7/PEEK(IM7/APC2)
Fiber Layup:	$[0, \pm 45,90]_S$	$[\pm 30, 0_4]_S$
Process:	ICI-Fiberite autoclave cycle C-29. All panels were consolidated in a platen press at 735°F under an applied pressure of 100 psi for 20 min. The panels were cooled down at ≥ 13°F/minute while the 100 psi pressure was maintained until below 200°F. Full vacuum was maintained throughout consolidation cycle.	
Condition:	As-fabricated	As-fabricated
Dimensions:	12-in. x 12-in. x 0.040-in.	12-in. x 12-in. x 0.060-in.
Ply Thickness:	0.005-in.	0.005-in.
Prepeg Batch No.:	N89-0032	N89-0032
Fiberite Code No.:	12737 P1-P5	12738 P1-P5
Martin Marietta ID#:	(CK)(SQ)(AP)	(CK)(SZ)(AP)

2.2.2 Product Evaluation

(a) Density

- IM7/PEEK $[0, \pm 45, 90]_S$ and $[\pm 30, 0_4]_S$

IM7 Fiber: 0.0643 lb/in^3 (1.78 gm/cm^3)

PEEK: 0.046 lb/in^3 (1.27 gm/cm^3)

IM7/PEEK: 0.0569 lb/in^3 (1.575 gm/cm^3)

(b) Fiber Volume

- IM7/PEEK $[0, \pm 45, 90]_S$: 62.0%

  Std. Dev.: 0.7

  Void Volume: ≤0.5%

- IM7/PEEK $[\pm 30, 0_4]_S$: 62.0%

  Std. Dev.: 0.8

  Void Volume: ≤0.5%

(c) Non-Destructive Evaluation

Visual, X-radiographic and ultrasonic techniques were used to inspect all IM7/PEEK $[0, \pm 45, 90]_S$ and $[\pm 30, 0_4]_S$ flat panels. Each panel appeared to be of good quality without any surface imperfections. X-radiographic inspection examination revealed that fiber collimation was excellent. Ultrasonic C-scan (Figure 2.2-1)showed no major defect such as cracks or delaminations except a few air-bubble sites on the entire panel.

(d) Microstructure

Longitudinal and transverse photomicrographs of $[0, \pm 45, 90]_S$ and $[\pm 30, 0_4]_S$ IM7/PEEK specimens are shown in Figure 2.2-2 (a, b) and 2.2-3 (a, b) respectively. Each photomicrograph revealed nearly uniform fiber-matrix distribution with a few localized microvoids. Microstructural examination at different locations of the panel did not reveal any microcracks or large voids.

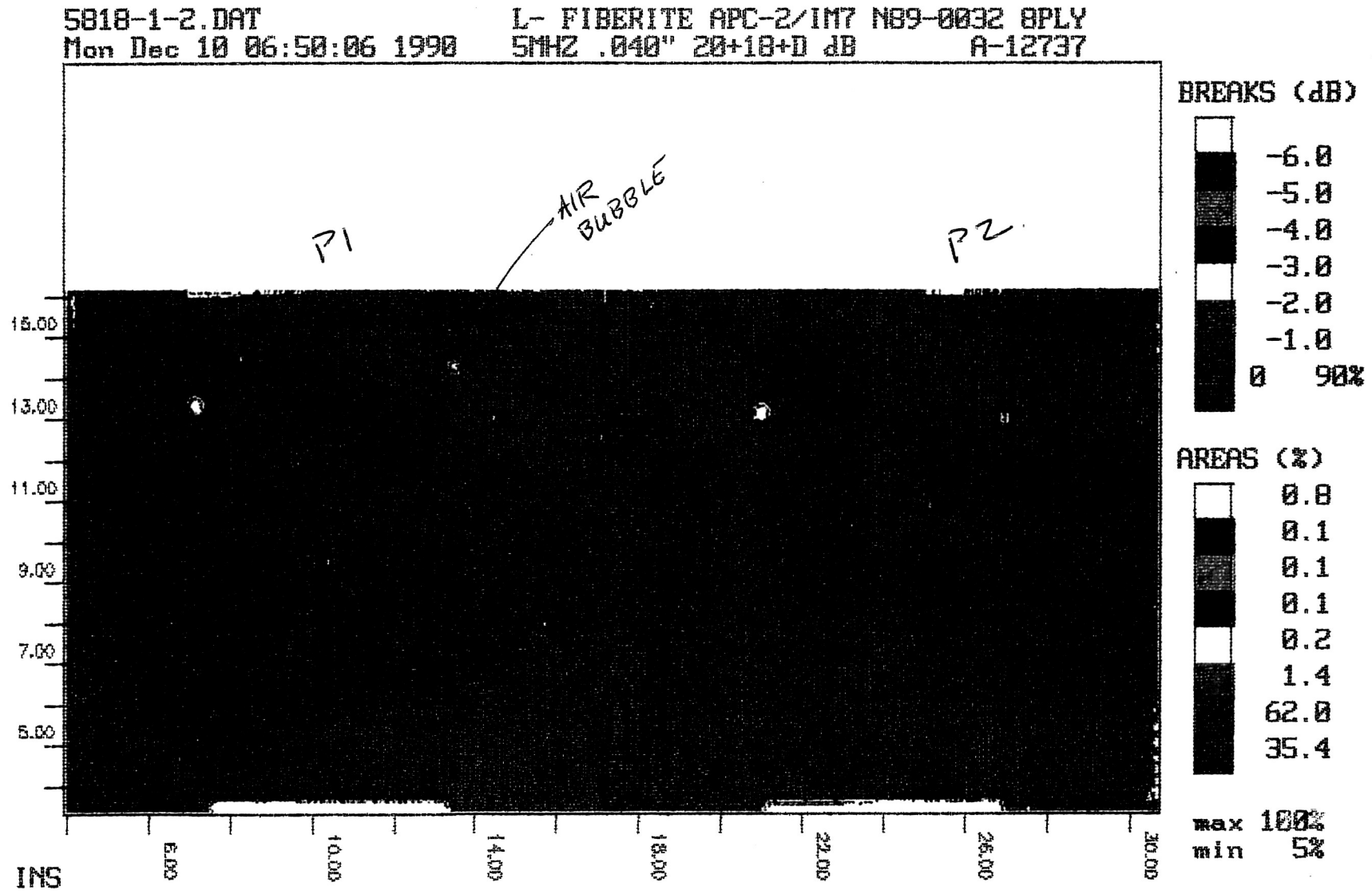

Figure 2.2-1 Ultrasonic C-Scan of IM7/PEEK [0, ±45, 90]$_s$

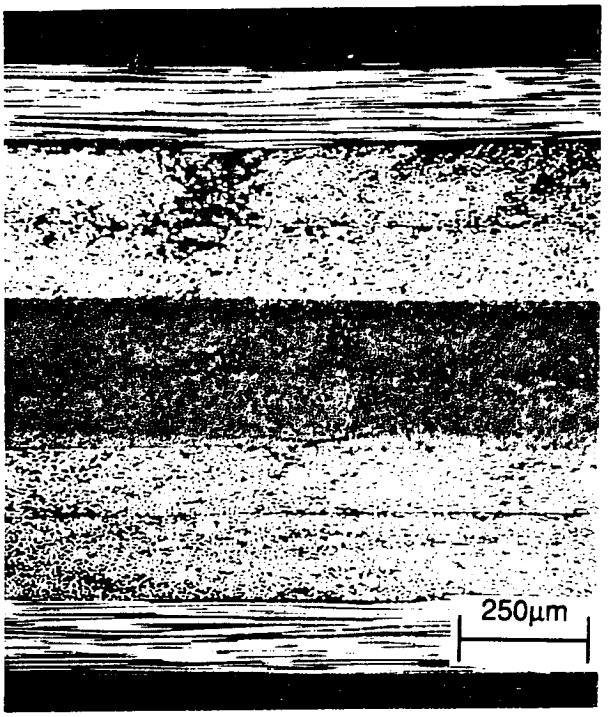

(a) Longitudinal

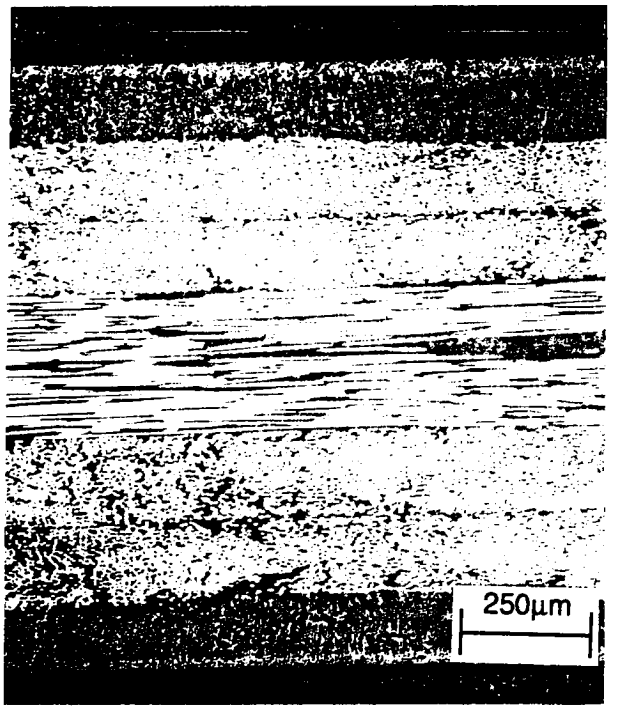

(b) Transverse

Figure 2.2-2 Longitudinal and Transverse Micrographs of Quasi-Isotropic $[0, \pm 45, 90]_s$ IM7/PEEK Laminate Showing Uniform Fiber Distribution and No Defects Such as Microvoids and Disbonds

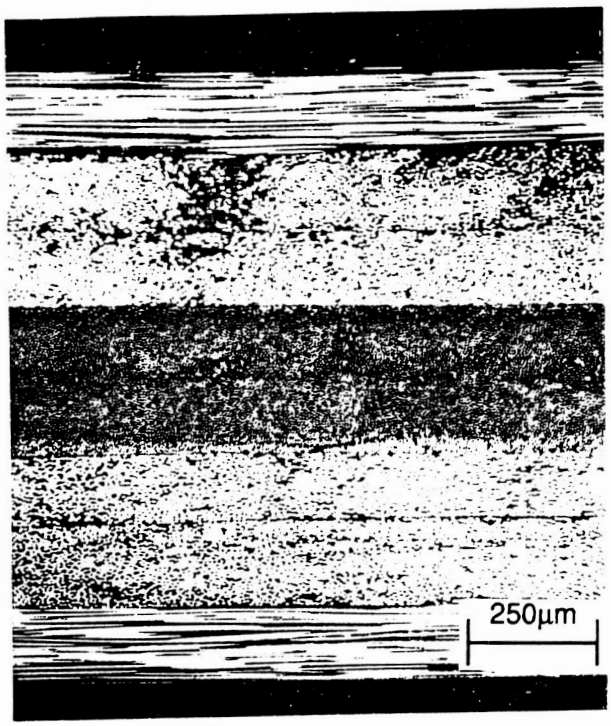

(a) Longitudinal

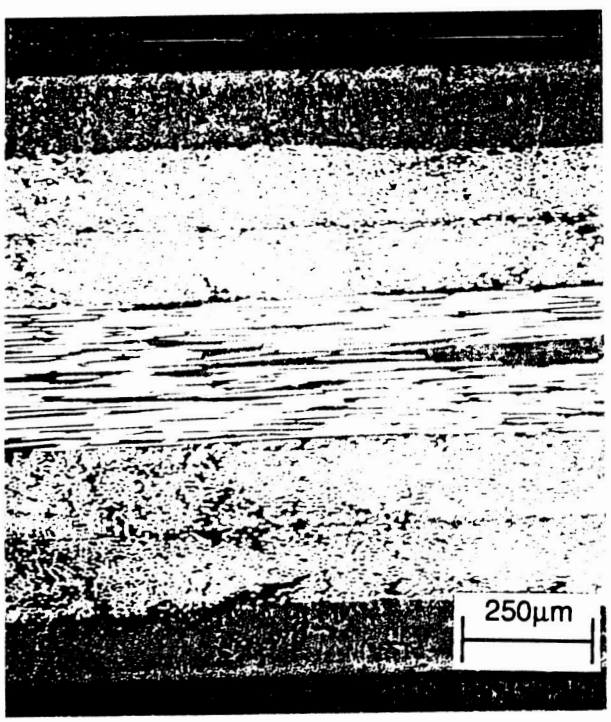

(b) Transverse

Figure 2.2-2 Longitudinal and Transverse Micrographs of Quasi-Isotropic $[0, \pm 45, 90]_s$ IM7/PEEK Laminate Showing Uniform Fiber Distribution and No Defects Such as Microvoids and Disbonds

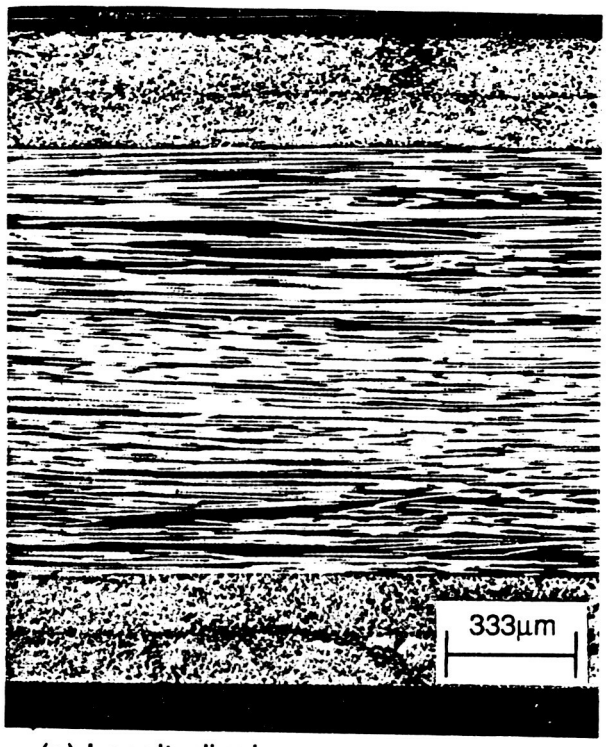

(a) Longitudinal

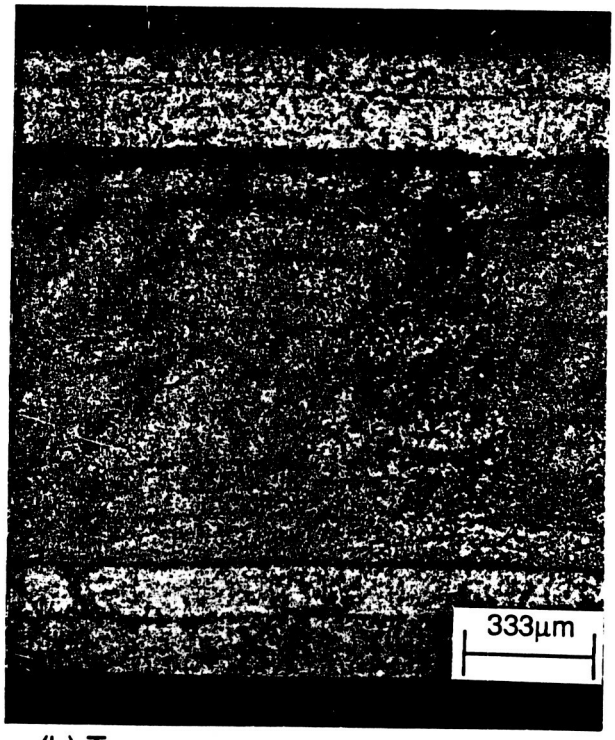

(b) Transverse

Figure 2.2-3 Longitudinal and Transverse Micrographs of $[\pm 30, 0_4]_s$ IM7/PEEK Laminate Revealing Uniform Fiber Distribution Without Any Defects in Different Plies

2.2.3 Mechanical Properties

(a) Tension

Table 2.2-1 and 2.2-2 list the longitudinal and transverse tension properties respectively of $[0, \pm 45, 90]_s$ laminate, and Tables 2.2-3 and 2.2-4 list the longitudinal and transverse tensile properties of $[\pm 30, 0_4]_s$ laminate. During these tests, each specimen exhibited nearly linear elastic response up to about 90 ±5% of the failure stress. For both the laminates, the measured elastic modulus and strength values are consistent with the predicted values. For example, in the case of quasi-isotropic laminate measured strength of 134.8 ksi is in excellent agreement with the predicted value of 134 ksi; although the measured modulus of 7.3 Msi is somewhat lower than the predicted modulus value of 9.4 Msi. The $[0, \pm 45, 90]_s$ laminate exhibited the nearly isotropic response at each test temperatures. Also, in the case of $[\pm 30, 0_4]_s$, the measured modulus of 18.1 Msi was close to the predicted value of 19.8 Msi, and measured strength of 297.4 ksi was 98% of the predicted strength value of 303 ksi. Like unidirectional composite, the tensile modulus values at different test temperatures were nearly identical and the strength values at 250°F were lower than the values obtained at -150°F and RTO.

(b) Compression

Longitudinal and transverse compressive properties of IM7/PEEK $[0, \pm 45, 90]_s$ and $[\pm 30, 0_4]_s$ laminate are listed in Tables 2.2-5 to 2.2-8. Based on these results the compressive modulus values at different temperatures were nearly identical and about 95% of the tensile modulus values. The compressive strength values were about 45% of the tensile strength values, and generally decreased with the increasing temperature; e.g., for IM7/PEEK $[0, \pm 45, 90]_s$ compressive strength 96.85 ksi at -150°F, 67.7 ksi at RT, and 55.06 ksi at 250°F.

Table 2.2-1 Longitudinal Tensile Properties of IM7/PEEK $[0, \pm 45, 90]_s$

(a) at -150°F

Specimen # (CK) (SQ) (AP)	Elastic Modulus E_x^T (Msi)	Ultimate Tensile Strength (ksi)	Poisson Ratio ν_{xy}
TNL-1	6.89	128.18	0.310
TNL-2	6.94	130.23	0.290
TNL-3	7.69	134.49	0.270
TNL-4	—	—	—
TNL-5	—	—	—
Mean Value	7.17	130.97	0.290
Std. Dev.	0.45	3.21	0.020
CV (%)	6.27	2.45	6.900

(b) at RT

Specimen # (CK) (SQ) (AP)	Elastic Modulus E_x^T (Msi)	Ultimate Tensile Strength (ksi)	Poisson Ratio ν_{xy}
TNL-11	—	—	—
TNL-12	—	—	—
TNL-13	7.4	130.2	0.260
TNL-14	7.3	129.2	0.290
TNL-15	7.3	131.6	0.330
Mean Value	7.3	130.3	0.291
Std. Dev.	0.0	1.2	0.034
CV (%)	0.5	0.9	11.800

(c) at +250°F

Specimen # (CK) (SQ) (AP)	Elastic Modulus E_x^T (Msi)	Ultimate Tensile Strength (ksi)	Poisson Ratio ν_{xy}
TNL-6	7.29	119.1	0.330
TNL-7	7.56	115.2	0.330
TNL-8	7.07	119.5	0.310
TNL-9	7.43	104.0	0.330
TNL-10	6.96	—	0.350
Mean Value	7.26	114.5	0.331
Std. Dev.	0.25	7.2	0.013
CV (%)	3.40	6.3	4.000

Table 2.2-2 Transverse Tensile Properties of IM7/PEEK $[0, \pm 45, 90]_S$

(a) at -150°F

Specimen # (CK) (SQ) (AP)	Elastic Modulus E_y^T (Msi)	Ultimate Tensile Strength (ksi)	Poisson Ratio ν_{yx}
TNT-1	8.03	129.40	0.330
TNT-2	7.28	145.00	0.290
TNT-3	7.51	152.00	0.320
TNT-4	7.21	150.80	—
TNT-5	7.84	150.40	—
Mean Value	7.57	145.44	0.310
Std. Dev.	0.35	9.35	0.021
CV (%)	4.60	6.43	6.780

(b) at RT

Specimen # (CK) (SQ) (AP)	Elastic Modulus E_y^T (Msi)	Ultimate Tensile Strength (ksi)	Poisson Ratio ν_{yx}
TNT-11	8.32	131.10	0.360
TNT-12	7.54	138.97	0.338
TNT-13	7.27	122.00	0.313
TNT-14	7.65	136.90	0.314
TNT-15	7.77	145.03	—
Mean Value	7.71	134.80	0.334
Std. Dev.	0.39	8.70	0.020
CV (%)	5.06	6.45	6.000

(c) at +150°F

Specimen # (CK) (SQ) (AP)	Elastic Modulus E_y^T (Msi)	Ultimate Tensile Strength (ksi)	Poisson Ratio ν_{yx}
TNT-6	8.20	118.7	0.300
TNT-7	6.50	120.8	0.280
TNT-8	7.60	126.4	0.340
TNT-9	7.10	119.0	0.320
TNT-10	7.10	97.1	0.290
Mean Value	7.30	116.4	0.310
Std. Dev.	0.64	11.2	0.024
CV (%)	8.70	9.6	7.770

Table 2.2-3 Longitudinal Tensile Properties of IM7/PEEK [±30, 0_4]$_S$

(a) at -150°F

Specimen # (CK) (SZ) (AP)	Elastic Modulus E_x^T (Msi)	Ultimate Tensile Strength (ksi)	Poisson Ratio ν_{xy}
TNL-1	16.93	298.0	1.090
TNL-2	17.80	303.2	0.950
TNL-3	—	—	—
TNL-4	17.44	311.1	1.200
TNL-5	17.12	305.5	1.110
Mean Value	17.32	304.4	1.090
Std. Dev.	0.38	5.43	0.100
CV (%)	2.20	1.78	9.450

(b) at RT

Specimen # (CK) (SZ) (AP)	Elastic Modulus E_x^T (Msi)	Ultimate Tensile Strength (ksi)	Poisson Ratio ν_{xy}
TNL-11	18.3	—	1.030
TNL-12	18.0	—	0.970
TNL-13	17.9	305.3	1.040
TNL-14	17.8	295.1	1.000
TNL-15	18.4	291.8	1.000
Mean Value	18.1	297.4	1.020
Std. Dev.	0.3	7.04	0.033
CV (%)	1.5	2.3	3.300

(c) at +250°F

Specimen # (CK) (SZ) (AP)	Elastic Modulus E_x^T (Msi)	Ultimate Tensile Strength (ksi)	Poisson Ratio ν_{xy}
TNL-6	18.48	222.5	1.090
TNL-7	18.95	252.9	1.140
TNL-8	19.12	244.9	1.110
TNL-9	17.59	242.2	0.950
TNL-10	19.92	230.9	1.200
Mean Value	18.81	238.7	1.099
Std. Dev.	0.86	12.0	0.095
CV (%)	4.60	5.0	8.700

Table 2.2-4 Transverse Tensile Properties of IM7/PEEK $[\pm 30, 0_4]_s$

(a) at -150°F

Specimen # (CK) (SZ) (AP)	Elastic Modulus E_y^T (Msi)	Ultimate Tensile Strength (ksi)	Poisson Ratio ν_{yx}
TNT-1	1.690	15.35	0.072
TNT-2	1.690	15.54	0.078
TNT-3	1.700	14.88	0.086
TNT-4	1.700	16.04	0.082
TNT-5	1.670	16.05	0.081
Mean Value	1.690	15.57	0.080
Std. Dev.	0.012	0.49	0.005
CV (%)	0.700	3.14	6.200

(b) at RT

Specimen # (CK) (SZ) (AP)	Elastic Modulus E_y^T (Msi)	Ultimate Tensile Strength (ksi)	Poisson Ratio ν_{yx}
TNT-11	1.600	15.66	0.084
TNT-12	1.636	14.92	0.084
TNT-13	1.561	14.50	0.083
TNT-14	1.686	14.34	0.083
TNT-15	1.630	14.18	0.087
Mean Value	1.623	14.72	0.0842
Std. Dev.	0.046	0.59	0.0016
CV (%)	2.800	4.00	1.900

(c) at +150°F

Specimen # (CK) (SZ (AP)	Elastic Modulus E_y^T (Msi)	Ultimate Tensile Strength (ksi)	Poisson Ratio ν_{yx}
TNT-6	1.28	12.5	0.090
TNT-7	—	—	—
TNT-8	1.15	12.9	0.090
TNT-9	1.19	13.4	0.080
TNT-10	0.96	11.5	0.110
Mean Value	1.15	12.6	0.093
Std. Dev.	0.14	0.8	0.011
CV (%)	11.90	6.5	11.600

Table 2.2-5 Longitudinal Compressive Properties of IM7/PEEK [0, ±45, 90]$_S$

(a) at -150°F

Specimen # (CK) (SQ) (AP)	Elastic Modulus E_x^C (Msi)	Ultimate Compressive Strength (ksi)	Poisson Ratio ν_{xy}
CML-1	9.43	106.00	0.340
CML-2	8.80	91.32	0.300
CML-3	10.54	96.77	0.290
CML-4	9.67	106.16	0.260
CML-5	7.23	84.01	0.330
Mean Value	9.13	96.85	0.304
Std. Dev.	1.23	9.56	0.030
CV (%)	13.47	9.87	9.870

(b) at RT

Specimen # (CK) (SQ) (AP)	Elastic Modulus E_x^C (Msi)	Ultimate Compressive Strength (ksi)	Poisson Ratio ν_{xy}
CML-11	6.9	60.8	0.290
CML-12	7.6	70.5	0.290
CML-13	7.1	70.9	0.310
CML-14	7.1	63.1	0.360
CML-15	7.1	73.3	0.250
Mean Value	7.1	67.7	0.300
Std. Dev.	0.3	5.4	0.040
CV (%)	3.7	8.0	13.600

(c) at +250°F

Specimen # (CK) (SQ) (AP)	Elastic Modulus E_x^C (Msi)	Ultimate Compressive Strength (ksi)	Poisson Ratio ν_{xy}
CML-6	9.42	49.55	0.330
CML-7	9.74	60.96	0.340
CML-8	6.50	49.55	0.360
CML-9	6.19	56.73	0.320
CML-10	6.66	58.49	0.290
Mean Value	7.70	55.06	0.330
Std. Dev.	1.72	5.20	0.026
CV (%)	22.13	9.44	7.880

Table 2.2-6 Transverse Compressive Properties of IM7/PEEK [0, ±45, 90]$_s$

(a) at -150°F

Specimen # (CK) (SQ) (AP)	Elastic Modulus E_y^C (Msi)	Ultimate Compressive Strength (ksi)	Poisson Ratio ν_{yx}
CMT-1	9.63	64.41	0.230
CMT-2	8.61	66.58	0.290
CMT-3	8.80	63.08	0.310
CMT-4	—	55.51	0.300
CMT-5	8.91	56.68	0.350
Mean Value	8.98	61.25	0.296
Std. Dev.	0.445	4.89	0.043
CV (%)	4.95	7.98	14.500

(b) at RT

Specimen # (CK) (SQ) (AP)	Elastic Modulus E_y^C (Msi)	Ultimate Compressive Strength (ksi)	Poisson Ratio ν_{yx}
CMT-11	9.48	51.5	0.29
CMT-12	8.26	53.2	0.30
CMT-13	11.0	47.9	0.31
CMT-14	8.26	48.0	0.35
CMT-15	9.80	44.6	0.30
Mean Value	9.36	49.0	0.31
Std. Dev.	1.15	3.3	0.023
CV (%)	1.15	6.8	7.4

(c) at +250°F

Specimen # (CK) (SQ (AP)	Elastic Modulus E_y^C (Msi)	Ultimate Compressive Strength (ksi)	Poisson Ratio ν_{yx}
CMT-6	11.03	36.5	0.390
CMT-7	9.79	43.8	0.380
CMT-8	7.12	39.6	0.260
CMT-9	6.99	44.3	0.280
CMT-10	8.63	30.7	0.330
Mean Value	8.71	39.0	0.330
Std. Dev.	1.74	5.6	0.060
CV (%)	19.90	14.5	17.200

Table 2.2-7 Longitudinal Compressive Properties of IM7/PEEK $[\pm 30, 0_4]_s$

(a) at -150°F

Specimen # (CK) (SZ) (AP)	Elastic Modulus E_x^C (Msi)	Ultimate Compressive Strength (ksi)	Poisson Ratio ν_{xy}
CML-1	16.50	164.75	0.720
CML-2	16.34	145.35	0.830
CML-3	—	155.10	—
CML-4	—	162.80	—
CML-5	16.33	143.00	0.750
Mean Value	16.39	154.20	0.790
Std. Dev.	0.095	9.87	0.06
CV (%)	0.56	6.40	7.60

(b) at RT

Specimen # (CK) (SZ) (AP)	Elastic Modulus E_x^C (Msi)	Ultimate Compressive Strength (ksi)	Poisson Ratio ν_{xy}
CML-11	15.6	121.2	0.83
CML-12	15.3	120.1	0.81
CML-13	19.3	132.7	0.84
CML-14	20.4	140.6	0.82
CML-15	15.5	123.6	0.91
Mean Value	17.2	127.6	0.84
Std. Dev.	2.4	8.8	0.04
CV (%)	14.2	6.9	4.60

(c) at +250°F

Specimen # (CK) (SZ) (AP)	Elastic Modulus E_x^C (Msi)	Ultimate Compressive Strength (ksi)	Poisson Ratio ν_{xy}
CML-6	16.24	113.29	0.940
CML-7	15.70	122.76	0.880
CML-8	15.60	99.38	0.860
CML-9	16.20	96.49	0.850
CML-10	—	100.00	0.900
Mean Value	15.94	106.38	0.880
Std. Dev.	0.33	11.22	0.036
CV (%)	2.07	10.56	4.060

Table 2.2-8 Transverse Compressive Properties of IM7/PEEK $[\pm 30, 0_4]_s$

(a) at -150°F

Specimen # (CK) (SZ) (AP)	Elastic Modulus E_y^C (Msi)	Ultimate Compressive Strength (ksi)	Poisson Ratio ν_{yx}
CMT-1	2.09	40.56	0.180
CMT-2	1.87	40.93	0.130
CMT-3	1.95	35.26	0.110
CMT-4	2.08	35.78	0.130
CMT-5	—	—	—
Mean Value	2.00	38.13	0.140
Std. Dev.	0.10	3.02	0.030
CV (%)	5.00	7.92	21.40

(b) at RT

Specimen # (CK) (SZ) (AP)	Elastic Modulus E_y^C (Msi)	Ultimate Compressive Strength (ksi)	Poisson Ratio ν_{yx}
CMT-11	1.9	22.8	0.100
CMT-12	1.7	21.4	0.100
CMT-13	2.0	23.5	0.090
CMT-14	1.8	23.2	0.120
CMT-15	1.9	23.9	—
Mean Value	1.9	23.0	0.10
Std. Dev.	0.1	1.0	0.01
CV (%)	5.5	4.2	10.00

(c) at +250°F

Specimen # (CK) (SZ) (AP)	Elastic Modulus E_y^C (Msi)	Ultimate Compressive Strength (ksi)	Poisson Ratio ν_{yx}
CMT-6	1.33	19.7	0.110
CMT-7	1.53	17.6	0.090
CMT-8	1.40	18.5	0.100
CMT-9	1.38	19.0	0.120
CMT-10	1.40	19.8	0.110
Mean Value	1.41	18.9	0.100
Std. Dev.	0.07	0.9	0.010
CV (%)	5.20	4.9	10.00

(c) Flexure

Flexural modulus and strength values for the IM7/PEEK $[0, \pm 45, 90]_s$ and $[\pm 30, 0_4]_s$ specimens using four point bend tests are listed in Table 2.2-9. The flexural modulus of highly anisotropic laminates is a critical function of ply stacking sequence and does not necessarily correlate with the tensile modulus. During this test, the load deflection response is primarily influenced by the outermost lamina subjected to a tensile stress state. Therefore, the longitudinal flexural modulus of $[0, \pm 45, 90]_s$ specimen with the outermost [0] ply was higher than the transverse modulus with a [90°] outer ply.

(d) In-Plane Shear

Iosipescu shear test results of $[0, \pm 45, 90]_s$ and $[\pm 30, 0_4]_s$ laminates at different temperatures are listed in Tables 2.2-10 and 2.2-11 respectively. The $[0, \pm 45, 90]_s$ laminate exhibited a nearly isotropic response with longitudinal and transverse shear modulus value of 2.70 Msi and 2.43 Msi respectively. These test results also indicate that shear strength decreased with the increasing temperature whereas the shear modulus remained nearly identical:

	Shear Modulus (Msi) @			Shear Strength (ksi) @		
IM7/PEEK	-150°F	RT	250°F	-150°F	RT	250°F
$[0, \pm 45, 90]_s$	2.90	2.70	2.46	44.72	45.20	33.10
$[\pm 30, 0_4]_s$	2.04	1.93	1.81	36.30	34.60	25.70

(e) Interlaminar Shear Strength (ILSS)

The apparent interlaminar shear strength of $[0, \pm 45, 90]_s$, and $[\pm 30, 0_4]_s$ IM7/PEEK specimens are listed in Table 2.2-12.

Table 2.2-9 Flexural Properties of IM7/PEEK (a) $[0, \pm 45, 90]_s$ and (b) $[\pm 30, 0_4]_s$ at RT

(a)

Specimen # (CK)(SQ)(AP)	Longitudinal Flexural Modulus (Msi)	Longitudinal Flexural Strength (ksi)	Specimen # (CK)(SQ)(AP)	Transverse Flexural Modulus (Msi)	Transverse Flexural Strength (ksi)
FXL-1	13.7	165.40	FXT-1	3.2	47.1
FXL-2	13.1	135.60	FXT-2	2.5	35.5
FXL-3	13.1	180.10	FXT-3	2.8	40.9
FXL-4	13.4	138.60	FXT-4	3.1	44.1
FXL-5	14.0	148.20	FXT-5	3.4	50.8
Mean	13.5	153.60	Mean	3.0	43.7
Std. Dev.	0.4	18.84	Std. Dev.	0.4	5.9
CV (%)	3.1	12.30	CV (%)	12.2	13.4

(b)

Specimen # (CK)(SZ)(AP)	Longitudinal Flexural Modulus (Msi)	Longitudinal Flexural Strength (ksi)	Specimen # (CK)(SZ)(AP)	Transverse Flexural Modulus (Msi)	Transverse Flexural Strength (ksi)
FXL-1	11.35	170.0	FXT-1	2.1	26.0
FXL-2	11.82	168.6	FXT-2	2.0	24.1
FXL-3	10.52	166.2	FXT-3	2.1	25.8
FXL-4	10.87	170.6	FXT-4	2.0	23.8
FXL-5	11.49	163.4	FXT-5	2.1	23.7
Mean	11.21	167.8	Mean	2.0	24.7
Std. Dev.	0.51	3.0	Std. Dev.	0.1	1.1
CV (%)	4.60	1.8	CV (%)	3.7	4.6

Table 2.2-10 Inplane Shear Properties of IM7/PEEK [0, ±45, 90]$_s$

(a) at -150°F

Specimen # (CK)(SQ)(AP)	Longitudinal Shear Modulus (Msi)	Longitudinal Shear Strength (ksi)	Specimen # (CK)(SU)(AP)	Transverse Shear Modulus (Msi)	Transverse Shear Strength (ksi)
IPL-1	3.11	50.06	IPT-1	2.58	43.86
IPL-2	2.76	41.63	IPT-2	2.64	52.07
IPL-3	2.95	42.16	IPT-3	2.57	52.60
IPL-4	2.82	45.05	IPT-4	2.74	46.11
IPL-5	—	—	IPT-5	—	—
Mean	2.91	44.72	Mean	2.63	48.66
Std. Dev.	0.155	3.86	Std. Dev.	0.078	4.34
CV (%)	5.30	8.63	CV (%)	2.96	8.91

(b) at RT

Specimen # (CK)(SQ)(AP)	Longitudinal Shear Modulus (Msi)	Longitudinal Shear Strength (ksi)	Specimen # (CK)(SQ)(AP)	Transverse Shear Modulus (Msi)	Transverse Shear Strength (ksi)
IPL-11	2.66	45.5	IPT-11	2.63	40.8
IPL-12	2.64	45.1	IPT-12	2.51	47.0
IPL-13	2.89	45.6	IPT-13	2.08	36.7
IPL-14	2.56	43.7	IPT-14	2.48	48.8
IPL-15	2.77	46.2	IPT-15	2.44	44.9
Mean	2.70	45.2	Mean	2.43	43.6
Std. Dev.	0.13	0.9	Std. Dev.	0.21	4.9
CV (%)	4.70	2.0	CV (%)	8.60	11.3

(c) at 250°F

Specimen # (CK)(SU)(AP)	Longitudinal Shear Modulus (Msi)	Longitudinal Shear Strength (ksi)	Specimen # (CK)(SU)(AP)	Transverse Shear Modulus (Msi)	Transverse Shear Strength (ksi)
IPL-6	2.53	32.58	IPT-6	2.37	29.23
IPL-7	2.42	34.43	IPT-7	2.41	37.83
IPL-8	2.39	36.63	IPT-8	2.44	34.33
IPL-9	2.47	32.79	IPT-9	2.38	33.28
IPL-10	2.49	33.00	IPT-10	2.89	30.33
Mean	2.46	33.10	Mean	2.50	33.00
Std. Dev.	0.055	0.885	Std. Dev.	0.22	3.40
CV (%)	2.20	2.67	CV (%)	8.80	10.3

Table 2.2-11 Inplane Shear Properties of IM7/PEEK $[\pm 30, 0_4]_s$

(a) at -150°F

Specimen # (CK)(SZ)(AP)	Longitudinal Shear Modulus (Msi)	Longitudinal Shear Strength (ksi)	Specimen # (CK)(SZ)(AP)	Transverse Shear Modulus (Msi)	Transverse Shear Strength (ksi)
IPL-1	2.00	36.84	IPT-1	1.550	26.82
IPL-2	2.14	39.29	IPT-2	1.560	26.11
IPL-3	2.05	33.12	IPT-3	1.640	27.29
IPL-4	1.98	35.90	IPT-4	1.780	28.83
IPL-5	—	—	IPT-5	—	—
Mean	2.042	36.29	Mean	1.630	27.26
Std. Dev.	0.07	2.55	Std. Dev.	0.100	1.15
CV (%)	3.42	7.02	CV (%)	6.500	4.22

(b) at RT

Specimen # (CK)(SZ(AP)	Longitudinal Shear Modulus (Msi)	Longitudinal Shear Strength (ksi)	Specimen # (CK)(SZ)(AP)	Transverse Shear Modulus (Msi)	Transverse Shear Strength (ksi)
IPL-11	1.86	33.2	IPT-11	1.57	25.8
IPL-12	2.04	34.5	IPT-12	1.51	25.7
IPL-13	1.91	35.9	IPT-13	1.56	25.5
IPL-14	1.92	35.0	IPT-14	1.43	26.6
IPL-15	1.95	34.5	IPT-15	1.59	25.1
Mean	1.93	34.6	Mean	1.53	25.8
Std. Dev.	0.07	1.0	Std. Dev.	0.07	0.5
CV (%)	3.50	2.9	CV (%)	4.30	2.1

(c) at 250°F

Specimen # (CK)(SZ)(AP)	Longitudinal Shear Modulus (Msi)	Longitudinal Shear Strength (ksi)	Specimen # (CK)(SZ)(AP)	Transverse Shear Modulus (Msi)	Transverse Shear Strength (ksi)
IPL-6	1.85	26.45	IPT-6	1.54	20.76
IPL-7	1.70	26.77	IPT-7	1.40	22.22
IPL-8	1.74	25.23	IPT-8	1.48	21.90
IPL-9	1.98	25.04	IPT-9	1.23	20.41
IPL-10	1.80	24.98	IPT-10	1.55	21.25
Mean	1.814	25.70	Mean	1.44	21.31
Std. Dev.	0.109	0.849	Std. Dev.	0.13	0.76
CV (%)	6.00	3.30	CV (%)	9.03	3.56

Table 2.2-12 Apparent Interlaminar Shear Strength (ILSS) of IM7/PEEK

(a) at -150°F

IM7/PEEK $[0, \pm 45, 90]_s$		IM7/PEEK $[\pm 30, 0_4]_s$	
Specimen # (CK)(SQ)(AP)	ILSS-L (ksi)	Specimen # (CK)(SZ)(AP)	ILSS-L (ksi)
IL-1Q1	9.14	IL-4Z1	17.41
IL-1Q2	9.66	IL-4Z2	18.53
IL-1Q3	9.61	IL-4Z3	17.40
IL-1Q4	—	IL-4Z4	17.40
IL-1Q5	—	IL-4Z5	—
IL-1Q6	—	IL-4Z6	—
Mean	9.48	Mean	17.68
Std. Dev.	0.29	Std. Dev.	0.56
CV (%)	3.01	CV (%)	3.1

(a) at RT

IM7/PEEK $[0, \pm 45, 90]_s$		IM7/PEEK $[\pm 30, 0_4]_s$	
Specimen # (CK)(SQ)(AP)	ILSS-L (ksi)	Specimen # (CK)(SZ)(AP)	ILSS-L (ksi)
IL-1Q1	12.05	IL-4Z1	15.96
IL-1Q2	11.87	IL-4Z2	15.17
IL-1Q3	11.11	IL-4Z3	15.65
IL-1Q4	11.33	IL-4Z4	14.64
IL-1Q5	11.24	IL-4Z5	18.67
IL-1Q6	11.10	IL-4Z6	18.92
Mean	11.45	Mean	16.50
Std. Dev.	0.41	Std. Dev.	1.80
CV (%)	3.58	CV (%)	10.90

(a) at 250°F

IM7/PEEK $[0, \pm 45, 90]_s$		IM7/PEEK $[\pm 30, 0_4]_s$	
Specimen # (CK)(SQ)(AP)	ILSS-L (ksi)	Specimen # (CK)(SZ)(AP)	ILSS-L (ksi)
IL-1Q1	7.95	IL-4Z1	10.73
IL-1Q2	7.93	IL-4Z2	10.38
IL-1Q3	7.95	IL-4Z3	10.68
IL-1Q4	7.93	IL-4Z4	10.38
IL-1Q5	8.01	IL-4Z5	10.38
IL-1Q6	—	IL-4Z6	10.50
Mean	7.95	Mean	10.51
Std. Dev.	0.032	Std. Dev.	0.18
CV (%)	0.40	CV (%)	1.70

ILSS at RT = 11.45 ksi for $[0, \pm 45, 90]_s$

ILSS at RT = 16.5 ksi for $[\pm 30, 0_4]_s$ laminate

Based on these results, the apparent ILSS values of $[\pm 30, 0_4]_s$ also decreased with increasing temperature because the interlaminar shear response is primarily influenced by the matrix. It is likely that $[0, \pm 45, 90]_s$ laminate showed an anamolous response, as it exhibited lower strength at -150°F than at RT.

2.2.4 Thermophysical Properties

(a) CTE

Thermal expansion response of the $[0, \pm 45, 90]_s$ and $[\pm 30, 0_4]_s$ laminates is presented in Figures 2.2-4 to 2.2-7. The average CTE (obtained from the slope of a line joining the end points of response) residual strain are listed in Table 2.2-13. Also, the measured CTE values are in good agreement with the predicted values. For example, $[0, \pm 45, 90]_s$ laminate exhibited the quasi-isotropic response with the average CTE value of 1.27 ppm/°F in perfect agreement with the predicted value (1.27 ppm/°F).

(b) Specific Heat, Thermal Diffusivity and Thermal Conductivity

These thermophysical property test results of IM7/PEEK specimens for three different layups $[0]_8$, $[0, \pm 45, 90]_s$, and $[\pm 30, 0_4]_s$ are listed in Table 2.2-14 (longitudinal), Table 2.2-15 (transverse) and Table 2.2-16 (through-the-thickness) respectively. The specific heat (Cp) values for each laminate are nearly similar. For example @ 23°C:

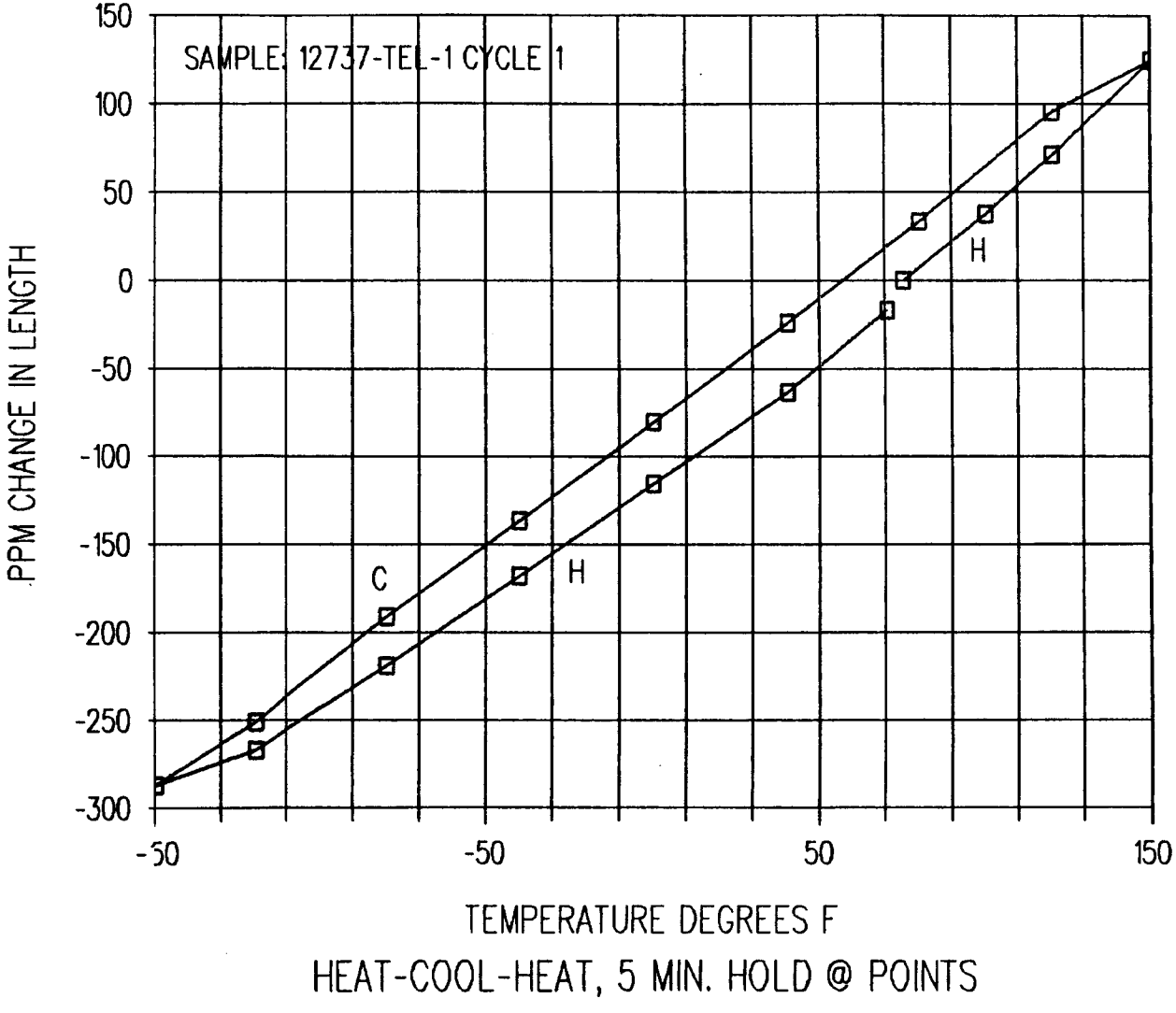

Figure 2.2-4 Thermal Expansion Behavior of Longitudinal IM7/PEEK [0, ±45, 90]$_s$ Specimen in a Heat-Cool -Heat Cycle Using Push Rod Dilatometer

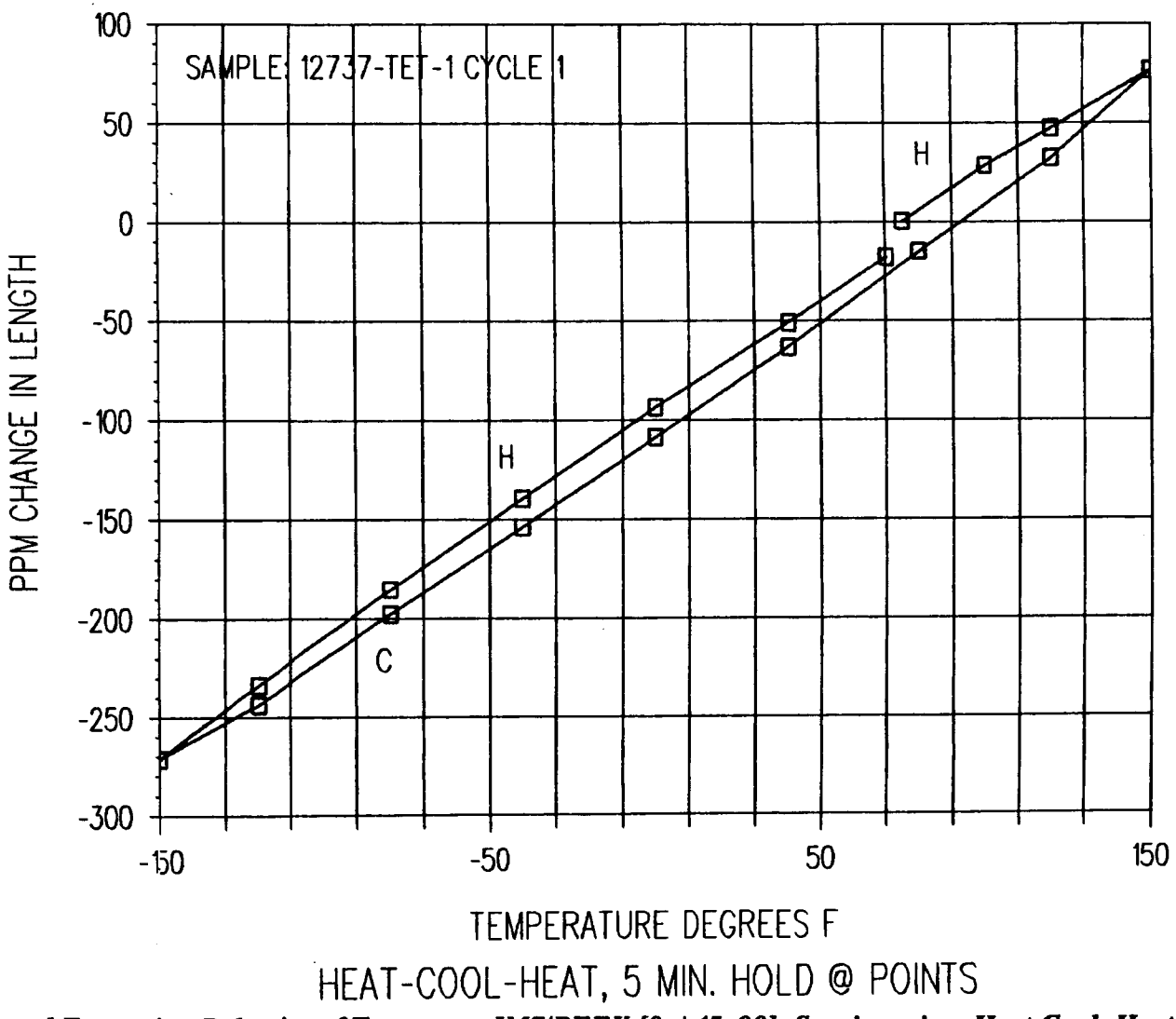

Figure 2.2-5 Thermal Expansion Behavior of Transverse IM7/PEEK [0, ±45, 90]$_s$ Specimen in a Heat-Cool -Heat Cycle Using Push Rod Dilatometer

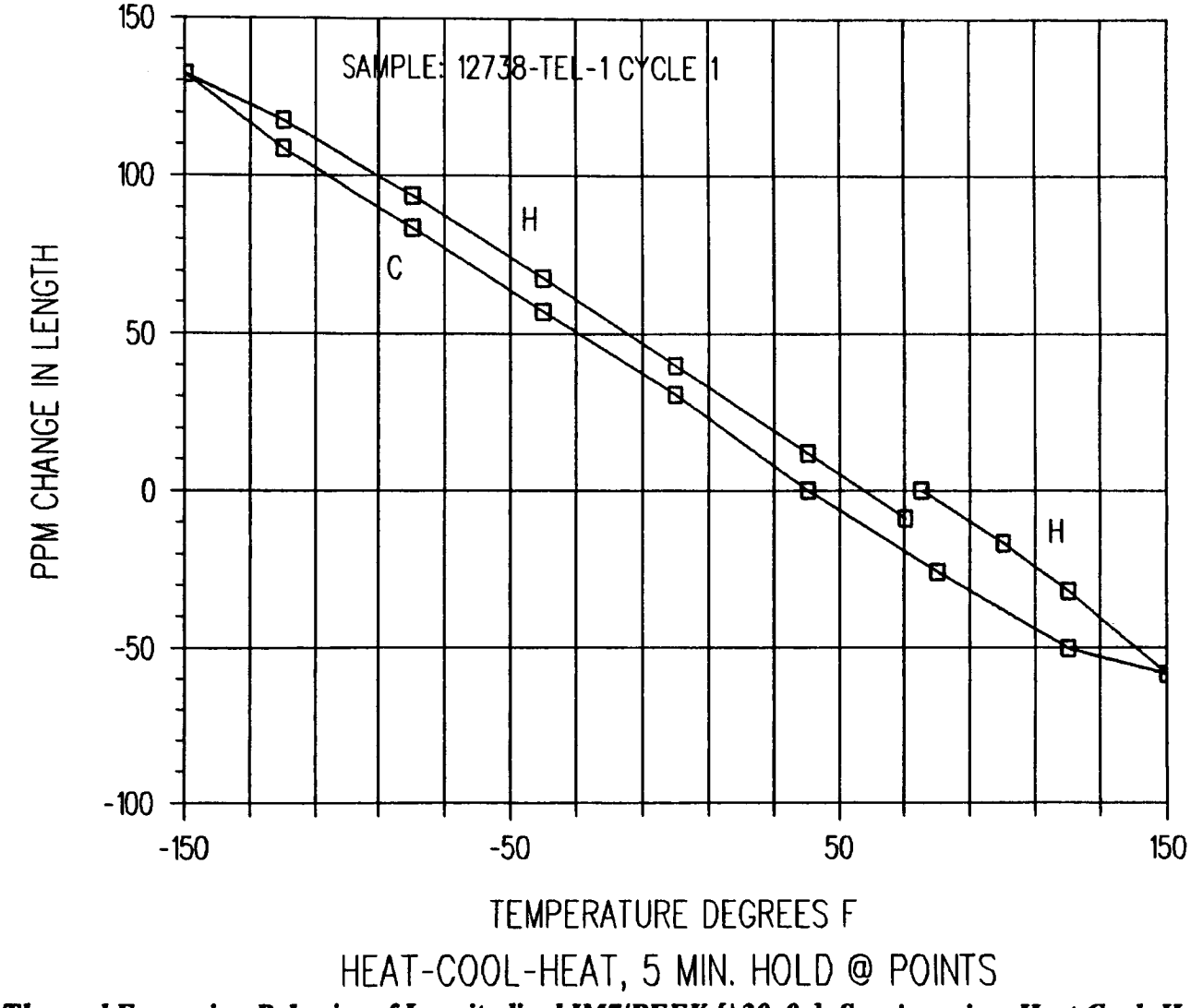

Figure 2.2-6 Thermal Expansion Behavior of Longitudinal IM7/PEEK [±30, 0_4]$_s$ Specimen in a Heat-Cool -Heat Cycle Using Push Rod Dilatometer

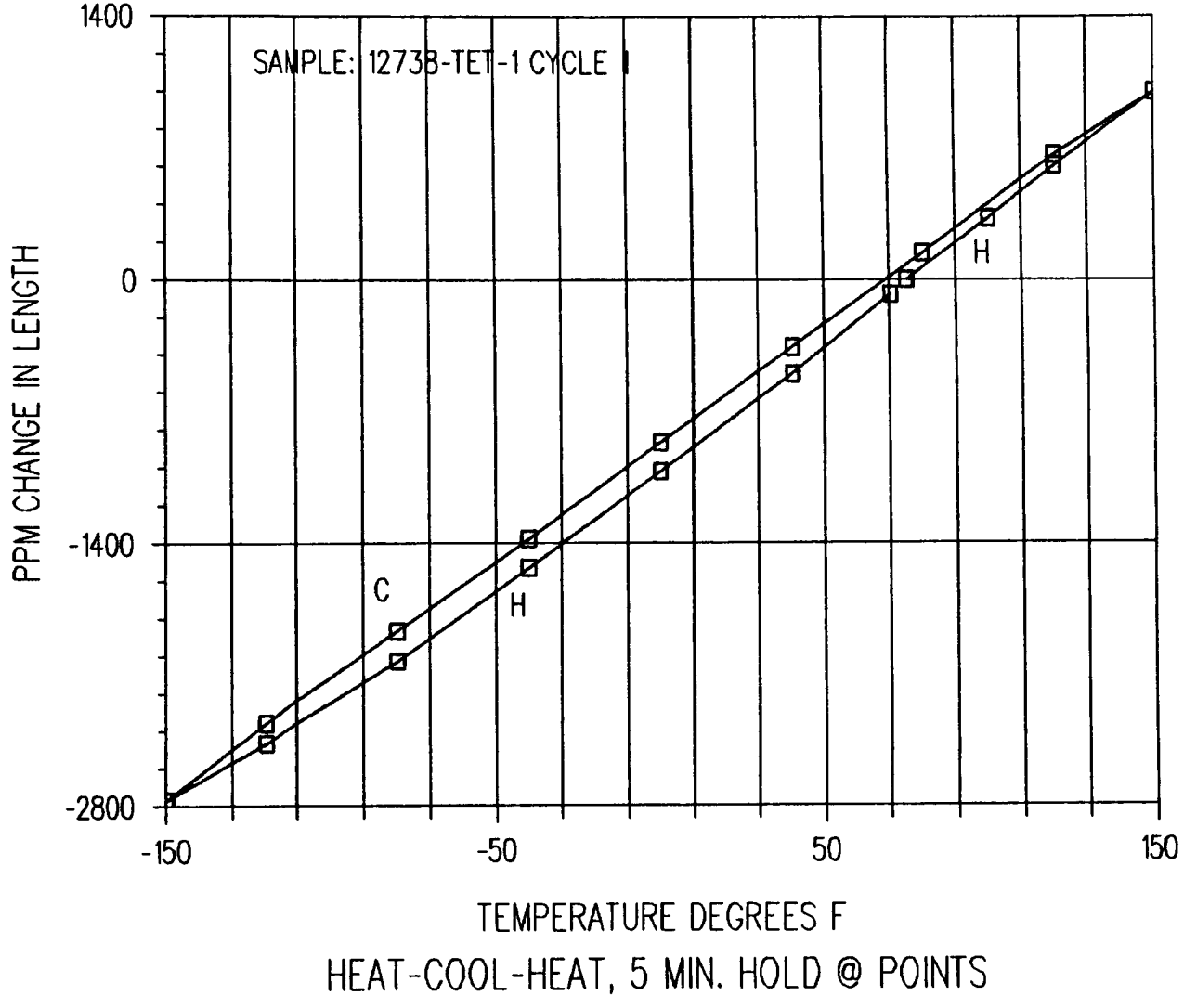

Figure 2.2-7 Thermal Expansion Behavior of Transverse IM7/PEEK [±30, 0_4]$_s$ Specimen in a Heat-Cool -Heat Cycle Using Push Rod Dilatometer

Table 2.2-13 Summary of Thermal Expansion Test Results for IM7/PEEK $[0, \pm 45, 90]_s$ and $[\pm 30, 0_4]_s$ Laminates in First Cycle Between -150°F and 150°F

THERMAL RESPONSE	IM7/PEEK			
	$[0, \pm 45, 90]_s$		$[\pm 30, 0_4]_s$	
	(L)	(T)	(L)	(T)
CTE ppm/°F (Predicted)	1.37 (1.27)	1.16 (1.27)	-0.62 (-0.63)	12.56 (11.70)
RT Hysteresis (ppm)	-25.87	140	-15.92	-15.02
Residual Strain (ppm)	-8.96	-80.40	-7.96	-18.09

	Cp (Ws gm^{-1} K^{-1})
IM7/PEEK $[0]_8$:	0.8230
IM7/PEEK $[0, \pm 45, 90]_s$:	0.8290
IM7/PEEK $[\pm 30, 0_4]_s$:	0.8270

For thermal conductivity tests, our experience has shown that Kohlrausch technique cannot be used for organic matrix composites because of the high electrical resistivity of constituent fiber and matrix. Therefore, diffusivity (D) and bulk density (ρ) measurements were made to calculate thermal conductivity (K) using the following relationship:

$$K = - D \cdot Cp \cdot \rho,$$

Test specimens were prepared for transverse, longitudinal, and through-the-thickness diffusivity measurements. In Table 2.2-14 these measured bulk density values obtained by weighing the specimens of known geometry are about two percent lower than the values obtained by ASTM D-792, based on Archimedes principle.

Table 2.2-14 Results of IM7/PEEK Thermophysical Property Test (Longitudinal)

Material	Temp. (C)	Density (gm cm $^{-3}$)	Specific Heat (W s mg $^{-1}$K $^{-1}$)	Diffusivity (cm ^{2}sec $^{-1}$)	Conduct-ivity (W cm $^{-1}$K $^{-1}$)	Conduct-ivity (BTU Units *)	Temp (F)
IM7/PEEK							
$[0]_8$	-150.0	1.549	0.2210	0.06620	0.02266	15.71	-238.0
$[0]_8$	-100.0	1.549	0.4300	0.05480	0.03650	25.31	-148.0
$[0]_8$	-50.0	1.549	0.6010	0.04720	0.04394	30.47	-58.0
$[0]_8$	0.0	1.549	0.7600	0.04230	0.04980	34.53	32.0
$[0]_8$	23.0	1.549	0.8230	0.04130	0.05265	36.50	73.4
$[0]_8$	75.0	1.549	0.9850	0.03950	0.06027	41.79	167.0
$[0]_8$	150.0	1.549	1.2390	0.03720	0.07139	49.50	302.0
$[0]_8$	225.0	1.549	1.4790	0.03550	0.08133	56.39	437.0
$[0]_8$	300.0	1.549	1.6570	0.03420	0.08778	60.86	572.0
$[0]_8$	350.0	1.549	1.8600**	0.03400	0.09796	67.92	662.0
IM7/PEEK							
$[0, \pm45, 90]_s$	-150.0	1.543	0.2290	0.04070	0.01438	9.97	-238.0
$[0, \pm45, 90]_s$	-100.0	1.543	0.4380	0.03310	0.02237	15.51	-148.0
$[0, \pm45, 90]_s$	-50.0	1.543	0.6110	0.02900	0.02734	18.96	-58.0
$[0, \pm45, 90]_s$	0.0	1.543	0.7690	0.02650	0.03144	21.80	32.0
$[0, \pm45, 90]_s$	23.0	1.543	0.8290	0.02560	0.03275	22.70	73.4
$[0, \pm45, 90]_s$	75.0	1.543	0.9970	0.02430	0.03738	25.92	167.0
$[0, \pm45, 90]_s$	150.0	1.543	1.2500	0.02250	0.04340	30.09	302.0
$[0, \pm45, 90]_s$	225.0	1.543	1.4890	0.02100	0.04825	33.45	437.0
$[0, \pm45, 90]_s$	300.0	1.543	1.6650	0.01970	0.05061	35.09	572.0
$[0, \pm45, 90]_s$	350.0	1.543	1.8890**	0.01950	0.05684	39.41	662.0
IM7/PEEK							
$[\pm30, 0_4]_s$	-150.0	1.556	0.2240	0.05510	0.01920	13.32	-238.0
$[\pm30, 0_4]_s$	-100.0	1.556	0.4330	0.04710	0.03173	22.00	-148.0
$[\pm30, 0_4]_s$	-50.0	1.556	0.6050	0.04290	0.04039	28.00	-58.0
$[\pm30, 0_4]_s$	0.0	1.556	0.7540	0.03990	0.04681	32.46	32.0
$[\pm30, 0_4]_s$	23.0	1.556	0.8270	0.03870	0.04980	34.53	73.4
$[\pm30, 0_4]_s$	75.0	1.556	0.9820	0.03720	0.05684	39.41	167.0
$[\pm30, 0_4]_s$	150.0	1.556	1.2280	0.03510	0.06707	46.50	302.0
$[\pm30, 0_4]_s$	225.0	1.556	1.4850	0.03300	0.07625	52.87	437.0
$[\pm30, 0_4]_s$	300.0	1.556	1.6320	0.03180	0.08075	55.99	572.0
$[\pm30, 0_4]_s$	350.0	1.556	1.7200**	0.03140	0.08404	58.27	662.0

* BTU in $hr^{-1}ft^{-2}F^{-1}$) ** Extrapolated

Table 2.2-15 Results of IM7/PEEK Thermophysical Property Test (Transverse)

Material	Temp. (C)	Density (gm/cm^{-3})	Specific Heat ($W\,s\,mg^{-1}K^{-1}$)	Diffusivity (cm^2sec^{-1})	Conduct-ivity ($W\,cm^{-1}K^{-1}$)	Conduct-ivity (BTU Units *)	Temp (F)
IM7/PEEK							
$[0]_8$	-150.0 +	1.536	0.2210	0.00781	0.00265	1.84	-238.0
$[0]_8$	-100.0	1.536	0.4300	0.00672	0.00444	3.08	-148.0
$[0]_8$	-50.0	1.536	0.6010	0.00606	0.00559	3.88	-58.0
$[0]_8$	0.0	1.536	0.7600	0.00552	0.00644	4.47	32.0
$[0]_8$	23.0	1.536	0.8230	0.00525	0.00664	4.60	73.4
$[0]_8$	75.0	1.536	0.9850	0.00471	0.00713	4.94	167.0
$[0]_8$	150.0	1.536	1.2390	0.00437	0.00832	5.77	302.0
$[0]_8$	225.0	1.536	1.4790	0.00394	0.00895	6.21	437.0
$[0]_8$	300.0	1.536	1.6570	0.00365	0.00929	6.44	572.0
$[0]_8$	350.0	1.536	1.8600	0.00361	0.01031	7.15	662.0
IM7/PEEK							
$[0, \pm45, 90]_s$	-150.0 +	1.515	0.2290	0.02920	0.01013	7.02	-238.0
$[0, \pm45, 90]_s$	-100.0	1.515	0.4380	0.02620	0.01739	12.05	-148.0
$[0, \pm45, 90]_s$	-50.0	1.515	0.6110	0.02450	0.02268	15.72	-58.0
$[0, \pm45, 90]_s$	0.0	1.515	0.7690	0.02280	0.02656	18.42	32.0
$[0, \pm45, 90]_s$	23.0	1.515	0.9290	0.02240	0.03153	21.86	73.4
$[0, \pm45, 90]_s$	75.0	1.515	0.9970	0.02140	0.03232	22.41	167.0
$[0, \pm45, 90]_s$	150.0	1.515	1.2500	0.02070	0.03920	27.18	302.0
$[0, \pm45, 90]_s$	225.0	1.515	1.4890	0.01940	0.04376	30.34	437.0
$[0, \pm45, 90]_s$	300.0	1.515	1.6650	0.01930	0.04868	33.75	572.0
$[0, \pm45, 90]_s$	350.0	1.515	1.8890	0.01940	0.05552	38.49	662.0
IM7/PEEK							
$[\pm30, 0_4]_s$	-150.0 +	1.558	0.2240	0.01380	0.00482	3.34	-238.0
$[\pm30, 0_4]_s$	-100.0	1.558	0.4330	0.01180	0.00796	5.52	-148.0
$[\pm30, 0_4]_s$	-50.0	1.558	0.6050	0.01050	0.00990	6.86	-58.0
$[\pm30, 0_4]_s$	0.0	1.558	0.7540	0.00910	0.01068	7.41	32.0
$[\pm30, 0_4]_s$	23.0	1.558	0.8270	0.00891	0.01148	7.96	73.4
$[\pm30, 0_4]_s$	75.0	1.558	0.9820	0.00784	0.01199	8.32	167.0
$[\pm30, 0_4]_s$	150.0	1.558	1.2280	0.00714	0.01366	9.47	302.0
$[\pm30, 0_4]_s$	225.0	1.558	1.4850	0.00689	0.01594	11.05	437.0
$[\pm30, 0_4]_s$	300.0	1.558	1.6320	0.00634	0.01612	11.18	572.0
$[\pm30, 0_4]_s$	350.0	1.558	1.7200	0.00565	0.01514	10.50	662.0

* BTU in $hr^{-1}ft^{-2}F^{-1}$) + Extrapolated

Table 2.2-16 IM7/PEEK Thermophysical Property Test (Through -the-Thickness))

Material	Temp. (C)	Density (gm/cm^{-3})	Specific Heat ($W\,s\,mg^{-1}K^{-1}$)	Diffusivity (cm^2sec^{-1})	Conduct-ivity ($W\,cm^{-1}K^{-1}$)	Conduct-ivity (BTU Units *)	Temp (F)
IM7/PEEK							
$[0]_8$	-150.0	1.579	0.2210	0.00802	0.00280	1.94	-238.0
$[0]_8$	-100.0	1.579	0.4300	0.00680	0.00462	3.20	-148.0
$[0]_8$	-50.0	1.579	0.6010	0.00584	0.00554	3.84	-58.0
$[0]_8$	0.0	1.579	0.7600	0.00558	0.00670	4.64	32.0
$[0]_8$	23.0	1.579	0.8230	0.00532	0.00691	4.79	73.4
$[0]_8$	75.0	1.579	0.9850	0.00497	0.00773	5.36	167.0
$[0]_8$	150.0	1.579	1.2390	0.00447	0.00875	6.06	302.0
$[0]_8$	225.0	1.579	1.4790	0.00396	0.00925	6.41	437.0
$[0]_8$	300.0	1.579	1.6570	0.00356	0.00931	6.46	572.0
$[0]_8$	350.0	1.579	1.8600**	0.00340	0.00999	6.92	662.0
IM7/PEEK							
$[0, \pm45, 90]_s$	-150.0	1.576	0.2290	0.00784	0.00283	1.96	-238.0
$[0, \pm45, 90]_s$	-100.0	1.576	0.4380	0.00664	0.00458	3.18	-148.0
$[0, \pm45, 90]_s$	-50.0	1.576	0.6110	0.00597	0.00575	3.99	-58.0
$[0, \pm45, 90]_s$	0.0	1.576	0.7690	0.00539	0.00653	4.53	32.0
$[0, \pm45, 90]_s$	23.0	1.576	0.8290	0.00521	0.00681	4.72	73.4
$[0, \pm45, 90]_s$	75.0	1.576	0.9970	0.00484	0.00760	5.27	167.0
$[0, \pm45, 90]_s$	150.0	1.576	1.2500	0.00428	0.00843	5.85	302.0
$[0, \pm45, 90]_s$	225.0	1.576	1.4890	0.00387	0.00908	6.30	437.0
$[0, \pm45, 90]_s$	300.0	1.576	1.6650	0.00349	0.00916	6.35	572.0
$[0, \pm45, 90]_s$	350.0	1.576	1.8890**	0.00336	0.01000	6.76	662.0
IM7/PEEK							
$[\pm30, 0_4]_s$	-150.0	1.561	0.2240	0.00821	0.00287	1.99	-238.0
$[\pm30, 0_4]_s$	-100.0	1.561	0.4330	0.00704	0.00476	3.30	-148.0
$[\pm30, 0_4]_s$	-50.0	1.561	0.6050	0.00626	0.00591	4.10	-58.0
$[\pm30, 0_4]_s$	0.0	1.561	0.7540	0.00567	0.00667	4.63	32.0
$[\pm30, 0_4]_s$	23.0	1.561	0.8270	0.00552	0.00713	4.94	73.4
$[\pm30, 0_4]_s$	75.0	1.561	0.9820	0.00498	0.00763	5.29	167.0
$[\pm30, 0_4]_s$	150.0	1.561	1.2280	0.00445	0.00853	5.91	302.0
$[\pm30, 0_4]_s$	225.0	1.561	1.4850	0.00400	0.00927	6.43	437.0
$[\pm30, 0_4]_s$	300.0	1.561	1.6320	0.00363	0.00925	6.41	572.0
$[\pm30, 0_4]_s$	350.0	1.561	1.7200**	0.00340	0.00913	6.33	662.0

* BTU in $hr^{-1}ft^{-2}F^{-1}$) ** Extrapolated

The longitudinal thermal conductivity values for each laminate are lower than the corresponding values for P75/PEEK specimens, because of inherently low conductivity of the IM7 fiber (0.15 W/cm-K) compared to P75 fiber (1.85 w/cm-K).

Figure 2.2-8 shows the specific heat values at different temperatures, indicating a sudden increase near 305°C due to the phase transformation in the PEEK matrix.. The results of longitudinal transverse and the through-the-thickness thermal conductivity values are presented in Figures 2.2-9, 2.2-10, and 2.2-11respectively. Each specimen exhibited 5 - 8 times higher thermal conductivity in the longitudinal direction than in the through-the-thickness direction. For example, @ RT (23°C):

	K_L (W cm^{-1} K^{-1})		K_T (W cm^{-1} K^{-1})		K_Z (W cm^{-1} K^{-1})	
Layup	IM7/PEEK	P75/PEEK	IM7/PEEK	P75/PEEK	IM7/PEEK	P75/PEEK
$[0, \pm 45, 90]_S$	0.0327	0.463	0.0315	0.4865	0.0068	0.015
$[\pm 30, 0_4]_S$	0.0498	0.7775	0.0115	0.0795	0.0071	0.016

(c) Optical Properties

The solar absorptance (α_S) and normal emissivity (ε_N) values of the as fabricated quasi-isotropic and $[\pm 30, 0_4]_S$ laminates are quite similar as shown below.

α_S: 0.90, ε_N: 0.75 for $[0, \pm 45, 90]_S$ and $[\pm 30, 0_4]_S$

Reflectance vs. Wavelength: Typical FTIR diffuse reflectance spectra of as received $[0, \pm 45, 90]_S$ and $[\pm 30, 0_4]_S$ laminates are shown in Figures 2.2-12, and 2.2-13 respectively. The measurements in the 2.0 to 14.0 micrometer wavelength were taken from specimens oriented longitudinally and transversely. In each case the reflectance spectra was nearly identical. These

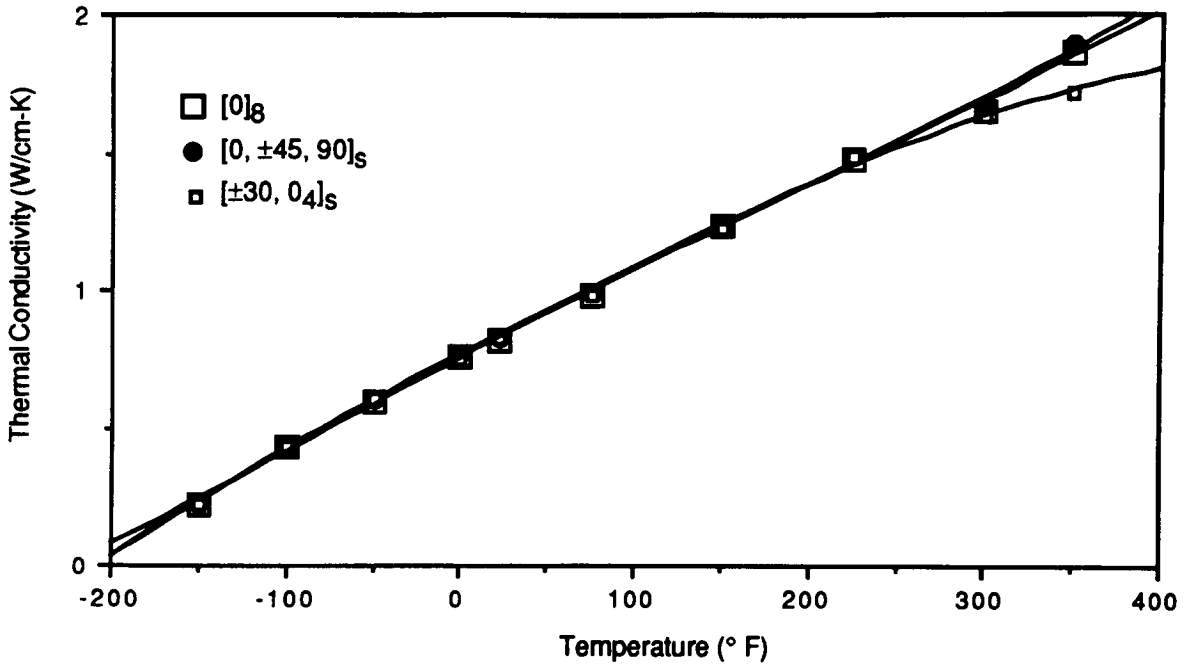

Figure 2.2-8 Specific Heat of IM7/PEEK Composites ($[0]_8$, $[0, \pm 45, 90]_s$, and $[\pm 30, 0_4]_s$) at Different Temperatures

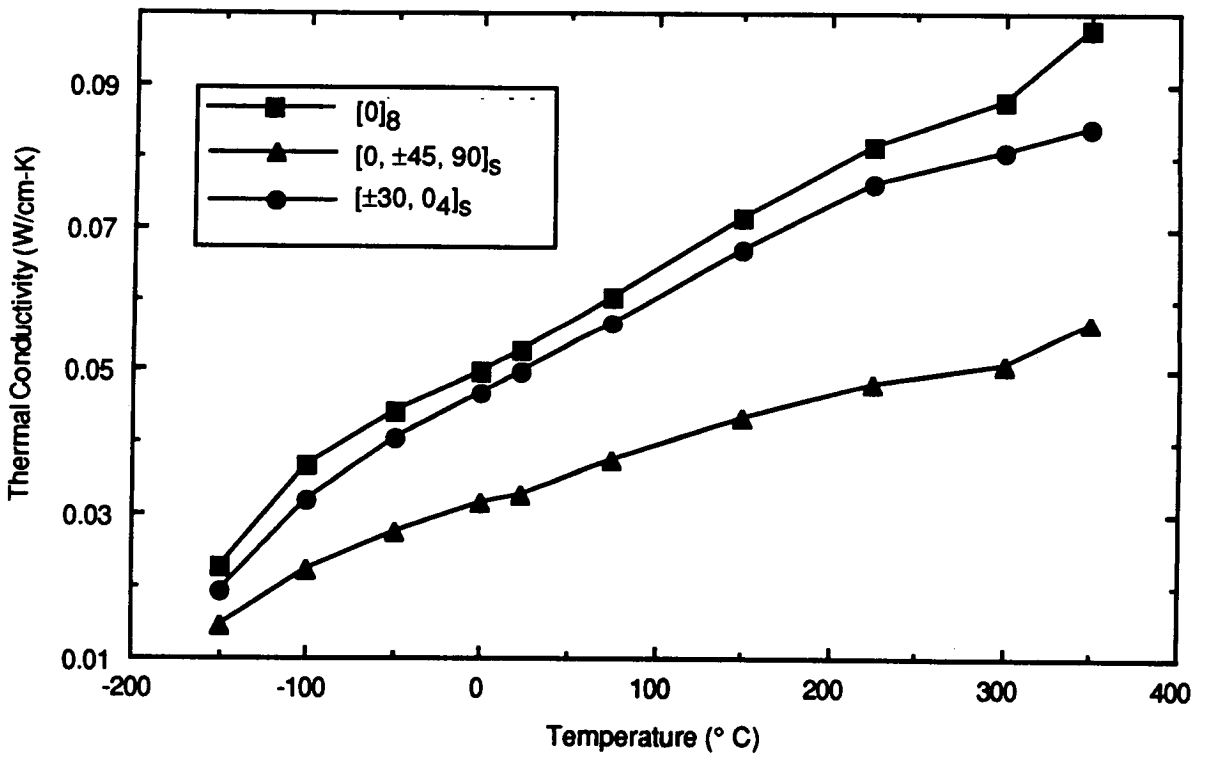

Figure 2.2-9 Longitudinal Thermal Conductivity of IM7/PEEK Specimens $[0]_8$, $[0, \pm 45, 90]_s$, and $[\pm 30, 0_4]_s$

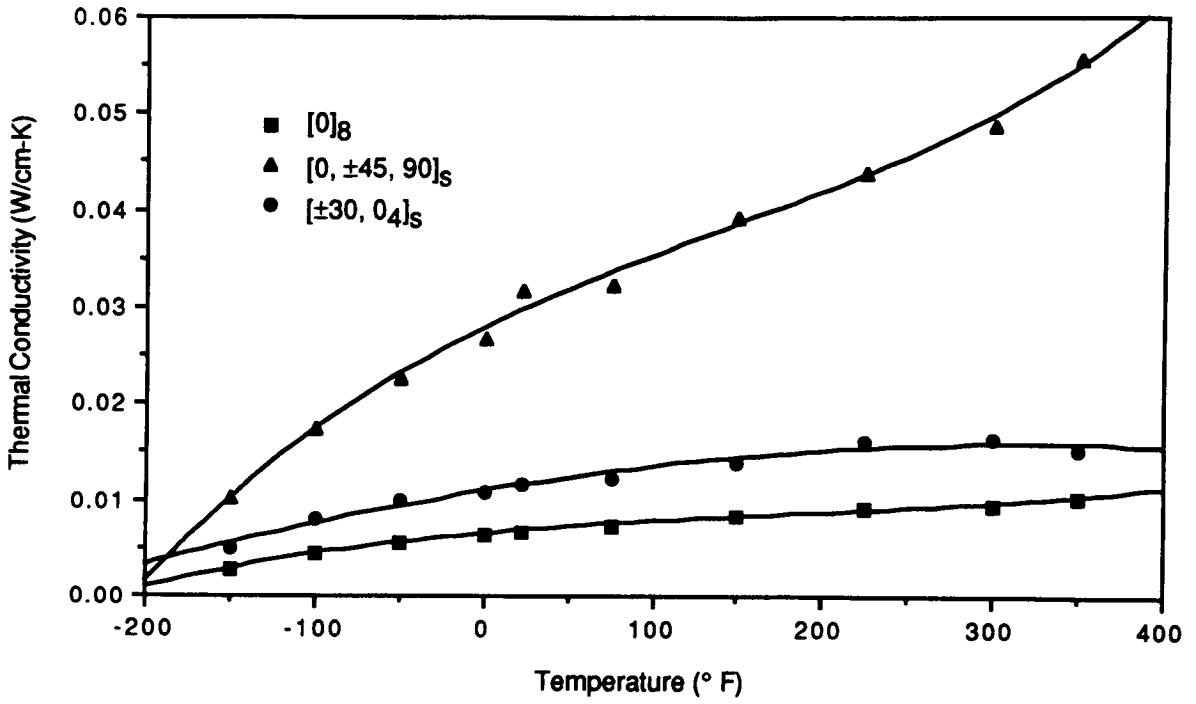

Figure 2.2-10 Transverse Thermal Conductivity of IM7/PEEK: ($[0]_8$, $[0, \pm45, 90]_s$, and $[\pm30, 0_4]_s$)

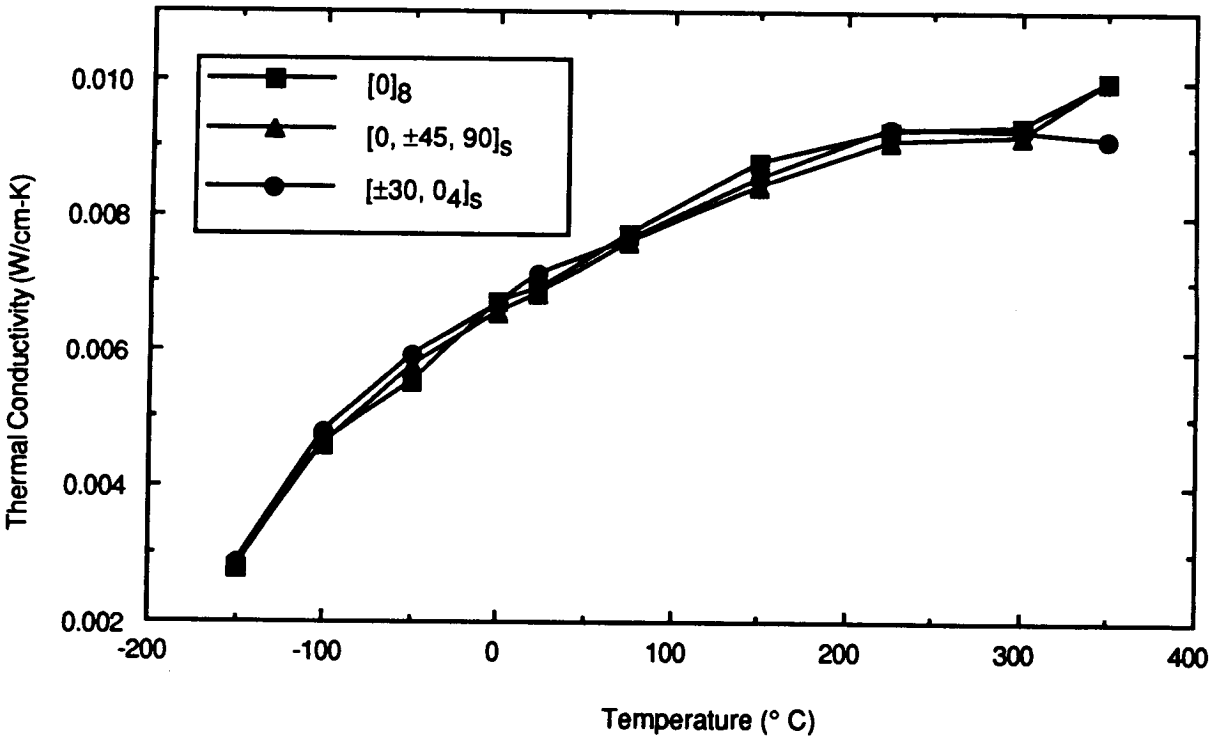

Figure 2.2-11 Through -the-Thickness (K_Z) Thermal Conductivity of IM7/PEEK: $[0]_8$, $[0, \pm45, 90]_s$, and $[\pm30, 0_4]_s$

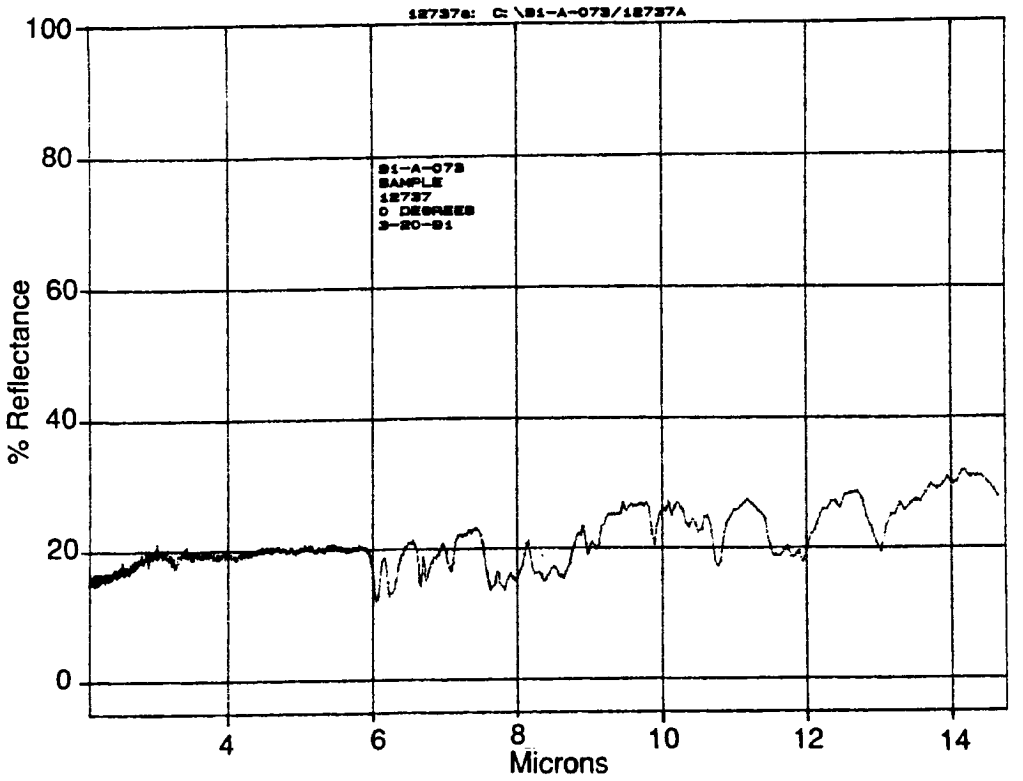

Figure 2.2-12 FTIR Reflectance Spectra of $[0, \pm 45, 90]_s$ IM7/PEEK

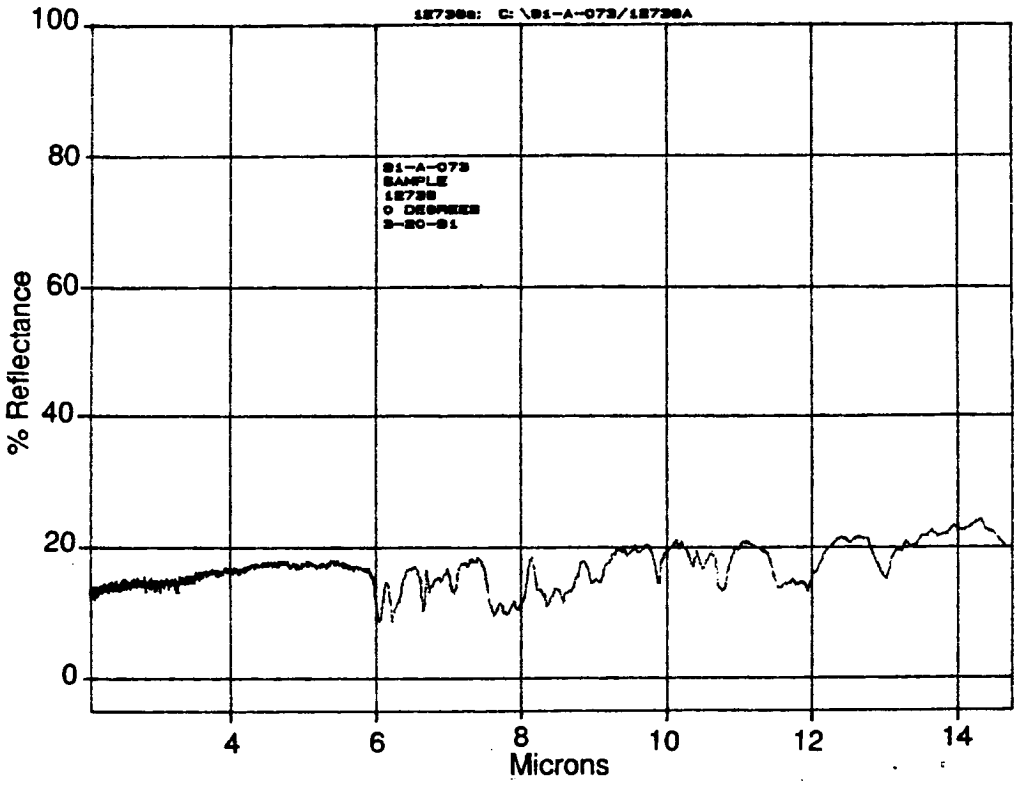

Figure 2.2-13 FTIR Reflectance Spectra of $[\pm 30, 0_4]_s$ IM7/PEEK

measurements indicated that at 10.6 μm average reflectance of $[0, \pm 45, 90]_s$ laminate was 20% and of $[\pm 30, 0_4]_s$ laminate was 19%.

2.3 SUMMARY OF IM7/PEEK TEST DATA

Material properties of $[0]_8$, $[0, \pm 45, 90]_s$, and $[\pm 30, 0_4]_s$ laminates are summarized in Table 2.3-1 and 2.3-2, and 2.3-3 respectively

Table 2.3-1 Graphite/Thermoplastic: IM7/PEEK $[0]_8$

NOT DESIGN ALLOWABLE DATA

PROPERTIES					TEMPERATURE (°F)			Std. Dev. / No. of Specimens at RT	Test Method
PHYSICAL			MECHANICAL & THERMAL			-150	Room	250		
Density (lb / in^3)			Longitudinal Tensile Strength	σ_x^{TU}	ksi	389.0	391.27	318.1		ASTM D-3039
Fiber volume fraction			Transverse Tensile Strength	σ_y^{TU}	ksi	11.08	10.5	9.03		ASTM D-3039
Void volume fraction			Longitudinal Comp. Strength	σ_x^{CU}	ksi	163.6	146.8	105.2		ASTM D-3410
Nominal ply thickness	in		Transverse comp. strength	σ_y^{CU}	ksi	25.86	17.8	12.3		ASTM D-3410
Max. cont. use temp.	°F		In-plane shear strength	IPSS	ksi	23.85	19.18	9.00		10° Off Axis
Ply Orientation	θ		Interlaminar shear strength	ILSS	ksi		15.38			ASTM D-2344
OPTICAL & ELECTRICAL (at room temperature)			Longitudinal tensile strain **	ε_x^T	%					ASTM D-3039
			Transverse tensile strain **	ε_y^T	%					ASTM D-3039
Solar Absorptance	α_s		Longitudinal comp. strain **	ε_x^C	%					ASTM D-3410
Normal Emissivity	ε_N		Transverse comp. strain **	ε_y^C	%					ASTM D-3410
			Longitudinal tensile modulus	E_x	Msi	21.9	23.87	24.3		ASTM D-3039
			Transverse tensile modulus	E_y	Msi	1.46	1.4	1.18		ASTM D-3039
			Longitudinal comp. modulus	E_x	Msi	22.53	22.8	21.72		ASTM D-3410
			Transverse comp. modulus	E_y	Msi	1.41	1.4	1.22		ASTM D-3410
			In-plane shear modulus	G	Msi	1.08	1.12	0.80		10° Off-Axis
			Longitudinal flexural modulus	F_x	Msi		23.13			ASTM D-790M
			Transverse flexural modulus	F_y	Msi		1.32			ASTM D-790M
			Long. tensile Poisson's ratio	ν_{xy}		0.295	0.289	0.276		ASTM D-3039
			Trans. tensile Poisson's ratio	ν_{yx}		0.018	0.02	0.016		ASTM D-3039
			Long. thermal conductivity	K_x	(1)	0.21	0.253	0.30		Kohlrausch
			Trans. thermal conductivity	K_y	(1)	0.026	0.031	0.041		Kohlrausch
			Thru thickness thermal cond.	K_z	(1)	0.026	0.033	0.04		
			Specific heat	C_p	(2)	0.10	0.20	0.26		ASTM E-1269
			Longitudinal CTE	α_x	(3)		-0.07			ASTM E-228
			Transverse CTE	α_y	(3)		17.42			ASTM E-228
			Thru thickness CTE	α_z	(3)					

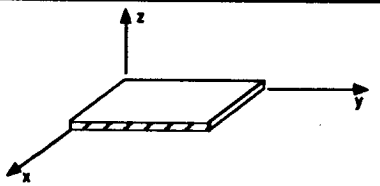

Notes: (**) - Strain to failure; (1) Btu/(hr·in·°F); (2) Btu/(lb·°F); (3) μin./in./°F

Table 2.3-2 Graphite/Thermoplastic: IM7/PEEK $[0, \pm 45, 90]_s$

NOT DESIGN ALLOWABLE DATA

PROPERTIES						TEMPERATURE (°F)			Std. Dev. / No. of Specimens at RT	Test Method
PHYSICAL			MECHANICAL & THERMAL			-150	Room	250		
Density (lb / in^3)		0.0569	Longitudinal Tensile Strength	σ_x^{TU}	ksi	130.97	130.3	114.5		ASTM D-3039
Fiber volume fraction		62.0	Transverse Tensile Strength	σ_y^{TU}	ksi	145.4	134.8	116.4		ASTM D-3039
Void volume fraction		≤ 0.5	Longitudinal Comp. Strength	σ_x^{CU}	ksi	96.85	67.7	55.06		ASTM D-3410
Nominal ply thickness	In	0.005	Transverse comp. strength	σ_y^{CU}	ksi	61.25	49.0	39.0		ASTM D-3410
Max. cont. use temp.	°F		In-plane shear strength	IPSS	ksi	44.72	45.2	33.1		10° Off Axis
Ply Orientation	θ	$[0, \pm 45, 90]_s$	Interlaminar shear strength	ILSS	ksi	9.48	11.45	7.95		ASTM D-2344
OPTICAL & ELECTRICAL (at room temperature)			Longitudinal tensile strain **	ε_x^T	%					ASTM D-3039
Solar Absorptance	α_s		Transverse tensile strain **	ε_y^T	%					ASTM D-3039
Normal Emissivity	ε_N		Longitudinal comp. strain **	ε_x^C	%					ASTM D-3410
			Transverse comp. strain **	ε_y^C	%					ASTM D-3410
			Longitudinal tensile modulus	E_x	Msi	7.17	7.3	7.26		ASTM D-3039
			Transverse tensile modulus	E_y	Msi	7.57	7.71	7.3		ASTM D-3039
			Longitudinal comp. modulus	E_x	Msi	9.13	7.1	7.7		ASTM D-3410
			Transverse comp. modulus	E_y	Msi	8.98	9.36	8.71		ASTM D-3410
			In-plane shear modulus	G	Msi	2.91	2.70	2.46		10° Off-Axis
			Longitudinal flexural modulus	F_x	Msi		13.5			ASTM D-790M
			Transverse flexural modulus	F_y	Msi		3.2			ASTM D-790M
			Long. tensile Poisson's ratio	ν_{xy}		0.291	0.291	0.33		ASTM D-3039
			Trans. tensile Poisson's ratio	ν_{yx}		0.31	0.334	0.31		ASTM D-3039
			Long. thermal conductivity	K_x	(1)	0.13	0.158	0.18		Kohlrausch
			Trans. thermal conductivity	K_y	(1)	0.109	0.151	0.155		Kohlrausch
			Thru thickness thermal cond.	K_z	(1)	0.22	0.033	0.041		
			Specific heat	C_p	(2)	0.10	0.20	0.26		ASTM E-1269
			Longitudinal CTE	α_x	(3)		1.37			ASTM E-228
			Transverse CTE	α_y	(3)		1.16			ASTM E-228
			Thru thickness CTE	α_z	(3)					

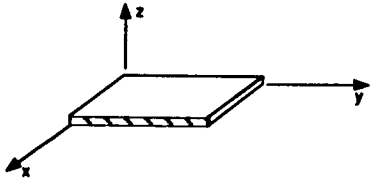

Notes: (**) - Strain to failure; (1) Btu/(hr·in·°F); (2) Btu/(lb·°F); (3) μin./in./°F

Table 2.3-3 Graphite/Thermoplastic: IM7/PEEK $[\pm 30, 0_4]_s$

NOT DESIGN ALLOWABLE DATA

PROPERTIES							TEMPERATURE (°F)			Std. Dev. / No. of Specimens at RT	Test Method
PHYSICAL			MECHANICAL & THERMAL				-150	Room	250		
Density (lb / in^3)	X	0.0569	Longitudinal Tensile Strength	σ_x^{TU}	ksi		304.4	297.4	238.7		ASTM D-3039
Fiber volume fraction	X	62.0	Transverse Tensile Strength	σ_y^{TU}	ksi		15.57	14.72	12.6		ASTM D-3039
Void volume fraction	X	≤ 0.5	Longitudinal Comp. Strength	σ_x^{CU}	ksi		154.2	127.6	106.38		ASTM D-3410
Nominal ply thickness	In	0.005	Transverse comp. strength	σ_y^{CU}	ksi		39.13	23.0	18.9		ASTM D-3410
Max. cont. use temp.	°F		In-plane shear strength	IPSS	ksi		34.6	36.3	25.7		10° Off Axis
Ply Orientation	θ	$[\pm 45, 0_4]_s$	Interlaminar shear strength	ILSS	ksi		17.68	16.5	10.51		ASTM D-2344
OPTICAL & ELECTRICAL (at room temperature)			Longitudinal tensile strain **	ε_x^T	%						ASTM D-3039
			Transverse tensile strain **	ε_y^T	%						ASTM D-3039
Solar Absorptance	α_s		Longitudinal comp. strain **	ε_x^C	%						ASTM D-3410
Normal Emissivity	ε_N		Transverse comp. strain **	ε_y^C	%						ASTM D-3410
			Longitudinal tensile modulus	E_x	Msi		17.32	18.1	18.81		ASTM D-3039
			Transverse tensile modulus	E_y	Msi		1.69	1.62	1.15		ASTM D-3039
			Longitudinal comp. modulus	E_x	Msi		16.39	17.2	15.94		ASTM D-3410
			Transverse comp. modulus	E_y	Msi		2.0	1.9	1.41		ASTM D-3410
			In-plane shear modulus	G	Msi		2.04	1.93	1.81		10° Off-Axis
			Longitudinal flexural modulus	F_x	Msi			11..21			ASTM D-790M
			Transverse flexural modulus	F_y	Msi			2.0			ASTM D-790M
			Long. tensile Poisson's ratio	ν_{xy}	X		1.09	1.02			ASTM D-3039
			Trans. tensile Poisson's ratio	ν_{yx}	X		0.080	0.084	0.093		ASTM D-3039
			Long. thermal conductivity	K_x	(1)		0.194	0.24	0.27		Kohlrausch
			Trans. thermal conductivity	K_y	(1)		0.047	0.055	0.058		Kohlrausch
			Thru thickness thermal cond.	K_z	(1)		0.028	0.034	0.041		
			Specific heat	C_p	(2)		0.10	0.20	0.26		ASTM E-1269
			Longitudinal CTE	α_x	(3)			-0.62			ASTM E-228
			Transverse CTE	α_y	(3)			12.56			ASTM E-228
			Thru thickness CTE	α_z	(3)						

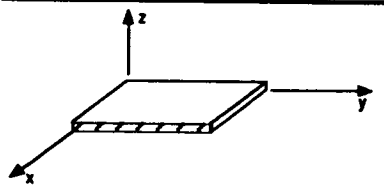

Notes: (**) - Strain to failure; (1) Btu/(hr·in·°F); (2) Btu/(lb·°F); (3) μin./in./°F

3.0 25 V/O DISCONTINUOUS SiC/Al

Discontinuous SiC/Al composites offer higher specific stiffness, a lower CTE, and an improved temperature capability compared to conventional metals used for spacecraft structural applications. In addition these composites have isotropic properties and can be readily fabricated into complex shaped structural components and attachment fittings. Therefore, 25 v/o SiC_p/2124-T6 and 25 v/o SiC_w/2124-T6 flat panels were procured to generate material property test data at three different temperatures: RT,-150° and 250°F. The material property tests at RT were performed during 1987-1990 technical effort, and documented in the NASA report #187472 entitled " Composite Materials for Space Applications" (65) (included in the summary tables at the end of this chapter). The fabrication data and the results of product evaluation, mechanical and thermophysical property tests performed at -150° and 250°F are discussed in this chapter.

3.1 FLAT PANELS

- 25 v/o SiC_p/2124-T6 and
- 25 v/o SiC_w/2124-T6

3.1.1 Fabrication Data

The particulate and whisker reinforced composite panels were procured from ACMC to generate representative data of SOA materials from a different batch that was used to generate room temperature material property test data. All the panels were fabricated by conventional powder metallurgy technique which included consolidation of billets followed by hot extrusion and hot rolling steps. After final hot rolling step, each panel was heat treated to -T6 condition.

Material:	25 v/o SiC_p/2124-T6	25 v/o SiC_w/2124-T6
Fabrication Process:	Powder metallurgy/hot extrusion and rolling	Powder metallurgy/hot extrusion and rolling
Manufacturer:	ACMC, SC	ACMC, SC
Base Matrix :	Atomized 2009 Al powder	
Dimension:	16-in. x 16-in. x 0.065-in. (from ACMC, SC)	16-in. x 16-in. x 0.065-in.
Warpage:	0.375-in./12-in. maximum	0.375-in./12-in. maximum
Lot No.:	239-01A	240-01-A
Martin Marietta ID:	(25PA)(CQ)(AP)	(25WA)(CQ)(AP)

3.1.2 Product Evaluation

(a) Density

- 25 v/o SiC_p/2124-T6: 0.101 lb/in^3

  Std. Dev.: 0.0005
- 25v/o SiC_w/2124-T6: 0.101 lb/in^3

  Std. Dev.: 0.0003

(b) Reinforcement Volume

- SiC_p/2124-T6: v/o: 25.22%

  Std. Dev.: 0.8
- SiC_w/2124-T6: v/o: 25.3%

  Std. Dev.: 1.1

In each case, void volume $\leq 0.1\%$

(c) Non-Destructive Evaluation

Based on visual examination, surface quality of each panel was good without voids and scratches. Also, in X-radiographs and ultrasonic C-scans of the panels, no voids, cracks, impurity stringers, or related defects were detected.

(d) Microstructure

Typical microstructures of both particulate and whisker reinforced composites are shown in Figure 3.1-1 and 3.1-2 respectively. These microstructures indicate that the overall reinforcement distribution is nearly uniform in both composites. In the particulate reinforced panels the average particle size was 3 μm. In SiC_w/Al panels, the average aspect ratio of whiskers was 12.6 (10 - 12 μm length and 0.6 - 1 μm diameter).

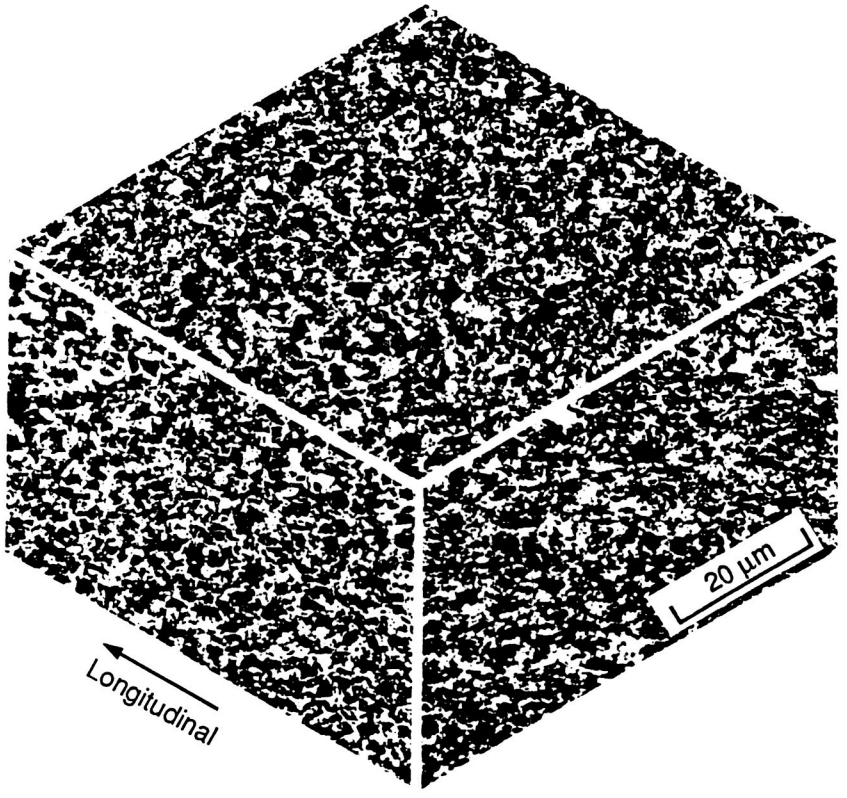

Figure 3.1-1 Three Dimensional Microstructure of 25 v/o SiC_p/2124-T6 Al

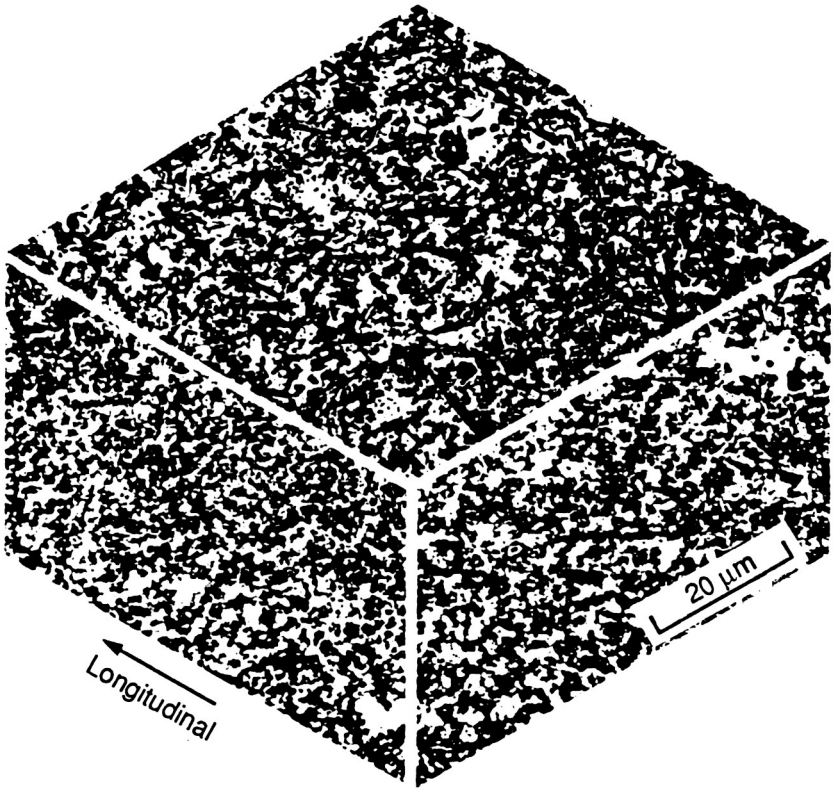

Figure 3.1-2 Three Dimensional Microstructure of 25 v/o SiC_w/2124-T6 Al

3.1.3 Mechanical Properties

Tension, compression, flexure, and inplane (Iosipescu) shear test results from both the 25 v/o SiC_p and SiC_w/2124-T6 panels were determined at -150° and 250°F. These test results are discussed below.

(a) Tension

25 v/o SiCp/2124-T6: Longitudinal and transverse tensile properties of these composites at -150°F and 250°F are listed in Table 3.1-1 and 3.1-2 respectively. In these tests, the stress-strain response of each specimen exhibited the elastic-plastic response, similar to RT tests.

Table 3.1-1- Longitudinal Tensile Properties of 25 v/o SiC_p/2124-T6

(a) at -150°F

Specimen # (25PA) (CQ) (AP)	Elastic Modulus E_x^T (Msi)	Yield Strength (ksi)	Ultimate Tensile Strength (ksi)	Poisson Ratio ν_{xy}
TNL-1	17.22	70.73	90.24	0.293
TNL-2	16.48	74.76	93.90	0.295
TNL-3	17.41	74.09	93.37	0.310
TNL-4	15.95	74.54	92.42	0.283
TNL-5	16.73	74.22	93.37	0.305
Mean Value	16.76	73.67	92.66	0.297
Std. Dev.	0.58	1.66	1.45	0.010
CV (%)	0.35	2.25	1.56	3.530

(b) at 250°F

Specimen # (25PA) (CQ) (AP)	Elastic Modulus E_x^T (Msi)	Yield Strength (ksi)	Ultimate Tensile Strength (ksi)	Poisson Ratio ν_{xy}
TNL-6	16.08	64.05	74.40	0.286
TNL-7	15.83	63.69	73.81	0.279
TNL-8	14.88	64.04	74.11	0.262
TNL-9	15.95	62.55	72.73	0.263
TNL-10	15.18	63.93	74.40	0.255
Mean Value	15.58	63.65	73.89	0.269
Std. Dev.	0.52	0.63	0.69	0.013
CV (%)	3.33	0.99	0.93	4.830

Table 3.1-2 Transverse Tensile Properties of 25 v/o SiC_p/2124-T6

(a) at -150°F

Specimen # (25PA) (CQ) (AP)	Elastic Modulus E_x^T (Msi)	Yield Strength (ksi)	Ultimate Tensile Strength (ksi)	Poisson Ratio ν_{yx}
TNT-1	16.62	74.21	91.22	0.301
TNT-2	15.66	75.00	87.50	0.289
TNT-3	15.65	76.69	93.86	0.276
TNT-4	15.97	74.85	92.63	0.307
TNT-5	16.72	74.25	91.90	0.275
Mean Value	16.12	75.00	91.42	0.289
Std. Dev.	0.51	1.008	2.40	0.015
CV (%)	3.19	1.30	2.60	5.150

(b) at 250°F

Specimen # (25PA) (CQ) (AP)	Elastic Modulus E_x^T (Msi)	Yield Strength (ksi)	Ultimate Tensile Strength (ksi)	Poisson Ratio ν_{yx}
TNT-6	15.03	64.29	73.81	0.250
TNT-7	15.29	64.12	72.94	0.263
TNT-8	16.48	65.61	74.39	0.276
TNT-9	15.25	64.94	74.70	0.258
TNT-10	16.18	64.48	74.03	0.257
Mean Value	15.65	64.69	73.97	0.261
Std. Dev.	0.64	0.60	0.67	0.0096
CV (%)	4.09	0.93	0.91	3.680

At -150°F, mean longitudinal elastic modulus (16.75 Msi) and strength (92.6 ksi) values were nearly identical to the transverse modulus (16.12 Msi) and strength (91.42 ksi) values, suggesting random distribution of particulates in the composite. The longitudinal elastic modulus value of 16.75 Msi at -150°F was close to the modulus value of 16.64 Msi obtained at RT from a different batch of material indicating the reproducibility of material and its properties. The measured properties at 250°F also indicate the isotropic behavior of the composite. Mean

mechanical properties (modulus, 0.2% offset yield strength and ultimate tensile strength) are lower than the corresponding values measured at -150°F, due to lower matrix strength at the 250°F test temperature.

25 v/o SiCw/2124-T6: Longitudinal and transverse tensile properties of 25 v/o SiCw/2124-T6 at -150°F and 250 °F are listed in Tables 3.1-3 and 3.1-4 respectively. These results indicate a slightly anisotropic response with a longitudinal tensile strength of 108.8 ksi and transverse tensile strength of 94.16 ksi. In addition, the whisker reinforced specimens exhibited tensile strength about 16% higher than the corresponding particulate reinforced composite. Still the measured modulus value obtained at 17.21 Msi at -150°F is nearly identical to the 17.6 Msi value obtained at RT from a different batch of composite material.

Like particulate reinforced composites, the average values of elastic modulus and strength obtained at 250°F are lower than the corresponding values measured at -150°F. In contrast to -150°F test data, the elastic modulus and strength results at +250°F indicate an anisotropic response, suggesting the whiskers align in the longitudinal direction during the exposure at 250°F test.

(b) Compression

25 v/o SiCp/2124-T6: Longitudinal and transverse compression test data of the composite specimens tested at -150°F and 250°F are listed in Table 3.1-5 and 3.1-6 respectively. The stress-strain response of each specimen exhibited the elastic-plastic response, similar to RT tests.

Based on these tests, average compressive strength value (109.67 ksi) was slightly higher than the corresponding tensile strength (92.66 ksi) value at -150°F. Measured longitudinal compressive modulus of 17.42 Msi was close (within 6.5% scatter) to the transverse modulus of

Table 3.1-3 Longitudinal Tensile Properties of 25 v/o SiCw/2124-T6

(a) at -150°F

Specimen # (25WA) (CQ) (AP)	Elastic Modulus E_x^T (Msi)	Yield Strength (ksi)	Ultimate Tensile Strength (ksi)	Poisson Ratio ν_{xy}
TNL-1	17.35	80.350	113.35	0.275
TNL-2 *	—	—	—	—
TNL-3	18.17	77.850	105.80	0.300
TNL-4	16.45	78.125	108.75	0.305
TNL-5	16.89	78.120	107.50	0.310
Mean Value	17.21	78.610	108.80	0.298
Std. Dev.	0.735	1.165	3.30	0.015
CV (%)	4.27	1.480	3.03	5.200

* Specimen got damaged during handling

(b) at 250°F

Specimen # (25WA) (CQ) (AP)	Elastic Modulus E_x^T (Msi)	Yield Strength (ksi)	Ultimate Tensile Strength (ksi)	Poisson Ratio ν_{xy}
TNL-6	17.95	72.05	91.93	0.303
TNL-7	17.81	72.00	94.38	0.291
TNL-8	17.95	75.15	96.89	0.297
TNL-9	17.36	72.50	91.25	0.280
TNL-10	17.27	71.25	90.63	0.303
Mean Value	17.67	72.59	93.02	0.295
Std. Dev.	0.329	1.50	2.59	0.0096
CV (%)	1.86	2.07	2.80	3.250

C-2

Table 3.1-4 Transverse Tensile Properties of 25 v/o SiC_w/2124-T6

(a) at -150°F

Specimen # (25WA) (CQ) (AP)	Elastic Modulus E_x^T (Msi)	Yield Strength (ksi)	Ultimate Tensile Strength (ksi)	Poisson Ratio ν_{yx}
TNT-1	16.82	71.09	96.77	0.310
TNT-2	16.56	69.57	94.72	0.280
TNT-3	17.69	70.32	92.36	0.299
TNT-4	---	---	92.55	---
TNT-5	17.06	68.94	94.41	0.298
Mean Value	17.03	69.98	94.16	0.297
Std. Dev.	0.483	0.93	1.804	0.0124
CV (%)	2.83	1.33	1.91	4.170

(b) at 250°F

Specimen # (25WA) (CQ) (AP)	Elastic Modulus E_x^T (Msi)	Yield Strength (ksi)	Ultimate Tensile Strength (ksi)	Poisson Ratio ν_{yx}
TNT-6	15.24	63.75	75.62	0.237
TNT-7	15.24	63.75	76.25	0.268
TNT-8	15.61	64.15	76.73	0.253
TNT-9	15.27	64.15	76.10	0.267
TNT-10	15.17	63.49	75.28	0.255
Mean Value	15.31	63.86	76.00	0.256
Std. Dev.	0.174	0.287	0.56	0.012
CV (%)	1.14	0.45	0.74	4.690

Table 3.1-5 Longitudinal Compressive Tensile Properties of 25 v/o SiC_p/2124-T6

(a) at -150°F

Specimen # (25PA) (CQ) (AP)	Elastic Modulus E_x^C (Msi)	Yield Strength (ksi)	Ultimate Compressive Strength (ksi)	Poisson Ratio ν_{xy}
CML-1	17.87	65.40	97.41	0.277
CML-2	17.11	76.36	104.84	0.239
CML-3	—	—	108.58	—
CML-4	17.23	84.70	131.43	0.229
CML-5	17.46	84.60	106.10	0.257
Mean Value	17.42	77.76	109.67	0.251
Std. Dev.	0.335	9.12	12.86	0.021
CV (%)	1.92	11.7	11.70	8.360

(b) at 250°F

Specimen # (25PA) (CQ) (AP)	Elastic Modulus E_x^C (Msi)	Yield Strength (ksi)	Ultimate Compressive Strength (ksi)	Poisson Ratio ν_{xy}
CML-6	16.60	62.80	79.92	0.286
CML-7	15.90	—	70.74	0.270
CML-8	16.10	63.10	72.88	0.262
CML-9	16.40	—	70.02	—
CML-10	15.80	62.90	72.22	0.255
Mean Value	16.16	62.93	73.16	0.268
Std. Dev.	0.336	0.15	3.95	0.013
CV (%)	2.08	0.24	5.40	4.850

Table 3.1-6 Transverse Compressive Tensile Properties of 25 v/o SiC_p/2124-T6

(a) at -150°F

Specimen # (25PA) (CQ) (AP)	Elastic Modulus E_Y^C (Msi)	Yield Strength (ksi)	Ultimate Compressive Strength (ksi)	Poisson Ratio ν_{yx}
CMT-1	16.51	85.50	94.70	0.222
CMT-2	16.41	86.00	101.00	0.253
CMT-3	—	—	113.52	0.234
CMT-4	15.90	85.10	127.69	0.267
CMT5	16.28	84.30	109.98	0.300
Mean Value	16.28	85.20	109.38	0.255
Std. Dev.	0.27	0.72	12.60	0.030
CV (%)	1.66	0.84	11.50	11.900

(b) at 250°F

Specimen # (25PA) (CQ) (AP)	Elastic Modulus E_Y^C (Msi)	Yield Strength (ksi)	Ultimate Compressive Strength (ksi)	Poisson Ratio ν_{yx}
CMT-6	—	63.10	66.18	—
CMT-7	15.39	66.20	72.76	0.276
CMT-8	16.08	—	75.89	0.283
CMT-9	16.02	63.10	73.23	0.279
CMT-10	15.63	62.90	74.15	0.268
Mean Value	15.78	63.83	72.44	0.277
Std. Dev.	0.33	1.59	3.70	0.006
CV (%)	2.09	2.49	5.10	2.300

16.76 Msi at -150°F. Whereas, at 250°F longitudinal compressive modulus of 16.16 Msi was nearly identical to the transverse modulus value of 15.78 Msi, inidcating the random distribution of particulates, as was also evident in the microstructural examination. For both particulate and whisker reinforced composites, the average compressive strength (yield and ultimate) decreased with increasing temperature due to the slight decrease (about 8%) in the matrix strength. For example, the ultimate compressive strength value of 109.67 ksi at -150°F compared to the strength of 73.16 ksi at 250°F.

25 v/o SiCw/2124-T6: Longitudinal and transverse compressive properties at -150°F and 250°F and listed in Tables 3.1-7 and 3.1-8 respectively. These results indicate that the longitudinal modulus of 17.57 Msi at -150°F is identical to the longitudinal modulus of 17.33 Msi at 250°F. However, the yield and ultimate compressive strength (80.04 and 106.56 ksi respecitvely) at -150°F are consistently higher than the corresponding yield and ultimate strength (62.65 and 81.28 ksi respectively) at 250°F, due to the increased matrix strength at low temperatures. A comparison of longitudinal and transverse compression test results at 250°F showed an anomalous response in compression modulus measurements: For example:

Longitudinal Compressive Modulus:	17.33 Msi at 250°F
Transverse Compressive Modulus:	14.6 Msi at 250°F

To ascertain that anomalous response is either the typical behavior or due to localized microstructural (such as v/o or whisker alignment) changes, more specimens should be tested.

Table 3.1-7 Longitudinal Compressive Porperties of 25 v/o SiC_w/2124-T6

(a) at -150°F

Specimen # (25WA) (CQ) (AP)	Elastic Modulus E_x^C (Msi)	Yield Strength (ksi)	Ultimate Compressive Strength (ksi)	Poisson Ratio ν_{xy}
CML-1	17.70	—	105.57	—
CML-2	17.09	78.77	102.77	0.269
CML-3	—	—	105.51	0.259
CML-4	17.79	79.20	107.13	0.256
CML-5	17.70	82.17	111.83	0.272
Mean Value	17.57	80.04	106.56	0.264
Std. Dev.	0.32	1.85	3.34	0.008
CV (%)	1.82	2.31	3.13	2.910

(b) at 250°F

Specimen # (25WA) (CQ) (AP)	Elastic Modulus E_x^C (Msi)	Yield Strength (ksi)	Ultimate Compressive Strength (ksi)	Poisson Ratio ν_{xy}
CML-6	17.74	62.80	83.06	0.293
CML-7	18.06	—	76.00	0.285
CML-8	16.04	59.90	74.03	0.288
CML-9	17.65	63.80	85.26	0.302
CML-10	17.16	64.10	88.04	0.299
Mean Value	17.33	62.65	81.28	0.293
Std. Dev.	0.785	1.91	6.02	0.007
CV (%)	4.53	3.04	7.40	2.400

Table 3.1-8 Transverse Compressive Porperties of 25 v/o SiC_w/2124-T6

(a) at -150°F

Specimen # (25WA) (CQ) (AP)	Elastic Modulus E_Y^C (Msi)	Yield Strength (ksi)	Ultimate Compressive Strength (ksi)	Poisson Ratio ν_{yx}
CMT-1	18.30	71.10	96.90	0.310
CMT-2	17.56	73.20	116.10	0.280
CMT-3	—	—	—	—
CMT-4	16.60	74.10	92.60	0.290
CMT5	17.30	76.60	103.10	0.298
Mean Value	17.44	73.75	102.18	0.295
Std. Dev.	0.702	2.28	10.20	0.013
CV (%)	4.00	3.10	9.98	4.400

(b) at 250°F

Specimen # (25WA) (CQ) (AP)	Elastic Modulus E_Y^C (Msi)	Yield Strength (ksi)	Ultimate Compressive Strength (ksi)	Poisson Ratio ν_{yx}
CMT-6	16.96	—	65.20	0.254
CMT-7	14.72	61.54	66.77	0.262
CMT-8	14.07	—	66.63	0.241
CMT-9	14.30	62.79	66.94	0.253
CMT-10	13.00	60.79	70.00	0.254
Mean Value	14.60	61.70	67.10	0.253
Std. Dev.	1.460	1.01	3.00	0.0075
CV (%)	10.00	1.60	4.50	2.980

(c) Flexure

25 v/o SiCp/2124-T6: Flexure test results obtained at -150°F and 250°F are listed in Table 3.1-9. These measurements indicate an isotropic response at both the test temperatures. Average flexural modulus value (16.76 Msi) is identical to the tensile modulus (16.75 Msi) value. However, the calculated flexural strength value of 135.9 ksi is higher than the measured tensile strength value of 92.66 ksi at -150°F.

25 v/o SiCw/2124-T6: Flexure test results of 25 v/o SiCw 2124-T6 obtained at -150°F and 250°F are listed in Table 3.1-10. Like particulate reinforced composites, the flexural modulus vlaues (17.59 Msi at -150°F) are nearly identical to the tensile modulus (17.21 Msi at -150°F) values, and the calculated flexural strength values are significantly higher than the measured tensile strength at the test temperature.

(d) Inplane Shear

The shear modulus and strength values of both particulate and whisker reinforced composites were obtained by Iosipescu test method at RT, -150°F and 250°F. The results of longitudinal and trasnverse specimens of 25 v/o SiC_p/2124-T6 and 25 v/o SiC_w/2124-T6 are listed in Table 3.1-11 (at RT), 3.1-12 (at -130°F) and 3.1-13 (at 250°F). These results indicate the following:

(1) Measured modulus and strength values indicate nearly isotropic response in both the composites at each test temperature. For example:

	Shear Modulus (x, y) (Msi)	
Test Temperature	25 v/o SiC_p/2124-T6	25 v/o SiC_w/2124-T6
at Room Temperature	5.94, 5.51	6.19, 5.46
at -150°F	6.00, 5.59	5.40, 5.59
at 250°F	5.03, 5.09	5.23, 5.21

Table 3.1-9 Flexural Properties of 25 v/o SiC_p/2124-T6

(a) at -150°F

Specimen # (25PA)(CQ)(AP)	Longitudinal Flexural		Specimen # (25PA)(CQ)(AP)	Transverse Flexural	
	Modulus (Msi)	Strength (ksi)		Modulus (Msi)	Strength (ksi)
FXL-1	16.84	133.9	FXT-1	15.29	133.80
FXL-2	17.38	142.7	FXT-2	16.64	134.80
FXL-3	17.10	136.9	FXT-3	17.50	139.98
FXL-4	16.20	135.3	FXT-4	15.32	130.20
FXL-5	16.30	130.6	FXT-5	17.47	135.10
Mean	16.76	135.9	Mean	16.44	134.60
Std. Dev.	0.51	4.5	Std. Dev.	1.09	3.15
CV (%)	3.00	3.3	CV (%)	6.63	2.34

(b)at 250°F

Specimen # (25PA)(CQ)(AP)	Longitudinal Flexural		Specimen # (25PA)(CQ)(AP)	Transverse Flexural	
	Modulus (Msi)	Strength (ksi)		Modulus (Msi)	Strength (ksi)
FXL-1	16.24	137.15	FXT-1	16.98	123.97
FXL-2	16.75	142.38	FXT-2	17.50	131.98
FXL-3	15.92	121.38	FXT-3	16.55	130.06
FXL-4	16.65	121.38	FXT-4	16.24	131.31
FXL-5	16.68	129.39	FXT-5	16.81	143.42
Mean	16.45	130.37	Mean	16.82	132.15
Std. Dev.	0.36	9.39	Std. Dev.	0.47	7.05
CV (%)	2.19	7.20	CV (%)	2.80	5.33

Table 3.1-10 Flexural Properties of 25 v/o SiC_w/2124-T6

(a) at -150°F

Specimen # (25WA)(CQ)(AP)	Longitudinal Flexural		Specimen # (25WA)(CQ)(AP)	Transverse Flexural	
	Modulus (Msi)	Strength (ksi)		Modulus (Msi)	Strength (ksi)
FXL-1	17.18	138.74	FXT-1	17.98	138.74
FXL-2	17.78	143.80	FXT-2	16.65	144.60
FXL-3	18.36	144.36	FXT-3	16.65	134.30
FXL-4	17.15	119.82	FXT-4	16.55	138.46
FXL-5	17.46	145.11	FXT-5	17.18	146.50
Mean	17.59	138.36	Mean	17.00	140.52
Std. Dev.	0.50	10.66	Std. Dev.	0.60	4.96
CV (%)	2.84	7.70	CV (%)	3.50	3.53

(b)at 250°F

Specimen # (25WA)(CQ)(AP)	Longitudinal Flexural		Specimen # (25WA)(CQ)(AP)	Transverse Flexural	
	Modulus (Msi)	Strength (ksi)		Modulus (Msi)	Strength (ksi)
FXL-1	17.11	144.38	FXT-1	16.68	131.98
FXL-2	17.52	144.00	FXT-2	16.69	139.60
FXL-3	17.11	147.00	FXT-3	17.08	134.50
FXL-4	17.54	144.20	FXT-4	16.84	131.80
FXL-5	17.12	149.40	FXT-5	16.45	132.07
Mean	17.28	145.80	Mean	16.75	133.98
Std. Dev.	0.23	2.36	Std. Dev.	0.23	3.32
CV (%)	1.33	1.62	CV (%)	1.37	2.48

Table 3.1-11 Inplane Shear Properties of Discontinuous SiC/Al at RT

(a) 25 v/o SiCp/2124-T6

Specimen # (25PA)(CQ)(AP)	Longitudinal Shear		Specimen # (25PA)(CQ)(AP)	Transverse Shear	
	Modulus (Msi)	Strength (ksi)		Modulus (Msi)	Strength (ksi)
IPL-11	5.64	36.46	IPT-11	5.35	42.81
IPL-12	5.86	42.39	IPT-12	5.06	44.31
IPL-13	6.05	42.96	IPT-13	5.70	49.23
IPL-14	6.41	38.27	IPT-14	6.30	50.07
IPL-15	5.76	37.60	IPT-15	5.14	48.18
Mean	5.94	39.54	Mean	5.51	46.92
Std. Dev.	0.30	2.90	Std. Dev.	0.506	3.18
CV (%)	5.00	7.30	CV (%)	9.18	6.77

(b) 25 v/o SiCw/2124-T6

Specimen # (25WA)(CQ)(AP)	Longitudinal Shear		Specimen # (25WA)(CQ)(AP)	Transverse Shear	
	Modulus (Msi)	Strength (ksi)		Modulus (Msi)	Strength (ksi)
IPL-11	6.31	47.10	IPT-11	5.57	46.6
IPL-12	6.10	46.40	IPT-12	6.08	48.8
IPL-13	6.12	37.90	IPT-13	5.01	45.3
IPL-14	5.61	41.60	IPT-14	4.87	41.8
IPL-15	6.83	47.20	IPT-15	5.77	44.6
Mean	6.19	44.00	Mean	5.46	45.4
Std. Dev.	0.44	4.14	Std. Dev.	0.51	2.58
CV (%)	7.10	9.40	CV (%)	9.40	5.70

Table 3.1-12 Inplane Shear Properties of Discontinuous SiC/Al at -150°F

(a) 25 v/o SiCp/2124-T6

Specimen # (25PA)(CQ)(AP)	Longitudinal Shear		Specimen # (25PA)(CQ)(AP)	Transverse Shear	
	Modulus (Msi)	Strength (ksi)		Modulus (Msi)	Strength (ksi)
IPL-1	5.34	44.64	IPT-1	6.10	47.46
IPL-2	5.62	29.12	IPT-2	5.22	38.69
IPL-3	6.19	35.85	IPT-3	5.35	46.77
IPL-4	6.84	32.28	IPT-4	5.17	48.04
IPL-5	—	29.81	IPT-5	6.11	39.78
Mean	6.00	34.34	Mean	5.59	44.20
Std. Dev.	0.66	6.33	Std. Dev.	0.47	4.58
CV (%)	11.10	18.40	CV (%)	8.40	10.36

(b) 25 v/o SiCw/2124-T6

Specimen # (25WA)(CQ)(AP)	Longitudinal Shear		Specimen # (25WA)(CQ)(AP)	Transverse Shear	
	Modulus (Msi)	Strength (ksi)		Modulus (Msi)	Strength (ksi)
IPL-1	5.06	44.10	IPT-1	6.02	50.60
IPL-2	5.27	49.70	IPT-2	5.60	41.03
IPL-3	5.44	46.50	IPT-3	5.57	49.83
IPL-4	5.60	49.60	IPT-4	5.16	51.18
IPL-5	5.61	51.00	IPT-5	—	47.04
Mean	5.40	48.20	Mean	5.59	47.94
Std. Dev.	0.23	2.82	Std. Dev.	0.35	4.17
CV (%)	4.30	5.80	CV (%)	6.30	8.70

Table 3.1-13 Inplane Shear Properties of Discontinuous SiC/Al at 250°F

(a) 25 v/o SiCp/2124-T6

Specimen # (25PA)(CQ)(AP)	Longitudinal Shear		Specimen # (25PA)(CQ)(AP)	Transverse Shear	
	Modulus (Msi)	Strength (ksi)		Modulus (Msi)	Strength (ksi)
IPL-1	5.34	44.64	IPT-1	6.10	47.46
IPL-2	5.62	29.12	IPT-2	5.22	38.69
IPL-3	6.19	35.85	IPT-3	5.35	46.77
IPL-4	6.84	32.28	IPT-4	5.17	48.04
IPL-5	—	29.81	IPT-5	6.11	39.78
Mean	6.00	34.34	Mean	5.59	44.20
Std. Dev.	0.66	6.33	Std. Dev.	0.47	4.58
CV (%)	11.10	18.40	CV (%)	8.40	10.36

(b) 25 v/o SiCw/2124-T6

Specimen # (25WA)(CQ)(AP)	Longitudinal Shear		Specimen # (25WA)(CQ)(AP)	Transverse Shear	
	Modulus (Msi)	Strength (ksi)		Modulus (Msi)	Strength (ksi)
IPL-1	5.06	44.10	IPT-1	6.02	50.60
IPL-2	5.27	49.70	IPT-2	5.60	41.03
IPL-3	5.44	46.50	IPT-3	5.57	49.83
IPL-4	5.60	49.60	IPT-4	5.16	51.18
IPL-5	5.61	51.00	IPT-5	—	47.04
Mean	5.40	48.20	Mean	5.59	47.94
Std. Dev.	0.23	2.82	Std. Dev.	0.35	4.17
CV (%)	4.30	5.80	CV (%)	6.30	8.70

(2) Average shear strength is not influenced by the test temperature. For example:

Longitudinal shear Strength: 44.0 ksi at RT;
48.2 ksi at -150°F; and
46.30 ksi at 250°F for 25 v/o SiC_w/2124-T6

(3) In 25 v/o SiC_p/2124-T6, the average longitudinal shear strengths at RT and -150°F (39.54 and 34.34 ksi respectively) were lower than the transverse shear strength values (46.92 and 44.2 ksi respectively), suggesting localized microstructural variation such as particulate orientation and volume percent in the as processed composite.

3.2 SUMMARY OF 25 V/O DISCONTINUOUS SIC/AL TEST DATA

Mechanical and thermophysical propert test data of 25 v/o discontinuous SiC/2124-T6 are summarized in the following tables:

25 w/o SiC_p/2124-T6 Al Panel:	Table 3.2-1
25 w/o SiC_w/2124-T6 Al Panel:	Table 3.2-2

*Table 3.2-1 25 v/o SiCp/Al 2124-T6 Panels **

NOT DESIGN ALLOWABLE DATA

PROPERTIES						TEMPERATURE (°F)			Std. Dev. / No. of Specimens at RT	Test Method
PHYSICAL			MECHANICAL & THERMAL			-150	Room	250		
Density (lb / in^3)		0.101	Longitudinal Tensile Strength	σ_x^{TU}	ksi	92.66	84.5	73.89	± 3.79 / 5	ASTM D-3552
Fiber volume fraction		0.25	Transverse Tensile Strength	σ_y^{TU}	ksi	91.42	77.5	73.97	±4.87 / 5	ASTM D-3552
Void volume fraction		<0.001	Longitudinal Comp. Strength	σ_x^{CU}	ksi	109.7	80.8	73.16	±2.071 / 5	ASTM D-3410
Nominal ply thickness	in	0.060	Transverse comp. strength	σ_y^{CU}	ksi	109.4	75.8	72.44	±1.610 / 5	ASTM D-3410
Max. cont. use temp.	°F	~550	In-plane shear strength	IPSS	ksi	34.31	39.54	47.91		
OPTICAL & ELECTRICAL (at room temperature)			Interlaminar shear strength	ILSS	ksi	----	----	----		
			Longitudinal tensile strain **	ε_x^T	%		1.258		±0.0045 / 5	ASTM D-3552
			Transverse tensile strain **	ε_y^T	%		1.18		±0.212 / 5	ASTM D-3552
			Longitudinal comp. strain **	ε_x^C	%		0.618		±0.0024 / 5	ASTM D-3410
			Transverse comp. strain **	ε_y^C	%		0.620		±0.006 / 5	ASTM D-3410
Solar Absorptance	α	0.57	Longitudinal tensile modulus	E_x	Msi	16.75	16.64	15.58	±0.410 / 5	ASTM D-3552
			Transverse tensile modulus	E_y	Msi	16.12	17.0	15.65	±0.324 / 5	ASTM D-3552
Normal Emissivity	ε	0.150	Longitudinal comp. modulus	E_x	Msi	17.42	18.5	16.16	±0.207 / 5	ASTM D-3410
			Transverse comp. modulus	E_y	Msi	16.28	17.9	15.78	±0.904 / 5	ASTM D-3410
Electrical Resistivity	R	8.5 μΩ·cm	In-plane shear modulus	G	Msi	6.00	5.94	5.03		
			Longitudinal flexural modulus	F_x	Msi	16.76	13.51	16.45	±0.156 / 3	ASTM D-790M
			Transverse flexural modulus	F_y	Msi	16.44	13.02	16.82	±0.4195 / 3	ASTM D-790M
			Long. tensile Poisson's ratio	ν_{xy}		0.291	0.267	0.269	±0.0023 / 5	ASTM D-3552
			Trans. tensile Poisson's ratio	ν_{yx}		0.289	0.279	0.261	±0.017 / 5	ASTM D-3552
			Long. thermal conductivity	K_x	(1)	3.373	5.740	6.486		Kohlrausch
			Trans. thermal conductivity	K_y	(1)	3.3026	5.6116	6.111		Kohlrausch
			Thru thickness thermal cond.	K_z	(1)					
			Specific heat	C_p	(2)	0.123	0.1984	0.243		ASTM E1269
			Longitudinal CTE	α_x	(3)		8.16			ASTM E-80
			Transverse CTE	α_y	(3)		7.86			ASTM E-80
			Thru thickness CTE	α_z	(3)		—			

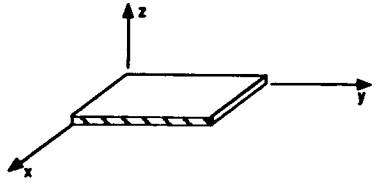

* RT Test Panels (0.040-in. thick) were from a different batch than the -150°F and 250°F test panels (0.060-in. thick)

Notes: (**) - Strain to failure; (1) Btu/(hr·in·°F); (2) Btu/(lb·°F); (3) μin./in./°F

*Table 3.2-2 25 v/o SiCw/Al 2124-T6 Panels **

NOT DESIGN ALLOWABLE DATA

PROPERTIES						TEMPERATURE (°F)			Std. Dev. / No. of Specimens at RT	Test Method
PHYSICAL			MECHANICAL & THERMAL			-150	Room	250		
Density (lb / in^3)	X	0.101	Longitudinal Tensile Strength	σ_x^{TU}	ksi	108.8	102.0	93.02	± 4.62 / 5	ASTM D-3552
Fiber volume fraction	X	0.25	Transverse Tensile Strength	σ_y^{TU}	ksi	94.16	97.4	76.0	± 1.54 / 5	ASTM D-3552
Void volume fraction	X	<0.001	Longitudinal Comp. Strength	σ_x^{CU}	ksi	106.56	102.5	81.28	± 1.57 / 4	ASTM D-3410
Nominal ply thickness	in	0.060	Transverse comp. strength	σ_y^{CU}	ksi	102.18	91.0	67.11	± 2.13 / 5	ASTM D-3410
Max. cont. use temp.	°F	~550	In-plane shear strength	IPSS	ksi	48.2	44.0	46.0		
OPTICAL & ELECTRICAL (at room temperature)			Interlaminar shear strength	ILSS	ksi					
Solar Absorptance	α	0.57	Longitudinal tensile strain **	ε_x^T	%		1.62		± 0.15 / 5	ASTM D-3552
Normal Emissivity	ε	0.150	Transverse tensile strain **	ε_y^T	%		1.83		± 0.048 / 5	ASTM D-3552
Electrical Resistivity	R	8.5 μΩ·cm	Longitudinal comp. strain **	ε_x^C	%		1.11		± 0.025 / 4	ASTM D-3410
			Transverse comp. strain **	ε_y^C	%		1.26		± 0.096 / 5	ASTM D-3410
			Longitudinal tensile modulus	E_x	Msi	17.21	17.6	17.67	± 0.415 / 5	ASTM D-3552
			Transverse tensile modulus	E_y	Msi	17.03	16.42	15.31	± 0.295 / 5	ASTM D-3552
			Longitudinal comp. modulus	E_x	Msi	17.57	18.15	17.33	± 0.265 / 4	ASTM D-3410
			Transverse comp. modulus	E_y	Msi	17.44	16.5	14.61	± 0.33 / 5	ASTM D-3410
			In-plane shear modulus	G	Msi	6.19	5.40	5.23		
			Longitudinal flexural modulus	F_x	Msi	17.59	13.1	17.2	± 0.208 / 3	ASTM D-790M
			Transverse flexural modulus	F_y	Msi	17.0	11.8	16.75	± 0.0577 / 3	ASTM D-790M
			Long. tensile Poisson's ratio	ν_{xy}	X	0.298	0.2934	0.295	± 0.0136 / 5	ASTM D-3552
			Trans. tensile Poisson's ratio	ν_{yx}	X	0.297	0.2717	0.256	± 0.00651 / 5	ASTM D-3552
			Long. thermal conductivity	K_x	(1)		4.87			Kohlrausch
			Trans. thermal conductivity	K_y	(1)		4.71			Kohlrausch
			Thru thickness thermal cond.	K_z	(1)		4.57			
			Specific heat	C_p	(2)		0.199			ASTM E1269
			Longitudinal CTE	α_x	(3)		8.03			ASTM E-80
			Transverse CTE	α_y	(3)		7.77			ASTM E-80
			Thru thickness CTE	α_z	(3)		----			

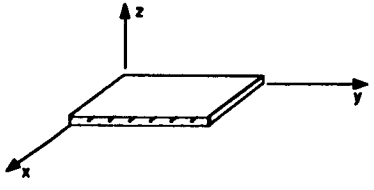

* RT Test Panels (0.040-in. thick) were from a different batch than the -150°F and 250°F test panels (0.060-in. thick)

Notes: (**) - Strain to failure; (1) Btu/(hr·in·°F); (2) Btu/(lb·°F); (3) μin./in./°F

APPENDIX A

A.0 MATERIAL PROPERTY TEST DATA

A.1 INTRODUCTION

Extensive mechanical and thermophysical property tests of various SOA composites have been conducted, and a reliable database has been constructed for spacecraft material selection. The composites included GRAPHITE/EPOXY (Gr/E), graphite/thermoplastic (Gr/TP), Graphite/thermoplastics (Gr/TP), discontinuous silicon carbide/aluminum (SiC/Al), graphite/aluminum (Gr/Al), graphite/magnesium (Gr/Mg), carbon/glass (C/Gl), and C/C materials. Of the test methods, American Society for Testing and Materials (ASTM) standards were used whenever they were applicable. In the absence of an ASTM Standard, DoD/NASA, Thermophysical Property Research Laboratory (TPRL), or Martin Marietta Astronautics Group recommended test methods were used.

Material property results for the majority of the as-fabricated composites were consistent with the predicted values, providing a measure of consolidation integrity attained during fabrication. To determine the effect of thermal cycling on mechanical properties and dimensional stability, approximately 500 composite specimens were exposed to ~10,000 cycles between -150°F and +150°F. These specimens were placed in a large (18-ft^3 workspace) thermal cycling chamber that was specially designed and fabricated in this program to simulate one year orbital thermal cycling (i.e., about 5840 cycles between -150°F and +150°F in low earth orbit (LEO) in 20 days. With this rate of thermal cycling, this is the largest thermal cycling unit in the country.

Reference specimens of each composite were also cycled in this chamber to examine the

extent of microcracking as a result of thermal cycling. After 10,000 thermal cycles, only a few new microcracks and delaminations were observed in the organic matrix composite (OMC) laminates indicating that the thermal stresses were mostly accommodated by the microcracks that were generated during the consolidation process. In unidirectional Gr/E, discontinuous SiC/Al, Gr/Al, C/Gl, and C/C no new cracks were detected. Material property measurements of the Gr/E, Gr/TP, and C/TP laminate specimens exhibited less than 25% decrease in strength, whereas, the remaining materials exhibited less than 8% decrease in strength. The thermal expansion response of each of the thermal cycled specimens revealed significant reduction in hysteresis and residual strain, and the average CTE values were close to the predicted values.

A.2 TEST DATA SUMMARY

The average mechanical and thermophysical properties obtained from room temperature tests of as-fabricated composites are summarized in Table A.2-1 and details of these results are discussed in Chapters 2 to 10 of NASA CR #187472. Measured properties of the composites are in agreement with the values predicted from the simple rule of mixture (ROM) equations (Appendix C) and the laminate properties estimated by the computer analysis (GENLAM). Quantitative comparison for each composite system are presented in respective chapters. In the modulus and strength measurements, the coefficient of variation (CV) is less than 6%, whereas in Poisson ratio and strain to failure measurements the CV is about 12%. This level of scatter is reasonable to expect in SOA composites. Of the various tests, in general compressive property measurements indicated more scatter in the data than other mechanical and thermophysical property tests. The extent of scatter in compressive properties can be attributed both to the test method (Celanese compression - using 0.5 in. gauge length) and to inherent material response.

Overall, the reasonable agreement between the measured and predicted properties (Table A.2-2)

Table A.2-1 As-Fabricated Composite Materials Tested at Room Temperature

MATERIAL PROPERTY			Gr/Ep P75/1962	Gr/Ep P75/1962	Gr/TP P75/PEEK	Gr/TP P75/PEEK	Gr/TP AS4/PES	Gr/TP AS4/PES
Density	ρ	lb/in^3	0.0624	0.0625	0.0628	0.0628	0.0578	0.0578
Fiber Volume Fraction	V_f		0.622	0.627	0.622	0.622	0.537	0.5496
Nominal Ply Thickness	t	in.	0.00463	0.00458	0.0050	0.005	0.005	0.005
Max. Continuous Use Temp.	T	°F	260	260	250	250	250	250
Ply Orientation	θ	deg	$[0/45/90/-45]_s$	$[30/-30/0_4]_s$	$[0/\pm45/90]_s$	$[30/-30/0_4]_s$	$[0/\pm45/90]_s$	$[30/-30/0_4]_s$
Longitudinal Tensile Strength	σ_x^{TU}	ksi	44.6	85.5	34.91	68.77	80.34	101.61
Transverse Tensile Strength	σ_y^{TU}	ksi	50.1	4.4	43.2	5.46	77.69	4.54
Longitudinal Comp. Strength	σ_x^{CU}	ksi	26.5	54.3	21.35	51.38	47.31	90.29
Transverse Comp. Strength	σ_y^{CU}	ksi	27.6	17.7	21.75	17.54	30.36	21.07
Interlaminar Shear Strength	ILSS	ksi	5.03	6.38	4.78	7.41	7.11	9.81
Longitudinal Tensile Strain	ε_x^T	---	0.261	0.243	0.263	0.23	1.35	0.90
Transverse Tensile Strain	ε_y^T	---	0.301	0.23	0.286	0.44	1.18	0.308
Longitudinal Tensile Modulus	E_x^T	Msi	15.2	32.68	13.3	30.06	6.38	14.18
Transverse Tensile Modulus	E_y^T	Msi	15.2	1.79	14.0	1.40	6.51	1.57
Longitudinal Comp Modulus	E_x^C	Msi	13.9	27.64	9.02	28.40	5.82	12.36
Transverse Comp Modulus	E_y^C	Msi	13.6	1.73	9.36	1.14	5.63	1.26
In-Plane Shear Modulus	G	Msi	---	---	---	---	---	---
Longitudinal Flexural Modulus	F_x	Msi	15.17	14.56	16.29	12.05	9.26	7.18
Transverse Flexural Modulus	F_y	Msi	6.35	1.90	2.4	0.943	1.68	1.34
Long. Tensile Poisson's Ratio	ν_{xy}	---	0.3066	1.2122	0.3487	1.3685	0.2918	0.8872
Trans. Tensile Poisson's Ratio	ν_{yx}	---	0.3146	0.0825	0.3378	0.0719	0.3240	0.083
Long. Thermal Conductivity	K_x	(1)	2.1	3.97	2.23	3.74	0.11	0.115
Trans. Thermal Conductivity	K_y	(1)	2.11	0.40	2.34	0.38	0.19	0.043
Specific Heat	Cp	(2)	0.193	0.193	0.203	0.193	0.197	0.196
Longitudinal CTE	α_x	(2)	-0.454	-1.02	-0.28	-0.39	1.08	-0.66
Transverse CTE	α_y	(3)	-0.014	+5.83	0.04	10.17	1.38	12.6

(1) Btu/(hr·in.·°F); (2) Btu/(lb·°F); (3) µin./in/°F

Table A.2-1 As-Fabricated Composite Materials Tested at Room Temperature (Cont')

MATERIAL PROPERTY			MMC's SiC_p/2124 Al	MMC's SiC_w/2124 Al	MMC's SiC_p/2124 Al	MMC's SiC_p/2124 Al	Gr/Metals P100/6061 Al	Gr/Metals P100/AZ91CMg
Density	ρ	lb/in^3	0.104	0.104	0.106	0.106	0.090	0.0683
Fiber Volume Fraction	V_f		25	25	35	35	0.422	0.301
Nominal Ply Thickness	t	in.	0.060	0.060	0.060	0.060	0.0216	0.0125
Max. Continuous Use Temp.	T	°F	550	550	550	550	550	550
Ply Orientation	θ	deg	N/A	N/A	N/A	N/A	$[0]_2$	$[16]_c$
Longitudinal Tensile Strength	σ_x^{TU}	ksi	84.5	102.0	96.5	85.7	131.3	61.2
Transverse Tensile Strength	σ_y^{TU}	ksi	77.5	97.4	97.0	57.7	3.62	3.69
Longitudinal Comp. Strength	σ_x^{CU}	ksi	80.8	102.5	103.3	97.0	46.62	29.1
Transverse Comp. Strength	σ_y^{CU}	ksi	75.8	91.0	103.4	82.4	15.21	---
Interlaminar Shear Strength	ILSS	ksi	---	---	---	---	5.487	---
Longitudinal Tensile Strain	ε_x^T	---	1.258	1.62	1.038	1.0	0.262	0.21
Transverse Tensile Strain	ε_y^T	---	1.18	1.83	1.074	0.9	0.0707	---
Longitudinal Tensile Modulus	E_x^T	Msi	16.64	17.6	19.9	18.8	49.71	25.44
Transverse Tensile Modulus	E_y^T	Msi	17.0	16.42	19.4	17.2	5.14	4.1
Longitudinal Comp Modulus	E_x^C	Msi	18.5	18.15	20.4	19.22	48.15	18.9
Transverse Comp Modulus	E_y^C	Msi	17.9	16.5	21.0	17.2	4.82	---
In-Plane Shear Modulus	G	Msi	---	—	---	---	2.62	---
Longitudinal Flexural Modulus	F_x	Msi	13.51	13.1	16.9	13.11	26.25	---
Transverse Flexural Modulus	F_y	Msi	13.02	11.8	17.0	11.8	4.16	---
Long. Tensile Poisson's Ratio	ν_{xy}	---	0.267	0.2934	0.2539	0.2711	0.2949	0.46
Trans. Tensile Poisson's Ratio	ν_{yx}	---	0.279	0.2717	0.2481	0.2363	0.0211	---
Long. Thermal Conductivity	K_x	(1)	5.740	4.87	5.75	4.24	15.278	---
Trans. Thermal Conductivity	K_y	(1)	5.616	4.71	5.42	4.28	3.333	---
Specific Heat	Cp	(2)	0.1984	0.199	0.189	0.189	0.194	0.219
Longitudinal CTE	α_x	(2)	8.16	8.03	5.86	5.91	-0.27	---
Transverse CTE	α_y	(3)	7.86	7.77	6.11	6.29	11.37	---

(1) Btu/(hr·in.·°F); (2) Btu/(lb·°F); (3) µin./in/°F

Table A.2-1 As-Fabricated Composite Materials Tested at Room Temperature (Cont')

MATERIAL PROPERTY			C/Glass HMU/7070	C/Glass HMU/7070	C/C P100/C	C/C P100/C		
Density	ρ	lb/in^3	0.072	0.071	0.060	0.060		
Fiber Volume Fraction	V_f		0.44	0.40	0.5248	0.53		
Nominal Ply Thickness	t	in.	0.052	0.052	0.017	0.017		
Max. Continuous Use Temp.	T	°F	1500	1500	3700	3700		
Ply Orientation	θ	deg	$[0]_{12}$	$[0/90]_6$	$[0]_3$	[0/90/0]		
Longitudinal Tensile Strength	σ_x^{TU}	ksi	95.5	>40.9	81.5	44.1		
Transverse Tensile Strength	σ_y^{TU}	ksi	---	---	2.04	29.0		
Longitudinal Comp. Strength	σ_x^{CU}	ksi	126.3	86.7	47.8	6.95		
Transverse Comp. Strength	σ_y^{CU}	ksi	---	78.4	4.6	9.4		
Interlaminar Shear Strength	ILSS	ksi	---	3.35	3.47	1.96		
Longitudinal Tensile Strain	ε_x^T	---	0.353	0.405	0.225	0.17		
Transverse Tensile Strain	ε_y^T	---	---	---	0.208	~0.15		
Longitudinal Tensile Modulus	E_x^T	Msi	26.43	11.7	43.7	32.4		
Transverse Tensile Modulus	E_y^T	Msi	---	---	1.45	20.3		
Longitudinal Comp Modulus	E_x^C	Msi	21.3	12.7	39.4	29.1		
Transverse Comp Modulus	E_y^C	Msi	---	11.9	1.3	15.5		
In-Plane Shear Modulus	G	Msi	2.6	---	1.44	---		
Longitudinal Flexural Modulus	F_x	Msi	---	---	---	---		
Transverse Flexural Modulus	F_y	Msi	---	---	---	---		
Long. Tensile Poisson's Ratio	ν_{xy}	---	0.227	0.033	0.3690	0.145		
Trans. Tensile Poisson's Ratio	ν_{yx}	---	---	---	0.0446	0.1		
Long. Thermal Conductivity	K_x	(1)	---	0.83	9.86	6.83		
Trans. Thermal Conductivity	K_y	(1)	---	0.83	0.38	3.25		
Specific Heat	Cp	(2)	---	0.18	---	0.169		
Longitudinal CTE	α_x	(2)	-0.38	-0.075	-0.98	-0.95		
Transverse CTE	α_y	(3)	---	---	-0.42	---		

(1) Btu/(hr·in.·°F); (2) Btu/(lb·°F); (3) µin./in/°F

Table A.2-2 Comparison of Measured and Predicted Properties of Selected Composite Materials

Composite	E_x^T (Msi)		CTE_x (ppm/°F)	
	Measured	Predicted	Measured †	Predicted
P75/1962, v/o = 62.2				
$[0]_8$	46.3	46.8	-0.69	-0.60
$[0, \pm45, 90]_s$	15.2	15.8	-0.454	-0.34
P75/PEEK v/o = 62.2				
$[0, \pm45, 90]_s$	14.0	16.0	-0.28	-0.30
$[\pm30, 0_4]_s$	30.06	34.5	-0.39*	-1.01
25 v/o SiC/Al	16.64	16.8	8.16	8.56
P100/6061 Al v/o = 42.2				
$[0]_2$	49.71	40.9	-0.27 **	0.73

† Slope of a line joining the extreme points (±150°F) of the first cycle thermal expansion curve

* After thermal cycling CTE_x = -0.81 ppm/°F

** After thermal cycling CTE_x = 0.99 ppm/°F

and low CV indicated that SOA composites have adequate consolidation quality. For example, of the organic matrix composites, Gr/E composites exhibited higher tensile strength and modulus than Gr/PEEK, for the same fiber orientation and fiber volume (Figure A.2-1). These property differences in terms of processing techniques and microstructural characteristics of GR/PEEK are discussed in chapter 3.0. The AS4/PES panels exhibited slightly lower strength values than expected due to the presence of disbonded and delaminated regions in the as-consolidated laminate. Thus, the presence of any internal defects created during the processing of the composite was verified by the anamolous response in material property tests. Of the discontinuous metal matrix composites (MMC's), 25 v/o SiC_w/2124-T6 exhibited the expected modulus and strength values and nearly isotropic response (Figure A.2-2), whereas the 35v/o SiC_w/2124-T6 showed lower than expected modulus in both the longitudinal and transverse direction. Reduced modulus in this composite was attributed to the absence of whisker/matrix bonding in random locations where the whiskers clustered and lacked matrix infiltration during consolidation. Measured mechanical properties of continuous fiber reinforced composites such

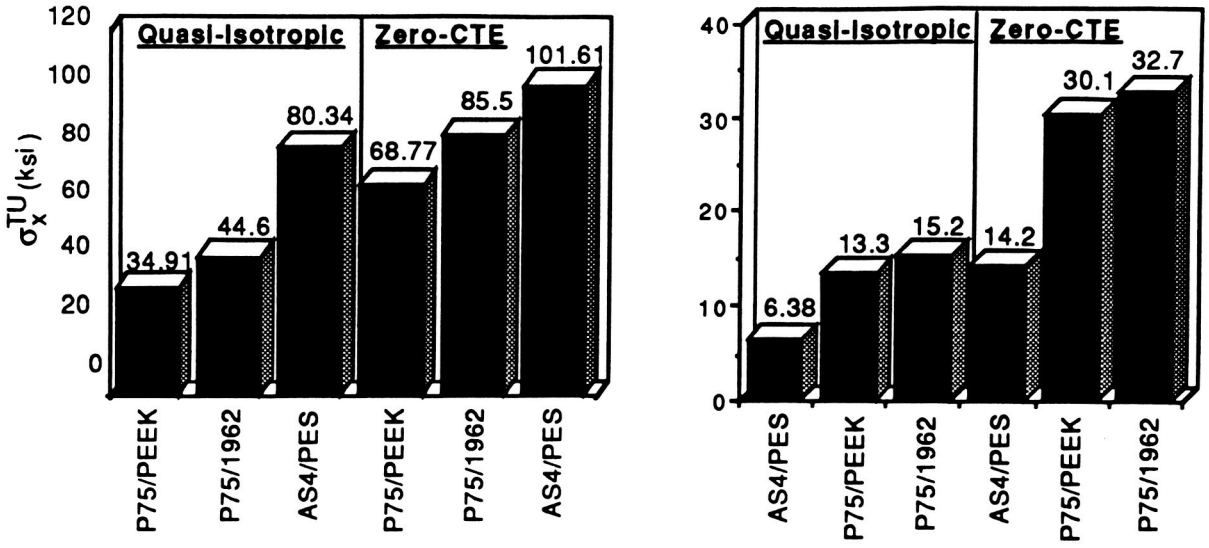

Figure A.2-1 Tensile Modulus and Strength Comparison of Gr/E and Gr/TP Composites

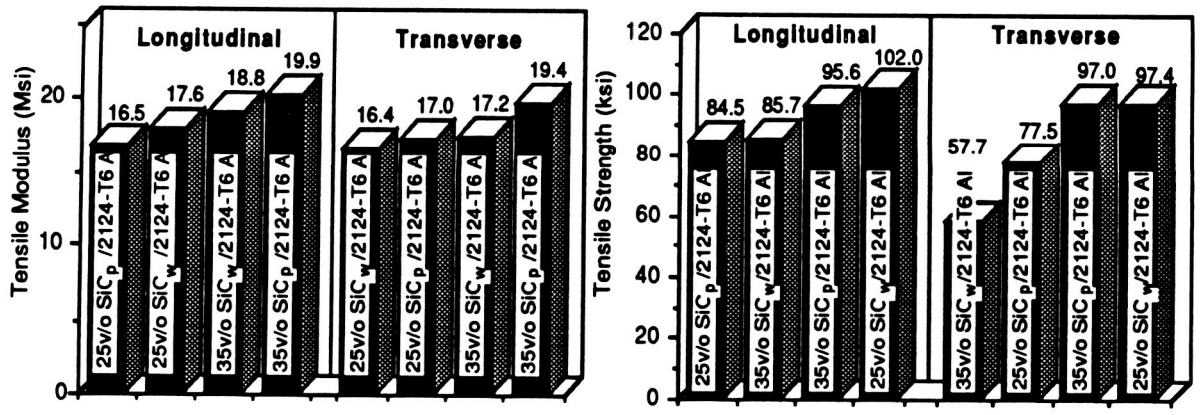

Figure A.2-2 Longitudinal and Transverse Modulus Comparison of Discontinuous SiC/Al Composites

as P100/Al, P100/Mg, and P100/C and C/Gl composites were in good agreement with the predicted values.

During thermophysical property tests, each composite exhibited reproducible thermal conductivity, specific heat and electrical resistivity values which were consistent with the expected values. The average CTE values (in Table A.2-2) were obtained by joining the extreme points of thermal expansion response curve in the first cycle (RT $\rightarrow$ +150°F $\rightarrow$ -150°F $\rightarrow$ RT) because it is difficult to assign a single CTE values when it continuously changes with temperature.

For the P75/1962 $[0]_8$, discontinuous SiC/Al, HMU/7070, and C/C composites, the measured CTE values were in close agreement with the predicted values. Whereas, in the remaining organic matrix and metal matrix composites, the difference in average CTE and predicted values were attributed to the following two reasons:

(i) First cycle response was significantly influenced by the residual stress state generated during fabrication, and

(ii) The push rod dilatometer has relatively poor strain resolution ($\approx$ 10 ppm) compared to 1 ppm for laser interferometric dilatometer (Details in Appendix C).

For example, the P75/PEEK and AS4/PES $[0, \pm45, 90]_s$ laminates do not exhibit nearly quasi-isotropic thermal expansion response (in the first cycle)because of fiber waviness and differences in residual stress state and defect density between the longitudinal and transverse directions. In general, the thermal expansion response of each composite exhibited maximum hysteresis and residual strain in the first cycle. As discussed in the literature (Ref 12, 31, 32, 40, 42, 54, 63-67), the hysteresis and residual strain are gradually reduced as the residual stresses at the reinforcement/matrix interface are relieved during subsequent thermal cycles.

A.3 EFFECT OF THERMAL CYCLING ON MATERIAL PROPERTIES

Thermal stress generated at the reinforcement/matrix interfaces during LEO cycling between -150°F and 150°F can induce microdamage in composites. This microdamage will change the thermal-mechanical properties of the material, and as a result significantly affect the dimensional stability and performance of the composite structure (Ref 11-18). Therefore, to examine the effect of thermal cycling, the technical approach included (1) dimensional change measurements (2) microstructural examination of damage, and (3) material property tests (tension, compression and CTE).

A.3.1 Dimensional Measurements

Length and width of thermal cycled specimens were determined and compared with their initial dimensions. Dial calipers used for measuring length and micrometers used for measuring width were calibrated, both with a sensitivity of 0.001-in. These measurements indicated that after 10,099 cycles, the transverse test specimens from $[30, -30, 0_4]_s$ laminate showed a slightly larger length increase than longitudinal specimens. These differences in transverse and longitudinal specimens were consistent with the changes in CTE due to thermal cycling. While the dimensional changes indicated a trend, their absolute values should be taken with caution for the following reasons (1) sensitivity limitation of the calipers and micrometers; and (2) flatness of edge finish.

A.3.2 Microstructural Examination of Damage

Initially the edges of a 1-in. x 1-in. reference specimen (from each composite) were polished, and subsequently examined under the optical microscope (at magnification 100x - 500x) to evaluate the damage during cycling. Microstructures of these specimens indicated that there was

a high incidence of microcrack initiation (and extension) in quasi-isotropic and zero-CTE P75/1962, P75/PEEK, and AS4/PES panels. In most cases a pre-existing microcrack propagated, though a few new cracks were also observed. In metal matrix, glass matrix and C/C composites, no detectable increase in the baseline microcrack density was observed. It appears that the thermal stresses generated during cycling of MMC are accommodated by microplastic deformation at the reinforcement matrix interface. Whereas in C/glass and C/C composite, thermal stresses at the interface may not be high enough to induce damage.

A.3.3 Material Property Tests

Material properties of thermal-cycled composites are listed in Table A.3-1. To determine the effect of the thermal cycling, the longitudinal and transverse mechanical properties have been compared with the properties of the as-fabricated composites in Tables A.3-2 and A.3-3 respectively. These results indicated ≤25% reduction in the tensile strength of the quasi-isotropic Gr/E, and zero-CTE Gr/E and AS4/PES laminates, whereas the Gr/PEEK composites exhibited no degradation of tensile or compressive properties. The mechanical property responses of thermal cycled Gr/Al, SiC_p/Al, C/C and C/Gl composites were nearly similar to the responses obtained in as-fabricated composites. In the case of SiC_w/Al, there was about a 10% decrease in strength without any significant change in the elastic modulus.

The CTE values of thermal cycled and as-fabricated composites are listed in Table A.3-4. As expected, the thermal expansion of cycled specimens exhibited reduced residual strain and RT hysteresis. The average CTE values were more consistent with the predicted values, as the residual stresses were relieved during cycling. For example the $[0, 45,90, -45]_s$ Gr/E, Gr/TP laminates exhibited the quasi-isotropic CTE values. For Gr/Al panel, the measured CTE of 0.99 ppm/°F was close to the predicted value of 0.73 ppm/°F. The CTE values of all composites were indicative of a stabilized thermal expansion response after cycling.

Table A.3-1 Thermal Cycled Composite Materials Tested at Room Temperature

MATERIAL PROPERTY			Gr/Ep P75/1962	Gr/Ep P75/1962	Gr/TP P75/PEEK	Gr/TP P75/PEEK	Gr/TP AS4/PES	Gr/TP AS4/PES
Density	ρ	lb/in^3	0.0624	0.0625	0.0628	0.0628	0.0578	0.0578
Fiber Volume Fraction	V_f		0.622	0.627	0.622	0.622	0.537	0.5496
Nominal Ply Thickness	t	in.	0.00463	0.00458	0.005	0.005	0.005	0.005
Max. Continuous Use Temp.	T	°F	260	260	250	250	250	250
Ply Orientation	θ	deg	$[0/45/90/-45]_s$	$[30/-30/0_4]_s$	$[0/\pm45/90]_s$	$[30/-30/0_4]_s$	$[0/\pm45/90]_s$	$[30/-30/0_4]_s$
Longitudinal Tensile Strength	σ_x^{TU}	ksi	31.5	64.9	37.2	68.14	77.1	78.4
Transverse Tensile Strength	σ_y^{TU}	ksi	42.2	4.06	39.7	5.61	71.4	5.21
Longitudinal Comp. Strength	σ_x^{CU}	ksi	26.5	49.71	24.21	40.2	45.45	76.38
Transverse Comp. Strength	σ_y^{CU}	ksi	25.08	17.58\	25.46	17.96	26.67	17.65
Interlaminar Shear Strength	ILSS	ksi	---	---	---	---	---	---
Longitudinal Tensile Strain	ε_x^T	---	---	---	---	---	---	---
Transverse Tensile Strain	ε_y^T	---	---	---	---	---	---	---
Longitudinal Tensile Modulus	E_x^T	Msi	14.35	28.2	13.3	31.6	6.41	14.5
Transverse Tensile Modulus	E_y^T	Msi	15.5	1.70	13.6	1.21	6.7	1.46
Longitudinal Comp Modulus	E_x^C	Msi	13.9	23.09	10.3	21.43	5.42	10.86
Transverse Comp Modulus	E_y^C	Msi	11.58	1.44	9.43	1.17	5.95	1.25
In-Plane Shear Modulus	G	Msi	---	---	---	---	---	---
Longitudinal Flexural Modulus	F_x	Msi	---	---	---	---	---	---
Transverse Flexural Modulus	F_y	Msi	---	---	---	---	---	---
Long. Tensile Poisson's Ratio	ν_{xy}	---	---	---	---	---	---	---
Trans. Tensile Poisson's Ratio	ν_{yx}	---	---	---	---	---	---	---
Long. Thermal Conductivity	K_x	(1)	---	---	---	---	---	---
Trans. Thermal Conductivity	K_y	(1)	---	---	---	---	---	---
Specific Heat	Cp	(2)	---	---	---	---	---	---
Longitudinal CTE	α_x	(2)	-0.585	-1.02	-0.248	-0.81	0.65	-0.37
Transverse CTE	α_y	(3)	-0.395	2.92	-0.201	7.60	0.285	10.68

(1) Btu/(hr·in.·°F); (2) Btu/(lb·°F); (3) µin./in/°F

Table A.3-1 Thermal Cycled Composite Materials Tested at Room Temperature (Cont')

MATERIAL PROPERTY			MMC's SiC_p/2124 Al	MMC's SiC_w/2124 Al	MMC's SiC_p/2124 Al	MMC's SiC_p/2124 Al		
Density	ρ	lb/in^3	0.101	0.101	0.104	0.104		
Fiber Volume Fraction	V_f		25	25	35	35		
Nominal Ply Thickness	t	in.	0.060	0.060	0.060	0.060		
Max. Continuous Use Temp.	T	°F	550	550	550	550		
Ply Orientation	θ	deg	N/A	N/A	N/A	N/A		
Longitudinal Tensile Strength	σ_x^{TU}	ksi	86.2	96.7	92.8	75.3		
Transverse Tensile Strength	σ_y^{TU}	ksi	90.6	93.0	91.92	56.7		
Longitudinal Comp. Strength	σ_x^{CU}	ksi	76.85	94.26	92.98	97.64		
Transverse Comp. Strength	σ_y^{CU}	ksi	86.33	75.76	97.7	95.33		
Interlaminar Shear Strength	ILSS	ksi	---	---	---	---		
Longitudinal Tensile Strain	ε_x^T	---	---	---	---	---		
Transverse Tensile Strain	ε_y^T	---	---	---	---	---		
Longitudinal Tensile Modulus	E_x^T	Msi	16.64	17.1	19.9	18.9		
Transverse Tensile Modulus	E_y^T	Msi	16.8	16.3	19.1	16.6		
Longitudinal Comp Modulus	E_x^C	Msi	16.5	16.13	18.18	19.28		
Transverse Comp Modulus	E_y^C	Msi	17.73	15.98	18.98	17.8		
In-Plane Shear Modulus	G	Msi	---	---	---	---		
Longitudinal Flexural Modulus	F_x	Msi	---	---	---	---		
Transverse Flexural Modulus	F_y	Msi	---	---	---	---		
Long. Tensile Poisson's Ratio	ν_{xy}	---	---	---	---	---		
Trans. Tensile Poisson's Ratio	ν_{yx}	---	---	---	---	---		
Long. Thermal Conductivity	K_x	(1)	---	---	---	---		
Trans. Thermal Conductivity	K_y	(1)	---	---	---	---		
Specific Heat	Cp	(2)	---	---	---	---		
Longitudinal CTE	α_x	(2)	8.69	8.56	6.78	---		
Transverse CTE	α_y	(3)	7.78	8.65	7.55	---		

(1) Btu/(hr·in.·°F); (2) Btu/(lb·°F); (3) µin./in/°F

Table A.3-1 Thermal Cycled Composite Materials Tested at Room Temperature (Cont')

MATERIAL PROPERTY			Gr/Metals P100/6061 Al	C/Gl HMU/7070	C/C P100/C			
Density	ρ	lb/in^3	0.090	0.071	0.0605			
Fiber Volume Fraction	V_f		0.422	0.40	0.53			
Nominal Ply Thickness	t	in.	0.0216	0.0052	0.017			
Max. Continuous Use Temp.	T	°F	550	1500	3700			
Ply Orientation	θ	deg	$[0]_2$	[0/90]6	[0/90/0]			
Longitudinal Tensile Strength	σ_x^{TU}	ksi	127.0	—	36.78			
Transverse Tensile Strength	σ_y^{TU}	ksi	---	—	28.7			
Longitudinal Comp. Strength	σ_x^{CU}	ksi	43.70	84.68	15.63			
Transverse Comp. Strength	σ_y^{CU}	ksi	20.30	74.57	8.63			
Interlaminar Shear Strength	ILSS	ksi	---		---			
Longitudinal Tensile Strain	ε_x^T	---	---		---			
Transverse Tensile Strain	ε_y^T	---	---		---			
Longitudinal Tensile Modulus	E_x^T	Msi	52.48		26.79			
Transverse Tensile Modulus	E_y^T	Msi	---		13.7			
Longitudinal Comp Modulus	E_x^C	Msi	45.33	12.44	28.58			
Transverse Comp Modulus	E_y^C	Msi	4.40	13.14	9.26			
In-Plane Shear Modulus	G	Msi	---		---			
Longitudinal Flexural Modulus	F_x	Msi	---		---			
Transverse Flexural Modulus	F_y	Msi	---		---			
Long. Tensile Poisson's Ratio	ν_{xy}	---	---		---			
Trans. Tensile Poisson's Ratio	ν_{yx}	---	---		---			
Long. Thermal Conductivity	K_x	(1)	---		---			
Trans. Thermal Conductivity	K_y	(1)	---		---			
Specific Heat	Cp	(2)	---		---			
Longitudinal CTE	α_x	(2)	0.99	0.28	-0.737			
Transverse CTE	α_y	(3)	---	0.40	-0.87			

(1) Btu/(hr·in.·°F); (2) Btu/(lb·°F); (3) µin./in/°F

Table A.3-2 Effect of Thermal Cycling on the Longitudinal Tensile and Compressive Properties of Composite Materials

Material	Density (lb/in^3)	Tension				Compression			
		E_x^T (Msi)		σ_x^{TU} (ksi)		E_x^C (Msi)		σ_x^{CU} (ksi)	
		AF	TC	AF	TC	AF	TC	AF	TC
P75/1962									
•62.2v/o, $[0, \pm45, 90]_s$	0.0623	15.2	14.35	44.6	31.5	13.9	9.88	26.5	25.66
•62.2v/o, $[\pm30, 0_4]_s$	0.0623	32.68	28.2	85.5	64.9	27.6	23.09	54.3	49.71
P75/PEEK									
•62.2v/o, $[0, \pm45, 90]_s$	0.063	13.3	13.3	34.91	37.2	9.02	10.30	21.35	24.21
•62.2v/o, $[\pm30, 0_4]_s$	0.063	30.06	31.6	68.77	68.14	28.40	21.43	51.38	40.2
AS4/PES									
•62.2v/o, $[0, \pm45, 90]_s$	0.058	6.38	6.41	80.34	77.1	5.82	5.42	47.31	45.45
•62.2v/o, $[\pm30, 0_4]_s$	0.058	14.18	14.5	101.61	78.4	12.36	10.86	90.29	76.88
SIC_p/Al									
•25 v/o, N/A	0.104	16.64	16.8	84.5	86.2	18.5	16.50	73.5	76.85
•35 v/o, N/A	0.106	19.9	19.9	95.6	92.8	20.4	18.18	103.3	92.98
SIC_w/Al									
•25 v/o, N/A	0.104	17.6	17.1	102.0	96.7	18.15	16.13	102.5	94.26
•35 v/o, N/A	0.106	18.8	18.9	85.7	75.3	19.22	19.28	97.02	97.64
P100/Al									
•42.2 v/o, [0, 0]	0.090	49.71	52.48	131.3	127.0	48.15	45.33	46.62	43.70
HMU/7070									
•44 v/o, $[0]_{12}$	0.072	26.43	—	95.5	—	21.3	21.66	126.3	115.34
•40.5 v/o, $[0/90]_6$	0.071	11.7	—	40.9	—	12.5	12.44	86.7	84.68
C-C									
•52.48 v/o, [0, 0, 0]	0.060	43.7	—	81.5	—	39.4	—	47.8	—
•53.0 v/o, [0/90/0]	0.060	32.4	—	44.1	36.78	29.1	28.58	6.95	15.63
SIC_p/Al Tubes									
•25 v/o, N/A	0.104	15.8	16.34	>63.4	85.5	17.3	16.33	90.1	84.6
•35 v/o, N/A	0.106	18.9	17.36	90.6	87.65	19.3	18.05	113.1	89.75
SIC_w/Al Tubes									
•25 v/o, N/A	0.104	19.8	17.73	>86.9	99.2	19.6	20.16	130.3	112.7
•35 v/o, N/A	0.106	22.3	19.93	>85.6	74.0	22.4	20.72	133.3	115.55

Table A.3-3 Effect of Thermal Cycling on the Transverse Tensile and Compressive Properties of Composite Materials

Material	Density (lb/in^3)	Tension				Compression			
		E_y^T (Msi)		σ_y^{TU} (ksi)		E_y^C (Msi)		σ_y^{CU} (ksi)	
		AF	TC	AF	TC	AF	TC	AF	TC
P75/1962									
•62.2v/o, $[0, \pm45, 90]_s$	0.0623	15.2	15.5	50.1	42.2	14.54	11.58	27.6	25.08
•62.2v/o, $[\pm30, 0_4]_s$	0.0623	1.79	1.70	4.4	4.06	1.73	1.44	17.7	17.58
P75/PEEK									
•62.2v/o, $[0, \pm45, 90]_s$	0.063	14.45	13.6	46.12	39.7	9.36	9.43	21.75	25.46
•62.2v/o, $[\pm30, 0_4]_s$	0.063	1.40	1.21	5.46	5.61	1.14	1.17	17.54	17.96
AS4/PES									
•62.2v/o, $[0, \pm45, 90]_s$	0.058	6.51	6.7	77.69	71.4	5.63	5.95	30.36	26.67
•62.2v/o, $[\pm30, 0_4]_s$	0.058	1.57	1.46	4.54	5.21	1.26	1.25	21.07	17.65
SiC_p/Al									
•25 v/o, N/A	0.104	17.0	16.8	77.5	90.6	17.9	17.73	75.8	86.33
•35 v/o, N/A	0.106	19.4	19.1	97.0	91.92	21.0	18.98	103.4	97.7
SiC_w/Al									
•25 v/o, N/A	0.104	16.42	16.3	97.4	93.0	16.5	15.98	91.0	75.76
•35 v/o, N/A	0.106	17.2	16.6	57.7	56.7	17.2	17.8	66.02	96.53
P100/Al									
•42.2 v/o, [0, 0]	0.090	5.14	—	3.62	—	4.82	4.40	15.21	20.30
HMU/7070									
•44 v/o, $[0]_{12}$	0.072	—	—	—	—	—	—	—	—
•40.5 v/o, $[0/90]_6$	0.071	11.9	—	78.4	—	—	13.14	—	74.57
C-C									
•52.48 v/o, [0, 0, 0]	0.060	1.45	—	2.04	—	1.3	—	4.6	—
•53.0 v/o, [0/90/0]	0.060	20.3	—	29.0	28.7	15.5	—	9.4	8.36
SiC_p/Al									
•25 v/o, N/A	0.104	—	—	—	—	—	—	—	—
•35 v/o, N/A	0.106	—	—	—	—	—	—	—	—
SiC_w/Al									
•25 v/o, N/A	0.104	—	—	—	—	—	—	—	—
•35 v/o, N/A	0.106	—	—	—	—	—	—	—	—

Table A.3-4 Summary of Thermal Expansion Response of Composite Specimens After 10, 099 Thermal Cycles Between -150°F and +150°F

					Thermal Expansion Response After 10,099 Cycles			0 Cycles
Material		Layup	v/o	Test Dir.	RT Hysteresis ppm	Residual Strain, ppm	CTE* ppm/°F	CTE* ppm/°F
PANELS								
1	P75/1962	$[0, \pm45, 90]_s$	62.2	x	-30.15	-4.02	-0.585	-0.454
2	P75/1962	$[0, \pm45, 90]_s$	62.2	y	-30.15	-35.17	-0.395	-0.14
3	P75/1962	$[\pm30, 0_4]_s$	62.7	x	-27.64	6.53	-1.00	-1.02
4	P75/1962	$[\pm30, 0_4]_s$	62.7	y	-45.22	-12.56	2.92	5.83
5	P75/PEEK	$[0, \pm45, 90]_s$	62.2	x	-57.79	26.13	-0.248	-0.28
6	P75/PEEK	$[0, \pm45, 90]_s$	62.2	y	-55.78	-9.045	-0.201	+0.04
7	P75/PEEK	$[\pm30, 0_4]_s$	62.2	x	-80.40	-188.44	-0.81	-0.39
8	P75/PEEK	$[\pm30, 0_4]_s$	62.2	y	5.78	-90.45	7.60	10.17
9	AS4/PES	$[0, \pm45, 90]_s$	53.7	x	-16.08	-50.25	0.65	1.08
10	AS4/PES	$[0, \pm45, 90]_s$	53.7	y	-12.90	15.58	0.285	1.38
11	AS4/PES	$[\pm30, 0_4]_s$	54.96	x	-42.72	-22.11	-0.37	-0.66
12	AS4/PES	$[\pm30, 0_4]_s$	54.96	y	-165.82	-201.00	10.68	12.60
13	P100/6061 Al	$[0]_2$	42.2	x	-10.05	4.02	0.99	-0.27**
14	SiC_p/2124-T6	N/A	25	x	55.28	-97.99	8.69	8.16
15	SiC_p/2124-T6	N/A	25	y	-100.50	-90.45	7.78	7.86
16	SiC_w/2124-T6	N/A	25	x	11.56	-100.50	8.56	8.03
17	SiC_w/2124-T6	N/A	25	y	50.25	-80.40	8.65	7.77
18	SiC_p/2124-T6	N/A	35	x	0.00	-75.38	6.78	5.91
19	SiC_p/2124-T6	N/A	35	y	50.25	-45.23	7.55	6.11
—	SiC_w/2124-T6	N/A	35	x	—	—	—	5.91
—	SiCw/2124-T6	N/A	35	y	—	—	—	6.29
20	Carbon-Carbon	[0/90/0]	53.0	x	-50.25	-12.56	-0.737	-0.95
21	Carbon-Carbon	[0/90/0]	53.0	y	-40.95	-13.57	-0.87	-0.87
22	Carbon-Carbon	$[0]_3$	52.48	x	-29.65	-21.10	-0.94	-0.98
23	Carbon-Carbon	$[0]_3$	52.48	y	-65.32	-47.70	0.29	-0.42
24	HMU/7070	$[0/90]_6$	40.5	x	8.75	-2.00	0.28	-0.075
25	HMU/7070	$[0/90]_6$	40.5	y	-13.00	-2.50	0.40	—
TUBES								
26	P100/Al, DB	$[0]_2$	43.63	x	10.01	-10.01	0.50	0.33
27	P100/Al, PT	$[0]_2$	44.35	x	-4.00	6.00	0.38	0.37
—	P100/AZ91C Mg	$[\pm16°]_s$	23.7	x	—	—	—	1.52
—	P100/AZ91C Mg	$[\pm16°]_s$	27.9	x	—	—	—	0.80
—	P100/AZ91C Mg	$[\pm16°]_s$	30.1	x	—	—	—	—

*Slope of a line joining extreme points at +150° and -150°F
**Calculated CTE: 0.70 ppm/°F

A.4 CONCLUDING REMARKS

Although extensive material property data of several composites exist, use of this data in structural design efforts is severely limited due to lack of standardized test methods and procedures, and the large number of organizations reporting the limited data. In response to these needs, the current program was designed to generate a viable database of advanced composite material properties by utilizing a singular contractor and implementing the same test methods and environments for the composites considered. This database, although limited, should prove extremely valuable to spacecraft designers for preliminary material trade-off studies. The test data listed in Table 1-5 (and discussed in Chapters 2 to 10) provides the typical material properties of SOA composites. Also, the test data presented in Table 1-7 to 1-10 (and discussed in Chapter 11) provides an assessment of the effect of thermal cycling on the mechanical properties and dimensional stability of these composites. The results of both the as-fabricated and thermal cycled composites have been included in the "Strategic Defense System (SDS) Spacecraft Structural Composite Materials Selection Guide" prepared by Ketema, Inc., Composite Materials Division, CA (Ref 21). While extensive data has been generated in this technical effort, a large number of specimens from different production batches should be tested before and after thermal cycling to build confidence in the reproducibility and reliability of composite material properties.

APPENDIX B TEST METHODS

B.1 TEST METHODS FOR COMPOSITE MATERIALS

To generate a reliable and consistent data base that may be used with confidence throughout industry, only those methods which produce repeatable, reliable, and easily obtainable results were included in this technical effort. These methods primarily included ASTM standards (whenever applicable), and ASTM, SACMA, DOD-NASA, TPRL, or Martin Marietta Astronautics Group recommended methods (Refs B1 to B5). For compression and torsion tests of tube specimens, specific fixtures were designed and fabricated at Martin Marietta Astronautics Group. The selected test methods are listed in Table B.1-1. For the mechanical property tests, the specimen design/fixture are shown schematically in Figures B.1-1 to B.1-7. For the thermophysical properties, key features of the test methods such as equipment, reference material and specimen size are listed in Table B.1-2.

B.2 THERMOPHYSICAL PROPERTY TEST METHOD

B.2.1 Coefficient of Thermal Expansion

Push Rod Dilatometer (PRD)

In a fused silica test chamber, a 3-in. long (0.5-in. wide) specimen is placed in contact with a freely-suspended probe rod (fused silica). As the specimen temperature changes, it expands or contracts and the resultant change in length is transmitted by the probe rod to the core of the LVDT transducer. The LVDT converts this displacement into a proportional voltage signal recorded as ΔL. These measurements were performed at Harrop Industries, Columbus, OH, using their model TDA-H2. The strain sensitivity of this technique is about ± 10 ppm/°F as

Table B.1-1 Selected Test Methods for Composites

• Density	
ASTM-D792	Specific Gravity of Plastics by Displacement Method
•Reinforcement Volume	
ASTM-D3553	Fiber Content by Digestion of MMC
ASTM-D3171	Fiber Content by Resin Matrix Composites by Matrix Digestion
ASTM-D2734	Void Content of Reinforced Plastics
• Mechanical Properties	
ASTM-D3552	Tensile Properties of Fiber Reinforced MMC
ASTM-D3039	Tensile Properties of Fiber Reinforced Resin Composites
ASTM-D3410	Compressive Properties of Unidirectional or Cross-Ply Fiber Resin Composites
ASTM-D3518	Inplane Shear Stress Strain Response of Unidirectional Reinforced Plastics
ASTM-D23444	Apparent Interlaminar Shear Strength of Fiber Composites by Short Beam Method
ASTM-D790	Flexural Properties of Plastics and Electrical Insulating Materials
NASA TN D-8215	10° Off-Axis Tensile Test for Interlaminar Shear Characterization of Fiber Composites
	Iosipescu Shear Test
• Thermophysical Properties	
ASTM-E228	Linear Thermal Expansion Using Vitreous Silica Dilatometer
ASTM-E80	Dilatometric Analysis of Metallic Material
ASTM-E1269	Specific Heat Capacity by Differential Scanning Calorimetry
TPRL (Recommended)	Kohlrausch Test Method for Determining Thermal Conductivity and Electrical Resistivity
TPRL (Recommended)	Laser Flash Method for Determining Thermal Diffusivity
ASTM-C835	Total Hemsipherical Emittance of Surfaces
ASTM-E903	Solar Absorptance, Reflectance and Transmittance of Materials
ASTM-E408	Total Normal Emittance of Surfaces Using Inspection Meter Techniques

Special Remarks

Laminate	No. of Plies (n)	Specimen Width b
$[0]_C$	n = 6	1/2
$[90]_C$	n = 15	1
$[0/90]_C$	n ≥ 3	1
$[0/\pm45/90]_C$	n ≥ 6	1

(1) Specimens may be individually molded or cut (diamond tool recommended) to width required.
(2) Inner ply of tab material should have fibers in the longitudinal direction.
(3) Self-aligning grips should be used, completely enclosing the tab area.
(4) The aspect ratio of the test area must be noted when testing off-axis orientations. The aspect ratio may be varied to represent a specific application.

Test Specimen

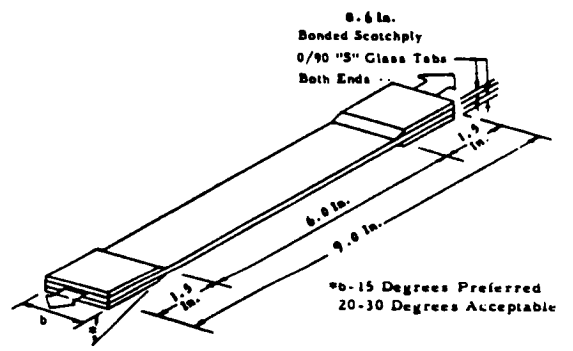

Method:
ASTM D3039

Figure B.1-1 Straight-sided Tension Test Specimen for Fiber Reinforced Composites

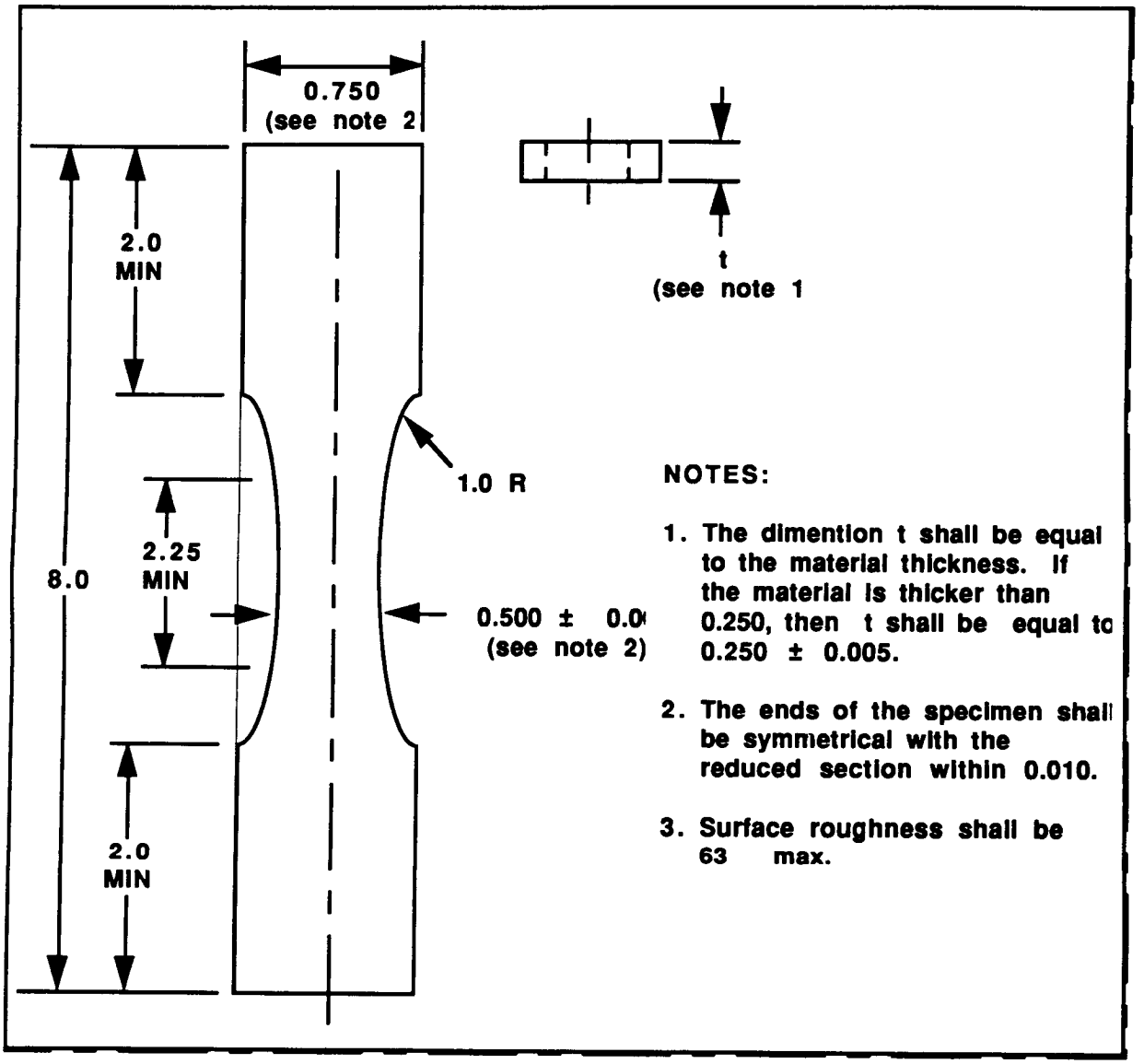

Figure B.1-2 Discontinuous Reinforced MMC Tension Test Specimens (ASTM D-3552)

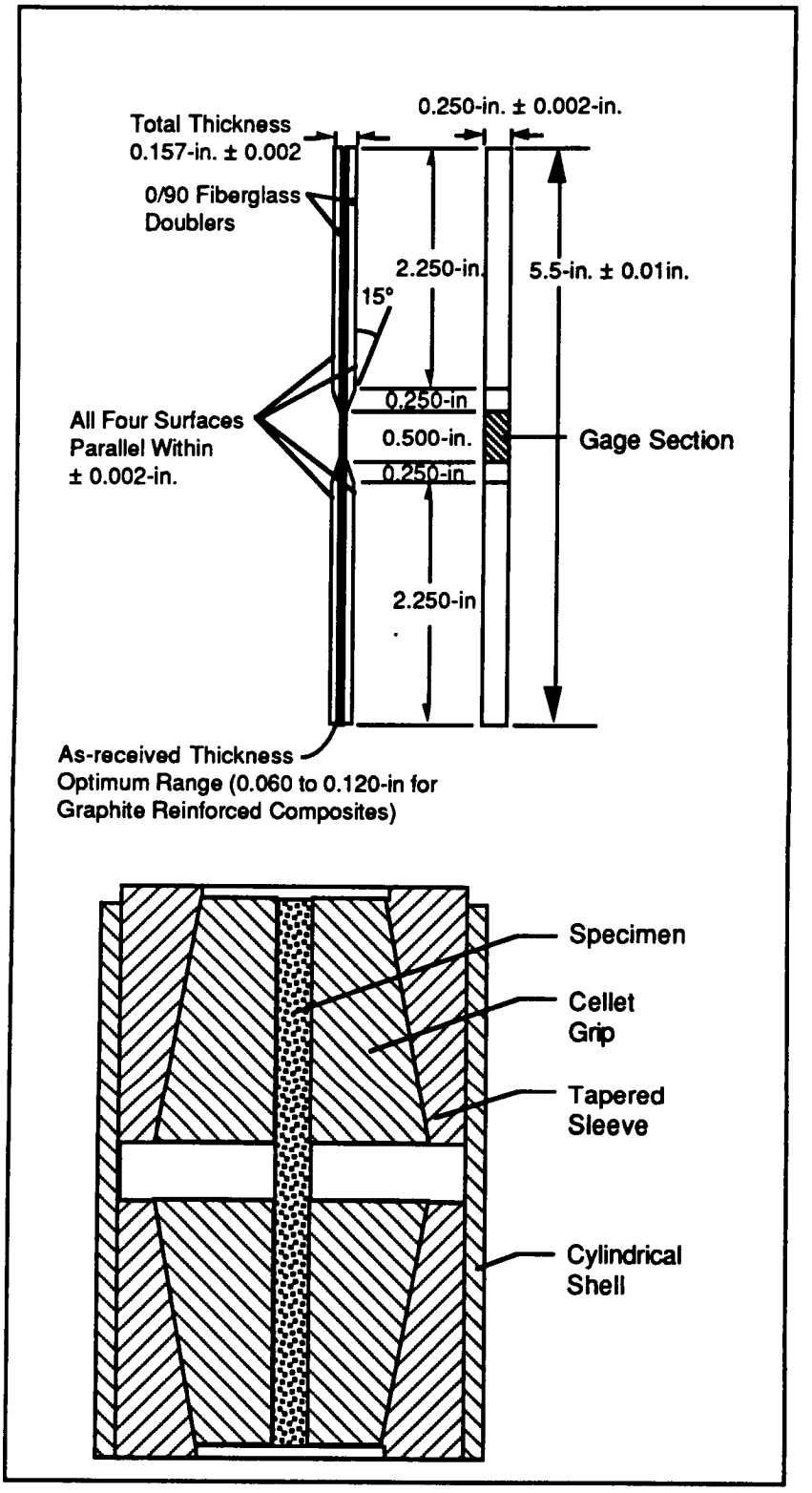

Figure B.1-3 Compression Test Specimen and Fixture (ASTM D-3410) for Composites

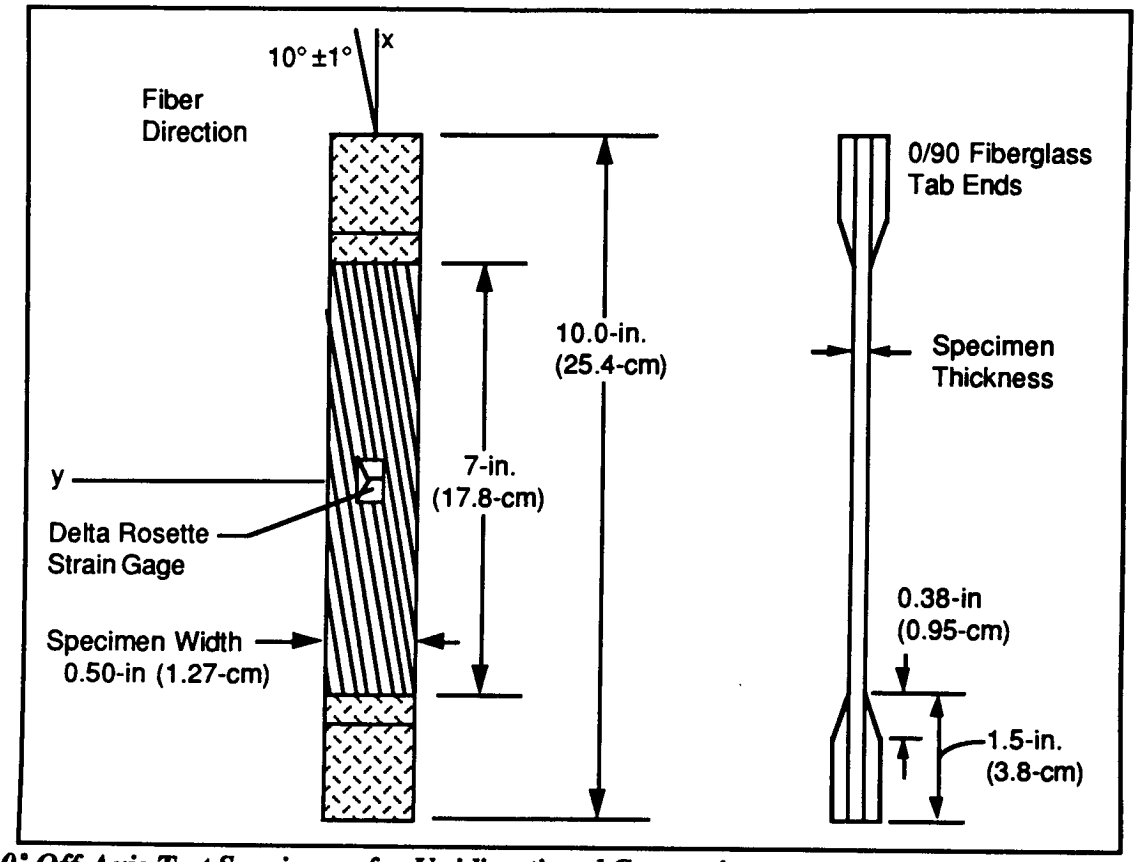

a) 10° Off-Axis Test Specimens for Unidirectional Composites

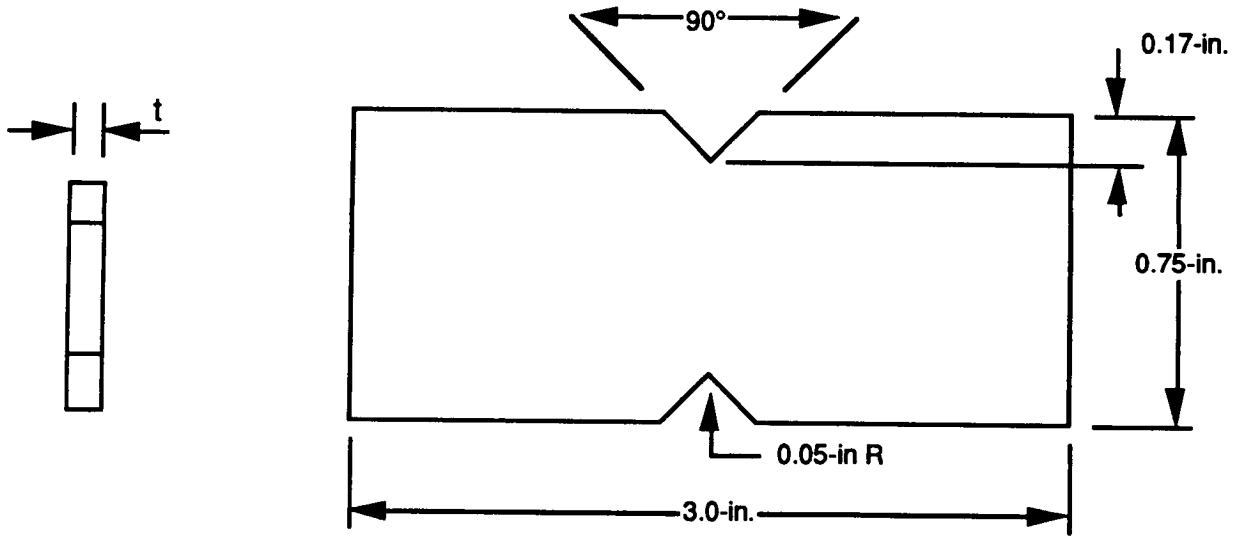

b) Typical Dimensions of the Iosipescu Shear Specimen for Composites

Figure B.1-4 Inplane Shear Test Specimen for Composites

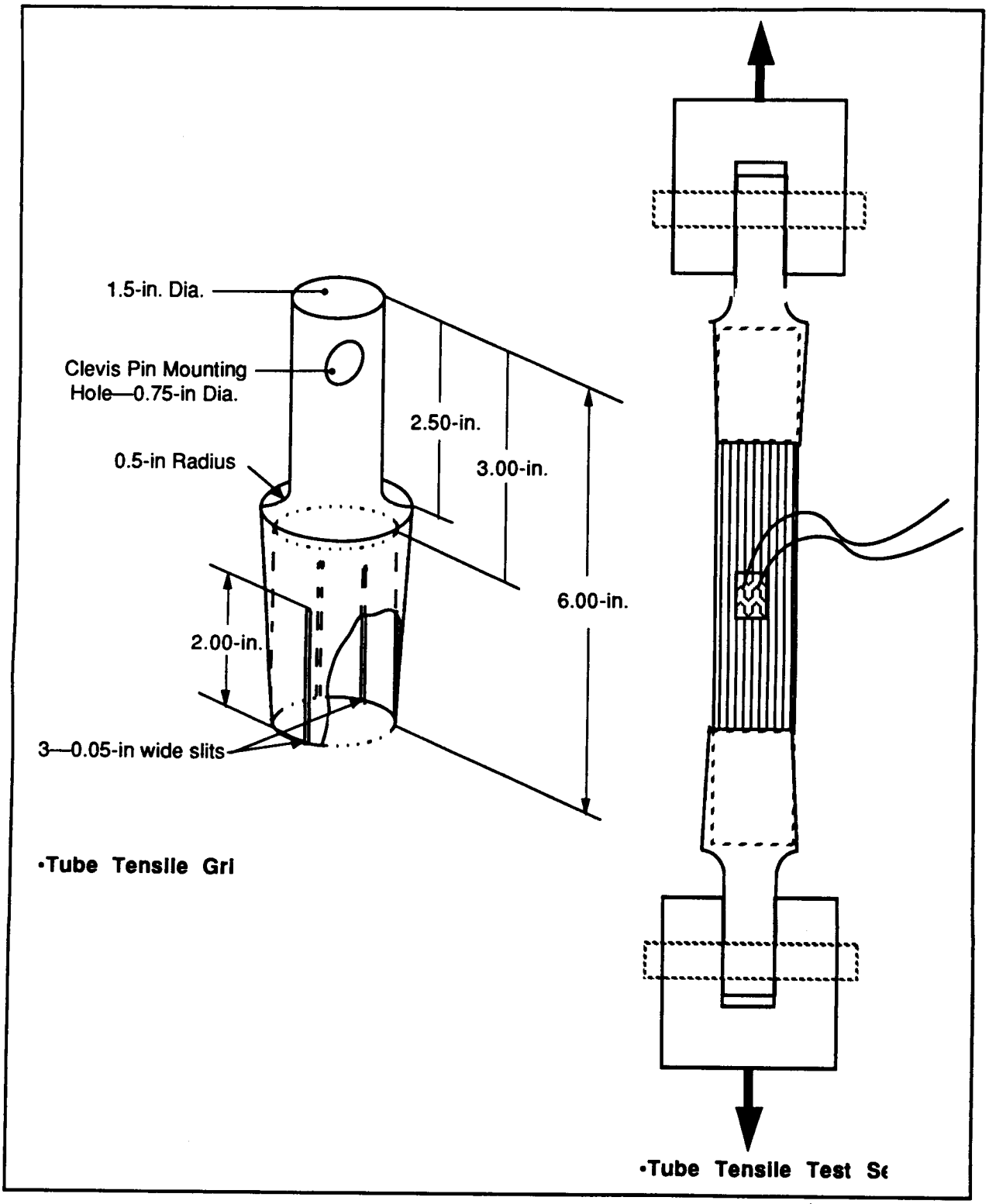

Figure B-1-5 Tension Test Grip and Setup for Composite Tube

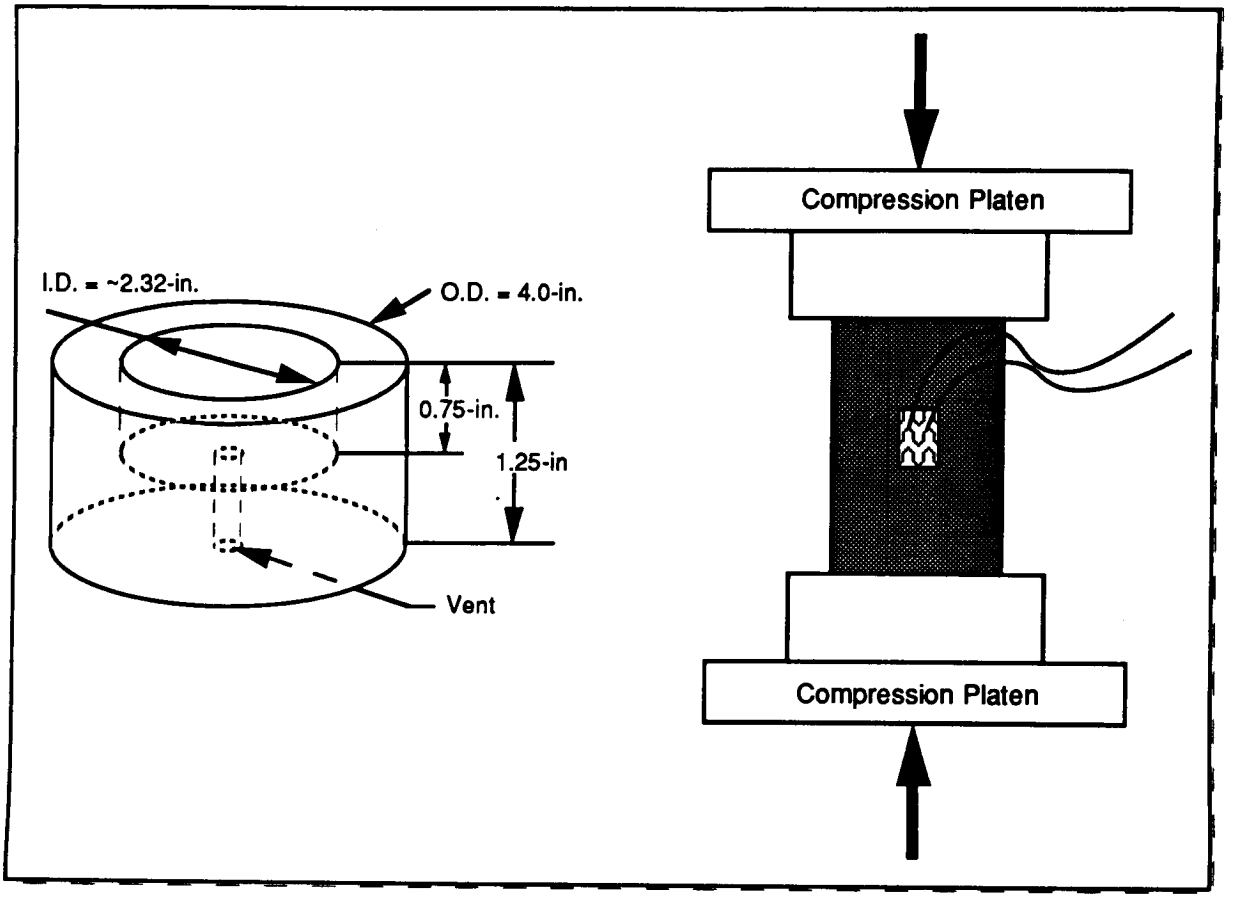

Figure B.1-6 Compression Test Grips and Composite Tubes

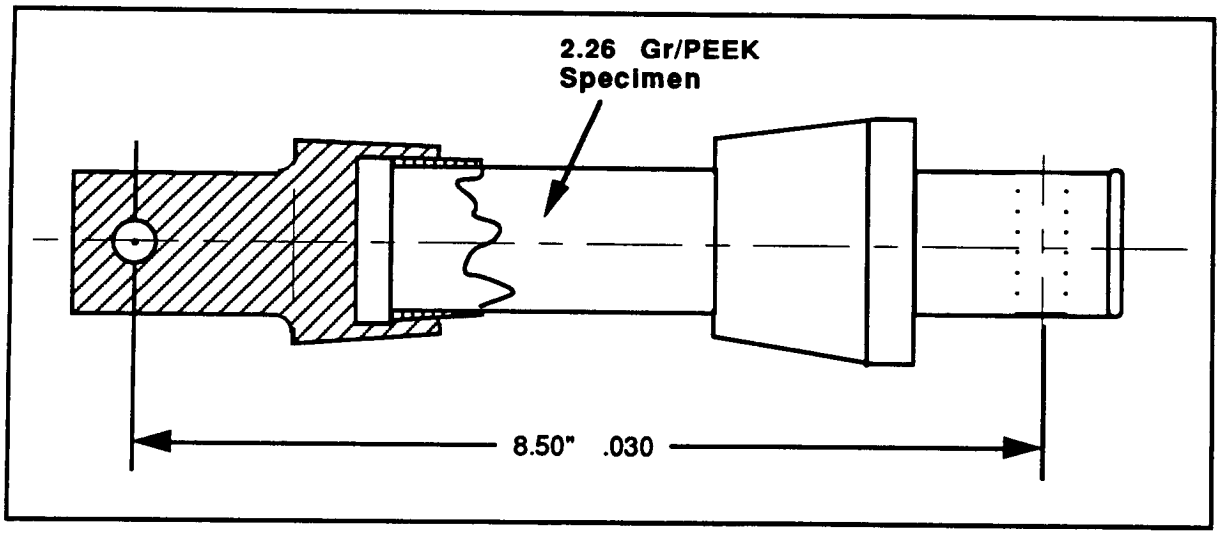

Figure B.1-7 Torsion Test Setup for Composite Tube

Table B.1-2 Key Features of Thermophysical Property Tests

Property	Apparatus	Specimen Dimensions
• Specific Heat (Cp)	Perkin Elmer DSC-2 Reference Material: Sapphire	0.16 ± 0.01 square inch x 0.060-in. thick
• Thermal Diffusivity (D)	TPRL Flash Diffusivity Reference Material: Sapphire	0.5 ± .005 square inch x 0.1 ± 0.001-in. thick
• Thermal Conductivity * :Kx, Ky	Kohlrausch Apparatus Reference Material: SRMS-739 SRMS-734 SRMS-735	3.5-in. ± 0.5 long x 0.25 ± 0.01-in. wide strips
:Kw = D · Cp · ρ	(From Cp & D Measurements)	0.5 ± 0.005 square inch x 0.1 ± 0.001-in. thick
• Electrical Resistivity *	Kohlrausch Apparatus	3.5-in. ± 0.5 long x 0.25-in. ± 0.01-in wide strips
• Solar Absorptance	Beckman Model DK2A Over Solar Spectra 0.3-4μm	1-in. square
• Normal Emittance	Gier-Dunkel Model DB-100	1-in. square
•Reflectance vs. Wavelength **	NICOLET 6000 FTIR Spectrophotmeter	1-in. square

* Refer to the schematic in Figure B.2-1, showing calculation of inplane thermal conductivity and electrical resistivity.

** Refer to Figure B.2-2, showing the schematic and brief description of test method.

compared to ±0.1 ppm°F for the laser interferometric dilatometer (Ref B-6). The temperature change is accomplished at a rate of 40°F/minute; compared to 22°F/hour in the case of laser interferometric dilatometer. The dimensional changes of the specimen-standard assembly were recorded at temperature levels of 10°F, and the specimen was held at the recording temperature for not more than 5 minutes. One complete thermal expansion test cycle included RT ⇒ 150°F ⇒ -150°F ⇒ RT. In the first test cycle, generally the thermal expansion response of a composite

specimen is a hysteresis loop as shown schematically in Figure B.2-1. From this thermal strain vs. temperature curve, it is difficult to assign a mean CTE value to the composite, because CTE varies continuously with temperature during a thermal cycle. (Often, a third order polynomial fit of test data points is obtained and CTE at a particular temperature is determined by taking the first derivative with respect to temperature.) From the first cycle, thermal expansion response of different composites, the average CTE value, RT hysteresis and residual strain has been determined, as follows (Refer to Figure B.2-3):

Average CTE:	The slope of a line (DB) connecting the strain values at temperature extremes (±150°F);
RT Hysteresis:	Dimensional change during RT ⇒ 150°F ⇒ RT measurements (i.e., AC); and
Residual Strain:	Thermal strain at the end of cycle.

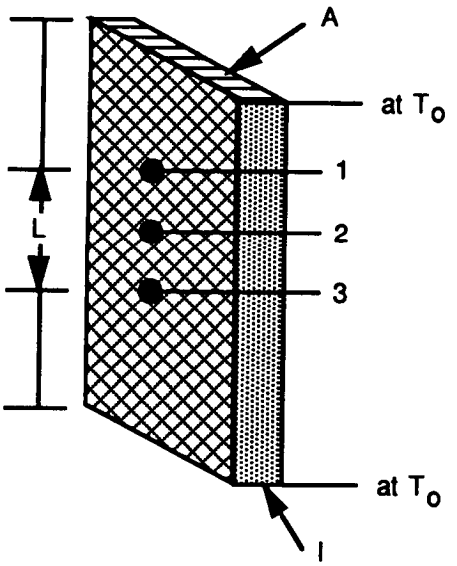

$$K \cdot \rho_e = \frac{(V_3 - V_1)^2}{4[2T_2 - (T_1 + T_3)]}$$

$$\rho_e = \frac{(V_3 - V_1)A}{IL}$$

Where:

K = Inplane Conductivity

ρ_e = Electrical Resistivity

I = Current

V_1, V_2, V_3 = Voltage at location 1, 2, 3

T_0, T_1, T_2, T_3 = Temperature at location 0, 1, 2, 3

Figure B.2-1 Schematic Showing Determination of Thermal Conductivity and Electrical Resistivity by Kohlrausch Method

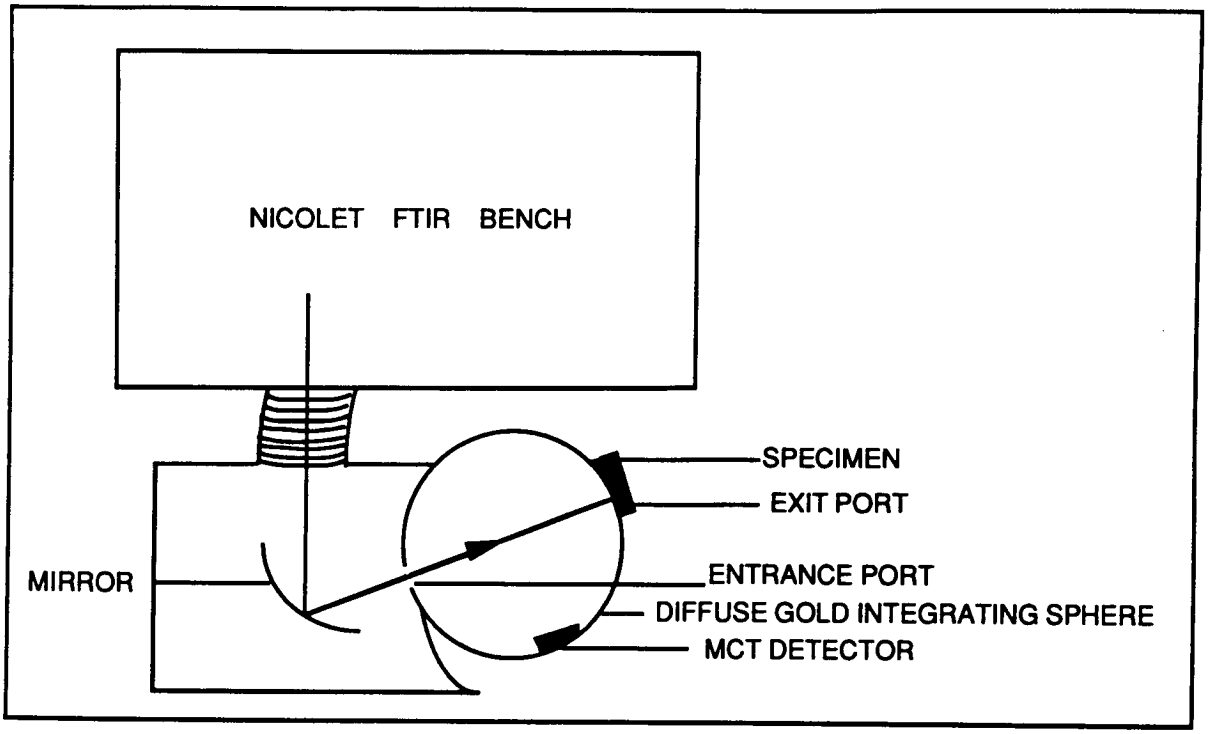

Figure B.2-2 Schematic Showing FTIR Spectrophotometer to Measure Reflectance at Different Wavelengths

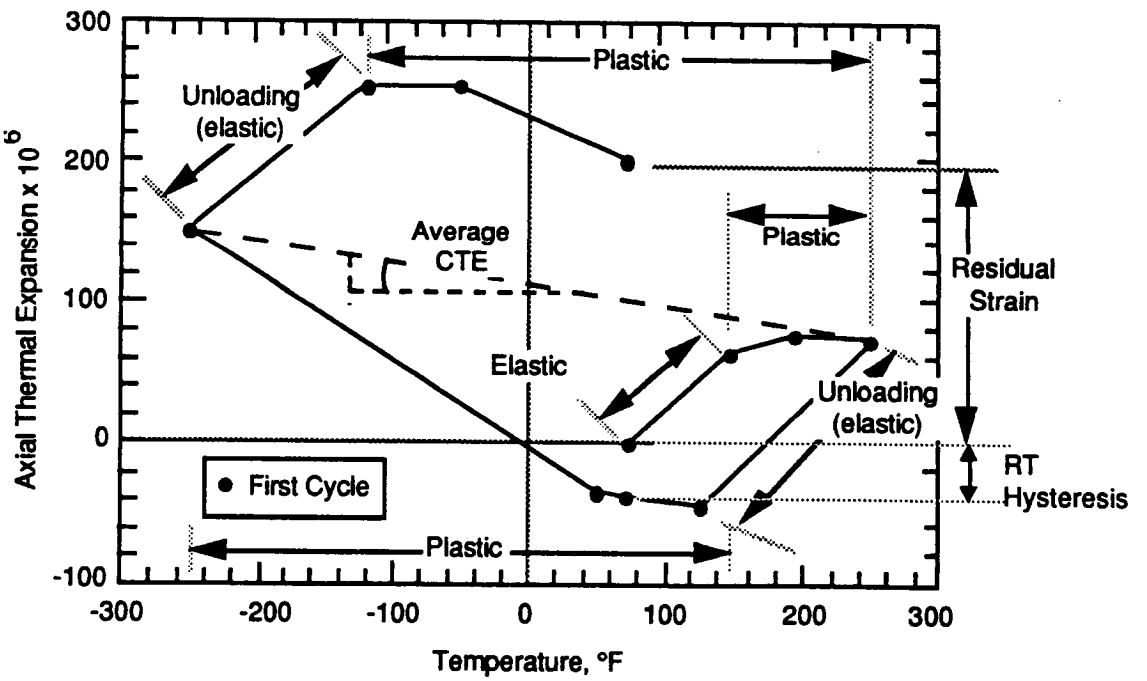

Figure B.2-3 Typical Thermal Expansion Response of a Composite Material During First Cycle (e.g., RT ⇒ 250°F ⇒ -250°F ⇒ RT)

These values of average CTE, RT hysteresis and residual strain do adequately describe the thermal expansion profile of the composite, although actual CTE value at a temperature has to be obtained from the curve.

B.2.2 Thermal Diffusivity (D)

Laser Flash Diffusivity Method

In the flash method, the front face of a small disc-shaped specimen is subjected to a short laser burst resulting in rise in rear face temperature. This transition temperature rise was recorded, and the time required to reach one-half of the maximum temperature rise, due to the laser flash was calculated to determine the thermal diffusivity. A highly developed apparatus exists at the TPRL and we have been involved in an extensive program to evaluate the technique and broaden its uses. The apparatus consists of a Korad K2 laser, a high vacuum system including a bell jar with windows for viewing the sample, a tantalum tube heater surrounding a sample holding assembly, a spring-loaded thermocouple or an infrared detector, appropriate biasing circuits, amplifiers, a-D converters, crystal clocks and a minicomputer based digital data acquisition system capable of accurately taking data in the 40 microsecond and long time domain. The computer controls the experiment, collects the data, calculated the results, and compares the raw data with the theoretical model.

B.2.3 Specific Heat (Cp)

Perkin-Elmer Model DSC-2 Differential Scanning Calorimeter

The sapphire standard and sample, both encapsulated in pans, were subjected to the same heat flux and the differential power required to heat the sample at the same rate was recorded using

the digital data acquisition system. From the mass of the sapphire standard, pans, the differential power, and the known specific heat of sapphire, the specific heat of the sample is computed. The experimental data is visually displayed as the experiment progresses. All measured quantities are directly traceable to NBS standards.

B.2.4 Thermal Conductivity

Kohlrausch Apparatus

The Kohlrausch method involves the determination of the product of the thermal conductivity "K" and the electrical resistivity "ρ_e". Since the electrical resistivity is also measured at the same time, K can be calculated. The method involves passing constant direct current through the specimen to heat the sample while the ends are kept at constant temperature. Radial heat losses are minimized by an external heater whose center temperatures are maintained at the sample's midpoint temperatures and whose ends are also water-cooled. With these provisions, at steady-state a parabola-like axial temperature profile is obtained. Thermocouples act as voltage probes. Numbering the center thermocouple as the "2" position (Figure B.1-8) and the other position as "1" and "3", it is possible to get the product of K and ρ_e:

$$K\rho_e = \frac{(V_3 - V_1)^2}{4[2T_2 - (T_1 + T_3)]}$$

where V(3) - V(1) is the voltage drop between the third and first thermocouple, T(1) + T(3) is the sum of the temperatures at the outside thermocouples and T(2) is the center temperature. Since ρ_e is also measured simultaneously, (ρ_e = (V(3) - V(1) A/IL where A is the cross-sectional area, I is the current and L is the distance between position 1 and 3), K can be calculated. The data collection (T(1), T(2), T(3), V(3), V(1), I) are computerized and the results calculated for a set of measurements performed while the sample is under vacuum and the heater temperature matched to that of T(2). Then additional current is used, a new set of equilibrium conditions is

obtained, and the process repeated.

Thermal conductivity values accurate well within 5% are obtained by the Kohlrausch method and all measured quantities are directly traceable to NBS standards. This method is a standard test procedure and has been tested with SRMS 730, 734, and 735. The results were all within 3% of the reference values.

B.2.5 Reflectance Measurements

FTIR Test Method

Test Specimen is mounted at 0.87-in. dia exit port at the exterior of the integrating sphere (ensure no light leaks). The specimen is irradiated by light emitted by a water-cooled Globar source located in the bench of the Nicolet 6000 Series FTIR Spectrometer (Figure B.2-2). the light exits the bench and is directed by a mirror into the diffuse gold-coated integrating sphere, where it directly irradiates the specimen (located at the exit port). The light reflects off the specimen and onto the walls of the sphere, and it continues to reflect off the walls of the sphere and eventually strikes the liquid nitrogen-cooled MCT (mercury-cadmium-telluride) detector. The amount of light reflected from the specimen is determined by its surface finish (a dark or dull specimen will reflect less than a lighter or shinier specimen). The reflectance of the sample is compared to the reflectance of a reference material (a diffuse gold specimen is used as a reference). It is customary to plot the spectrum of the specimen in % reflectance vs. wavelength (in microns) from the wavelength region of 2.0-14.0 microns.

B.3 REFERENCES

B1 Annual Book of ASTM Standards, 1989.

B2 DoD-NASA Advanced Composite Guide, Rockwell International, AFWAL/FDL, Chapter 4.2, July 1983.

B3 "Suppliers of Advanced Composite Materials Association Recommended Methods", T21-489-1, 1989.

B4 R. E. Taylor, "Thermophysical Property Research Laboratory, Purdue University, IN, Report No. TPRL 181A, 1989.

B5 S. P. Rawal, M. S. Misra, D. Goddard, and J. Jackson, "Novel Processing Techniques to Fabricate Graphite/Magnesium Composites for Space Applications", Martin Marietta Space Systems Report # MCR-88-635, 1988.

APPENDIX C COMPOSITE ANALYSIS

C.1 COMPOSITE ANALYSIS

Predicted mechanical and thermophysical properties of continuous fiber reinforced composite materials have been obtained by using various analytical tools that range from simple rule of mixture (ROM) equations through complex matrix operations of laminate analysis. The ROM equations and the names of computer codes which are often used to predict the material properties of different composites, are presented in this section.

C.2 RULE OF MIXTURES

The ROM equations are commonly used to predict properties of composites based on the properties of constituent reinforcement and matrix materials (Ref. C-1, C-2, C-3). These properties include elastic constants, CTE, specific heat, and thermal conductivity.

C.2.1 Elastic Constants

C.2.1.1 Continuous Fiber Reinforced Composites

- Transversely isotropic Composite

• Longitudinal Modulus: $E_x = E_{fx} V_f + E_m (1-V_f)$

• Transverse Modulus: $E_y = E_z = \dfrac{E_m}{1-\sqrt{V_f}\left(1-E_m/E_{fy}\right)}$

• Shear Modulus: $G_{xy} = G_{yz} = \dfrac{G_m}{1-\sqrt{V_f}\left(1-G_m/G_{fxy}\right)}$

• Poisson Ratio: $\nu_{xy} = \nu_{xz} = \nu_{fxy} V_f + (1-V_f) \nu_m$

V_f = fiber volume fraction

E_{fX} = fiber modulus (x direction)

E_m = matrix modulus

G_m = matrix shear modulus

G_f = fiber shear modulus

C.2.1.2 Discontinuous Reinforced Composite

• Elastic Modulus:

$$E_c = E_m \frac{E_m V_m + E_r (V_r + 1)}{E_r V_m + E_m (V_r + 1)}$$ (Hashin-Shritkman equation Ref C-4)

Where: E_r = Reinforcement modulus

V_r = Reinforcement volume fraction

C.2.2 Thermal Properties

C.2.2.1 Continuous Fiber Reinforced Composites

• Specific Heat: $$C_p = \frac{1}{\rho}\left(V_f \rho_f C_f + V_m \rho_m C_m\right)$$

• Longitudinal Conductivity: $K_x = V_f K_{fx} + K_m (1-V_f)$

• Transverse Conductivity: $$K_y = K_z = \left(1-\sqrt{V_f}\right) K_m + \frac{K_m \sqrt{V_f}}{1-\sqrt{V_f}\left(1-K_m / K_{fy}\right)}$$

• Longitudinal Thermal Expansion Coefficient: $$\alpha_x = \frac{V_f E_{fx} \alpha_{fx} + V_m E_m \alpha_m}{E_{fx} V_f + E_m V_m}$$

•Transverse Thermal

Expansion Coefficient: $$\alpha_y = \alpha_z = \alpha_{fy}\sqrt{V_f} + \alpha_m\left(1-\sqrt{V_f}\right)\left(1+\frac{V_f \nu_m E_{fx}}{E_{fx}V_f + E_m V_m}\right)$$

C.2.2.2 Discontinuous Reinforced Composites

• Coefficient of thermal expansion

- Random Particulate (Kerner Equation Ref C-5)

$$\alpha_c = \bar{\alpha} + \frac{\left(\alpha_m - \alpha_\rho\right)}{\left(\frac{1}{B_m} - \frac{1}{B_p}\right)}\left[\frac{1}{B_c} - \left(\frac{\bar{1}}{B}\right)\right]$$

Where:

$$\bar{\alpha} = V_m\alpha_m + V_\rho\alpha_p$$

$$\left(\frac{\bar{1}}{B}\right) = \frac{V_m}{B_m} + \frac{V_\rho}{B_p}$$

B = Bulk modulus

α = Thermal expansion coefficient

V = Volume fraction

B_c = Bulk modulus of composite (has lower and upper bounds)

B_p = Bulk modulus of particulate

- Transversely Isotropic, Aligned Whiskers (Kerner equation)

$$\alpha_x = \bar{\alpha} + \frac{\alpha_m - \alpha_\rho}{\left(\frac{1}{B_m} - \frac{1}{B_p}\right)}\left[\frac{3\left(1-2\nu_{xy}\right)}{E_x} - \left(\frac{\bar{1}}{B}\right)\right]$$

- Specific Heat

$$(C_p)_c = \frac{1}{\rho_c}\left[V_p \cdot \rho_p \cdot (C_p)_p + V_m \rho_m (C_p)_m\right]$$

- Thermal Conductivity (Lord Rayleigh Equation Ref D-6)

$$K_c = K_m \frac{1 + 2\,V_r \dfrac{(1 - K_m/K_r)}{(2\,K_m/K_r + 1)}}{1 - V_r \dfrac{(1 - K_m K_r)}{(K_m/K_r + 1)}}$$

C.3 COMPUTER ANALYSIS

Several computer codes have been developed to predict/analyze composite materials behavior. Of these codes, SQ5, GENLAM, and CLAM laminate analysis codes were used to predict thermal and mechanical properties of fiber reinforced composites.

C.4 REFERENCES

1. R. M. Jones, *Mechanics of Composite Materials*, Scripta Book Co., Washington, DC 1975.
2. R. M. Christensen, *Mechanics of Composite Materials*, John Wiley & Sons, New York , 1979.
3. J. C. Halpin, *Primer on Composite Materials*, 2nd ed., Technomic, Lancaster, PA, 1984.
4. J. Hashin and S. Shtrikman, A. Variational Approach to the Theory of Elastic Behavior of Multiphase Materials, *J. Mech. Phys.: Solids*, **11** (2), 127-140 (1963)
5. E. H. Kerner, The Elastic and Thermoelastic Properties of Composite Media, *Proc. Phys. Soc.*, **68** (b) 808-813 (1956).

6. Lord Rayleigh, On the Influence of Obstacles Arranged in Rectangular Order Upon the Properties of A Medium, *Phil Mag.*, **34**, 481-507 (1892)

REFERENCES

1. J. Persh, "Future of Metal Matrix Composites", Proceedings, Sixth Metal Matrix Composites Technology Conference, Monterey, CA, May 1985.
2. J. F. Garibotti, C. J. Northrup, and A. Gunderson, "Design Aspects of MMC in SDI Spacecraft", Proceedings, Seventh Metal Matrix Composites Technology Conference, pp1-1 - 1-28, Silver Spring, MD, 26-28 May 1987.
3. D. R. Tenney, "Structural Materials for Space Application", NASA/SDIO Space Environmental Effects of materials Workshop, L. A. Teichman, NASA CP-3035, Part 1, pp. 25 - 52, 1989.
4. M. S. Misra, "Engineered Materials for Space Applications", Martin Marietta Astronautics Group Journal, Volume 1, pp. 14 - 23, 1990.
5. D. R. Tenney, G. F. Sykes, and D. E. Bowles, "Composite Materials for Space Structures", Presented at the 3rd European Symposium on Spacecraft Materials in Space Environment, Noordwijk, The Netherlands, 1 - 4 October. 1979.
6. B. A. Stein, S. S. Tompkins, and W. D. Brewer, "Review of NASA Research on Low Temperature Metal-Matrix Composites for Aeronautics and Space", Presented at the 5th Metal Matrix Composites Technology Conference, May 1983.
7. J. F. Garibotti, W. E. Davis, and N. R. Adsit, "Materials and Structures for Space Applications", Presented at AIAA/NASA Space Systems Technology Conference, Costa Mesa, CA, 5 - 7 June 1984.
8. M. S. Misra, S. P. Rawal, B. J. Maclean, and R. G. Wendt, "Metal Matrix Composites for Precision Space Structures", Presented at AeroMat '90, Long Beach, CA, 21 - 24 May 1990.
9. L. A. Harris, "Composites in Space - Past, Present and Future", Composite Interfaces, H. Ishida and J. L. Koenig, Editors, pp. 1 - 8, Elsevier Publishing Co. Inc., 1986.

10. J. F. Garibotti, W. E. Davis, R. N. Levin, and V. L. Freeman, "The Impact of High Modulus Structural Carbon/Carbon on Spacecraft Survivability and Performance", ACMA CR 8601, Ametek, July 1986.

11. D. R. Tenney and D. E. Bowles, "Spacecraft Radiation Effects on Dimensional Stability of Composites", Proceedings of 4th International Symposium on Spacecraft Materials in Space Environment, Toulouse, France, 6 - 9 September 1988.

12. D. R. Tenney, G. F. Sykes, and D. E. Bowles, "Space Environmental Effects on Materials", Presented at the AGARD Conference on Environmental Effects on Materials for Space Applications, Conference Proceedings No. 327, Toronto, Canada, September 1982.

13. D. E. Bowles, "The Effects of Microcracking on the Thermal Expansion of Graphite/Epoxy Composites", Presented at the 3rd Annual LSST Conference, 16 - 19 November 1981, NASA-LaRC, NASA CP- 2215, Part 1, 1982, pp. 67-79.

14. D. E. Bowles, S. S. Tompkins, and G. F. Sykes, "Electron Radiation Effects on the Thermal Expansion of Graphite/Resin Composites", AIAA Journal of Spacecraft and Rockets, Vol. 23, No. 6, November - December 1986.

15. S. M. Milkovich, C. T. Herakovich, and G. F. Sykes, "Space Radiation Effects on Graphite-Epoxy Composite Materials", Center for Composite Materials, and Structures, VPI&SU, Report No. CCMS-84 08, Blacksburg, VA, June 1984.

16. G. F. Sykes, S. M. Milkovich, and C. T. Herakovich, "Simulated Space Radiation Effects on a Graphite/Epoxy Composite", Presented at the Spring National Meeting of the American Chemical Society, Miami Beach, FL, April 18 - May 3, 1985.

17. G. F. Sykes and D. E. Bowles, "Space Radiation Effects on the Dimensional Stability of a Toughened Epoxy Graphite Composite", SAMPE Quarterly, Nol. 17, No. 4, July 1986.

18. S. D. Adams, D. E. Bowles, and C. T. Herakovich, "Thermally Induced Transverse Cracking in Graphite/Epoxy Cross-Ply Laminates", Journal of Reinforced Plastics and Composites, Vol. 5, No. 3, July 1986.

19. J. Persh, "New Department of Defense Initiatives in Composite Materials and Structures", Ceramic Eng. Sci. Proc. 9, [7 - 8], pp. 529 - 540, 1988.

20. "DoD-NASA Advanced Composite Design Guide", AD-B080184, Rockwell International, AFWAL/FDL, July 1983.

21. "SDS Spacecraft Structural Composite Materials Selection Guide", Ketema Inc., Santa Ana, CA, Release 1.0, May 1989.

22. L. Rubin, "Data-Base Development for P100 Graphite/Aluminum Metal Matrix Composites", Aerospace Report No. TOR-0089 (4661-02)-1, 15 September 1989.

23. L. Rubin, "High Modulus Carbon Fiber Based Carbon-Carbon for Space Applications", The Aerospace Corporation, Report SD TR-86-45, 18 July 1986.

24. J. B. Andriulli, V. W. Campbell, R. E. Garvey, T. L. Knight, J. W. McKeever, and R. G. Rudness, "Thermoplastics Composites for Space Applications", 1989 Annual Report, ORNL/ATD-14, Vol. 1 and Vol. 2, Oak Ridge National Laboratory, Oak Ridge TN, September 1989.

25. "Proceedings of a Workshop on Advanced Structural Materials for Space Applications", Thermoplastic Composites, Vol. 1, Burlingame, CA, 11 - 14 September 1989.

26. "Proceedings of a Workshop on Advanced Structural Materials for Space Applications", Metal Matrix Composites, Vol. 2, Burlingame, CA, 11 - 14 September 1989.

27. "Spacecraft Applications for Carbon-Carbon Program Review Proceedings", NSWC, Silver Springs, 14 June 1989.

28. A. P. Divecha, S. G. Fishman, and S. D. Karmarker, Silicon Carbide Reinforced Aluminum - A Formable Composite, J. Met., September 1981.

29. K. Hall, B. Rodini, C. Thaw, and C. Zweben, "Metal Matrix, Carbon and Ceramic Matrix Composites 1985", NASA Conference Publication 2406, December 1985, pp. 116-121.

30. S. P. Rawal and M. S. Misra, "Large Graphite/Magnesium Tube Development", WRDC-TR-90-4062, August 1990.

31. G. A. Dries and S. S. Tompkins, "Effects of Thermal Cycling on Graphite-Fiber-Reinforced 6061 Aluminum", NASA TP-2612, October 1986.

32. D. W. Bowles and D. R. Tenney, "Thermal Expansion of Composites: Methods and Results", Presented at the 2nd Annual LSST Technical Review, NASA-LaRC, NASA CP 2168, November 1980.

33. B. L. Wingard, "Testing and Evaluation of Missile Materials - Task VI: Carbon-Carbon Materials for Space Structures", Southern Research Institute Quarterly Progress Report, July 1989.

34. A. L. Bertram, "Thin Ply Gr/Al for Space Structures", Proceedings DoD Eighth MMC Technology Conference, pp. 67-1 - 67-8, Monterey, CA, 19 - 23 June 1989.

35. K. Benner and B. K. Min, "MMC Truss Evaluation", Proceedings DoD Eighth MMC Technology Conference, pp.68-1, Monterey, CA, 19 - 23 June 1989.

36. D. E. Bowles and D. R. Tenney, "Composite Tubes for the Space Station Truss Structure", Presented at the 18th International SAMPE Technical Conference, Seattle, WA, October 1986.

37. M. S. Misra, "Role of Material Damping in the Control of Space Structures", Presented at AeroMat '90, Long Beach, CA, 21 - 24 May 1990.

38. H. H. Armstrong and A. M. Ellison, "Satellite Applications of Metal Matrix Composites", AFML-TR-79-4007, May 1979.

39. H. H. Armstrong, A. M. Ellison and D. H. Kintis, "Development of Graphite/Metal Advanced Composites for Applications", AFWAL-TR-83-4148, October 1983.

40. R. A. Mayor, J. R. Strife, and V. C. Nardone, "Metal Matrix Composites Structural Data Development," AFWAL-TR-86-4129, January 1987.

41. T. E. Steelman, A. D. Bakalyar, and L. Konopka, "Aluminum Matrix Composite Structural Design Development", AFWAL TR-86-3087, March 1987.

42. S. P. Rawal, M. S. Misra, D. Goddard, and J. Jackson, "Novel Processing Techniques to Fabricate Graphite/Magnesium Composites for Space Applications", Martin Marietta Space Systems Report #MCR-88-635, 1988.

43. R. G. Wendt, S. P. Rawal, and M. S. Misra, "Reproducibility of Filament-Wound Vacuum Cast Graphite Magnesium Tubes", Martin Marietta Space Systems Report #MCR-88-615, December 1988.

44. K. M. Prewo and V. C. Nardonne, " Carbon Fiber Reinforced Glass Matrix Composites for Space Based Applications", Report R86-917161-1, (UTRC) ONR Contract N0-0014-95-C-0332, September 1986.

45. W. K. Tredway and K. M Prewo, "Carbon Fiber Reinforced Glass Matrix Composites for Space Based Applications", Report 87-917470-1, Contract N00014-85-C-0332, August 1987.

46. W. C. Harrigan, Jr., "Heat Treatment of Silicon Catbide Reinforced 6061 Aluminum Composites," Presented at the AIME Fall Meeting, American Institute of Mining, Metallurgical and Petroleum Engineers, October 1982.

47. "Survivability of Satellite Structural Systems, Material Science Corporation", Technical Progress Report MSC-TPR-1725/1301, January 1987.

48. Annual Book of ASTM Standards, 1989.

49. DoD-NASA Advanced Composite Guide, Rockwell International, AFWAL/FDL, Chapter 4.2, July 1983.

50. Engineered Materials Handbook, Vol 1, Composites, ASM International, Metals Park, OH, 1987.

51. NASA RP 1092 - Standard Tests for Toughened Resin Composites, Revised Edition, July 1983.

52. "Suppliers of Advanced Composite Materials Association (SACMA) Recommended Methods, T2-489-1, 1989.

53. R. E. Taylor, "Determining the Thermophysical Properties of Selected Materials", Thermophysical Property Research Laboratory, Purdue University IN, Report No. TPRL 181A, 1989.

54. S. S. Tompkins, D. E. Bowles, and W. R. Kennedy,. "A Laser Interferometer for Thermal Expansion Measurements of Composites", SEM Experimental Mechanics, Vol. 26, No. 1, pp. 1 - 6, March 1986.

55. "Composite Materials", Testing and Design (Second Conference), STP-497, 04-497000-33, 1972.

56. "Composite Materials", Testing and Design (Third Conference), STP-546, 04-546000-33, 1974.

57. "Composite Materials", Testing and Design (Fifth Conference), STP-674, 04-674000-33, 1979.

58. "Composite Materials", Testing and Design (Sixth Conference), STP-787, 04-787000-33, 1982.

59. "Composite Materials", Testing and Design (Seventh Conference), STP-893, 04-893000-33, 1984.

60. C. C. Chamis and J. H. Sinclair, "10° Off-Axis Tensile Test for Interlaminar Shear Characterization of Fiber Composites", NASA-TN-D-8215, April 1976.

61. R. Francini, "Testing of Longitudinally Reinforced Graphite/Metal Composite Thin Wall Tubing", ASTM Proceeding on Test Methods, November. 1985.

62. D. F. Adams, " Properties/Characterization-Mechanical/Physical/Hygrothermal Properties Test Methods", Composites Technology, edited by Stuart M. Lee, published by Technonic Publishing Company, 1989, pp. 49-80.

63. L. J. Hart-Smith, "Generation of Higher Composite Material Allowables Using Improved Test Coupons", 36th International SAMPE Symposium, April 15 - 18, 1991.

64. D. F .Adams and D. E. Walrath, "Further Development of the Iosipescu Shear Test Method", Experimental Mechanics, June 1987, pp. 113 - 119.

65. S. P. Rawal, M. S. Misra, and R. G. Wendt, "Composite Materials for Space Applications", NASA Contractor Report 187472, August 1990.

National Aeronautics and Space Administration

Report Documentation Page

1. Report No.	2. Government Accession No.	3. Recipients Catalog No.
NASA CR-189552		

4. Title and Subtitle
Measurement of Mechanical and Thermophysical Properties of Dimensionally Stable Materials for Space Applications

5. Report Date
March 1992

6. Performing Organization Code

7. Author(s)
Suraj P. Rawal
Mohan S. Misra

8. Performing Organization Report No.
MCR-92-1320

10. Work Unit No.
506-43-21-04

9. Performing Organization Name and Address
Martin Marietta Astronautics Group
P.O. Box 179
Denver, CO 80201

11. Contract or Grant No.
NASA-18230

13. Type of Report and Period Covered
Contractor Report
11/12/90 - 8/22/91

12. Sponsoring Agency Name and Address
National Aeronautics and Space Administration
Langley Research Center
Hampton, VA 23665-5225

14. Sponsoring Agency Code

15. Supplementary Notes
Langely Technical Monitor: Louis A Teichman
Final Report - Task 12

16. Abstract

The objective of the program was to generate mechanical, thermal, and physical property test data for as-fabricated advanced composite materials at RT, -150° and 250° F. This report documents the results of mechanical and thermophysical property tests of IM7/PEEK and discontinuous SiC/Al (both particulate (p) and whisker (w) reinforced) composites which were tested at three different temperatures: -150°, RT and 250° F to determine the effect of temperature on material properties. The specific material systems tested were IM7/PEEK [0]8, [0, ±45, 90]s, [±30, 04]s, 25 volume percent (v/o) SiCp/Al, and 25 v/o SiCw/Al. Room temperature material property results of IM7/PEEK were in excellent agreement with the predicted values, providing a measure of consolidation integrity attained during fabrication. Results of mechanical property tests indicated that modulus values at each test temperature were identical, whereas the strength (e.g. tensile, compressive, flexural and shear) values were the same at -150°F and RT, and gradually decreased as the test temp-erature was increased to 250° F. Similar trend in the strength values was also observed in discontinuous SiC/Al composites. Based on these results, the effect of temperature was more pronounced on the strength values as compared to the modulus values as compared to the modulus values.

17. Key Words (Suggested by Author(s))	18. Distribution Statement
Dimensionally Stable Space Structures, Mechanical Properties,Thermophysical Properties, Non-Destructive Evaluation,Accelerated Thermal Cycling, Microcracking, Residual Stress,Delamination	Unlimited

19. Security Classif. (of this report)	20. Security Classif. (of this page)	21. No. of pages	22. Price
Unclassified	Unclassified	148	

NASA FORM 1626 OCT 86